



VCU

Virginia Commonwealth University
VCU Scholars Compass

Theses and Dissertations

Graduate School

2017

Nanomedicine Drug Delivery across Mucous Membranes

Michael G. Lancina III
Virginia Commonwealth University

Follow this and additional works at: <https://scholarscompass.vcu.edu/etd>



Part of the [Biomaterials Commons](#)

© The Author

Downloaded from

<https://scholarscompass.vcu.edu/etd/4979>

This Dissertation is brought to you for free and open access by the Graduate School at VCU Scholars Compass. It has been accepted for inclusion in Theses and Dissertations by an authorized administrator of VCU Scholars Compass. For more information, please contact libcompass@vcu.edu.

Nanomedicine Drug Delivery across Mucous Membranes

A dissertation submitted in partial fulfillment of the requirements for the degree of Doctor of
Philosophy in Biomedical Engineering at Virginia Commonwealth University

by

Michael George Lancina III,
B.S. Michigan Technological University 2013

Dr. Hu Yang, Chair
Dr. Daniel Conway
Dr. Rebecca L. Heise
Dr. Shahid Husain
Dr. Uday B. Kompella
Dr. Ning Zhang

Virginia Commonwealth University
Richmond, Virginia
June 2017

Acknowledgement

I would like to sincerely thank everyone who made this work possible. First and foremost, my academic advisor, Dr. Hu Yang. I have found his mentorship, patience, and support extraordinary. It is a leadership style I hope to emulate in my career moving forward. I would also like to thank the other members of my committee for their contributions to this work. Thank you to Dr. Shahid Husain for his close collaboration and hands-on training with the animal studies. Thank you to Dr. Uday Kompella for his expertise on ocular pharmacology and help with designing experiments. Finally, thank you to Dr. Ning Zhang, Dr. Rebecca Heise, and Dr. Daniel Conway for your guidance on the direction of the project and for taking the time to serve on my advisory committee.

I need to thank as well all of my current and former colleagues. In particular, Olga Zolotarskaya, Leyan Xu, Donald Aduba, and Juan Wang for donating their expertise and training me in experiments critical to this work. I am grateful also for all of my classmates and the faculty at Virginia Commonwealth University. Collectively you have made the last four years not just a period of personal and academic growth for me, but a fun one as well.

Lastly, my deepest gratitude is to my family. For 26 years my parents have sacrificed to provide me with the opportunity to chase my dream of becoming a scientist. For the last two, my wonderful fiancé Mary has been there to pick me up when an experiment failed or a paper was rejected. This work would truly not be possible without their unconditional love and support.

Michael Lancina III

Table of Contents

| | |
|--|-------------|
| Acknowledgements | iii |
| List of Tables | viii |
| List of Figures | ix |
| Abbreviations | xiii |
| Abstract | xv |
| Background and Significance | 1 |
| 1.1 Transmembrane Drug Delivery | 1 |
| 1.1.1 Ocular Drug Delivery: | 3 |
| 1.2 Nanoparticles | 5 |
| 1.2.1 Dendrimers: | 7 |
| 1.3 Electrospun Nanofibers | 9 |
| Dendrimer Application in Ocular Drug Delivery – A Literature Review⁵ | 11 |
| 2.1 Abstract | 11 |
| 2.2 Introduction | 11 |
| 2.3 Anatomy and Physiology of the Eye | 13 |
| 2.4 Routes of Administration | 14 |
| 2.4.1 Topical delivery: | 14 |
| 2.4.2 Systemic administration: | 14 |
| 2.4.3 Injections: | 15 |
| 2.5 Dendrimers | 15 |
| 2.5.1 Topical formulations: | 16 |
| 2.5.2 Injectable formulations: | 19 |
| 2.6 Conclusions & Future Directions | 21 |
| Chitosan Nanofibers for Oral Insulin Delivery | 23 |

| | |
|--|-----------|
| 3.1 Abstract | 23 |
| 3.2 Introduction | 23 |
| 3.3 Materials and Methods | 25 |
| 3.3.1 Materials: | 25 |
| 3.3.2 Electrospun fiber production: | 26 |
| 3.3.3 Mechanical tests: | 26 |
| 3.3.4 In vitro stability: | 26 |
| 3.3.5 In vitro insulin release: | 27 |
| 3.3.6 Insulin bioactivity: | 27 |
| 3.3.7 Trans-buccal permeation: | 28 |
| 3.4 Results | 28 |
| 3.4.1 Electrospun fiber production: | 28 |
| 3.4.2 Physiologic stability: | 29 |
| 3.4.3 In vitro insulin release: | 30 |
| 3.4.4 Insulin bioactivity: | 31 |
| 3.4.5 Buccal permeation: | 32 |
| 3.5 Discussion | 35 |
| 3.5.1 Synthesis: | 35 |
| 3.5.2 In vitro stability and insulin release: | 36 |
| 3.5.3 Bioactivity: | 37 |
| 3.5.4 Buccal permeability: | 38 |
| 3.6 Conclusion | 39 |
| Fast Dissolving Dendrimer Nanofiber (DNF) Mats as Alternative to Eye Drops for Antiglaucoma Drug Delivery | 40 |
| 4.1 Abstract | 40 |
| 4.2 Introduction | 41 |
| 4.3 Materials and Methods | 43 |
| 4.3.1 Materials: | 43 |
| 4.3.2 G3.0-mPEG synthesis: | 43 |

| | |
|---|-----------|
| 4.3.3 Electrospinning: | 44 |
| 4.3.4 Fiber characterization: | 44 |
| 4.3.5 In vitro drug release: | 45 |
| 4.3.6 Cornea permeability: | 45 |
| 4.3.7 In vitro cytocompatibility: | 45 |
| 4.3.8 IOP measurement: | 46 |
| 4.3.9 In vivo single dose response: | 46 |
| 4.3.10 Chronic use safety and efficacy: | 46 |
| 4.3.11 Ocular disposition: | 46 |
| 4.3.12 Statistical analysis: | 47 |
| 4.4 Results and Discussion | 47 |
| 4.4.1 Synthesis and fabrication: | 47 |
| 4.4.2 In vitro assessment: | 49 |
| 4.4.3 In vivo efficacy and safety: | 53 |
| 4.5 Conclusion | 59 |
| PAMAM Dendrimers for Improved Timolol Delivery | 60 |
| 5.1 Abstract | 60 |
| 5.2 Introduction | 60 |
| 5.3 Methods and Materials | 62 |
| 5.3.1 Synthesis: | 62 |
| 5.3.2 NMR spectra: | 63 |
| 5.3.3 HPLC analysis: | 63 |
| 5.3.4 Ex vivo permeability: | 63 |
| 5.3.5 In vitro cytotoxicity: | 64 |
| 5.3.6 In vivo efficacy: | 64 |
| 5.4 Results and Discussion | 65 |
| 5.4.1 Synthesis & characterization: | 65 |
| 5.4.2 In vitro assessment: | 67 |
| 5.4.3 In vivo safety and efficacy: | 68 |

| | |
|--|-----------|
| 5.5 Conclusions | 70 |
| Conclusions and Future Directions | 71 |
| 6.1 Summary | 71 |
| 6.2 Discussion | 73 |
| 6.2.1 Nanofiber patches as transmembrane drug delivery vehicles: | 73 |
| 6.2.2 Difficulties of Transmembrane Drug Delivery Models: | 74 |
| 6.3 Future Directions | 76 |
| 6.3.1 Layer-by-layer assemblies: | 76 |
| 6.3.2 Alternative ocular therapeutics: | 77 |
| 6.3.3 Targeted dendrimer vehicles as nanofiber patches: | 77 |
| References | 80 |

List of Tables

| | |
|---|-----------|
| Table 2.1: Preclinical ocular drug delivery studies utilizing dendrimer vehicles. _____ | 18 |
| Table 3.1: Electrospinning solutions content and final INS content. _____ | 26 |
| Table 3.2: CS:PEO fiber mechanical properties. _____ | 29 |
| Table 3.3: The insulin permeability coefficient and R^2 of the cumulative flux curve for CS:PEO fiber blends and naked insulin. _____ | 35 |
| Table 4.1: Permeability coefficient of rabbit corneas to brimonidine. _____ | 53 |

List of Figures

- Figure 1.1:** Typical mucosa structure. This schematic depicts the buccal mucosa, which lines the oral cavity, but in general all mucous membranes contain a mucous covered epithelium anchored to a basal lamina. For drugs to reach systemic circulation, they must penetrate to the vascularized lamina propia. Adapted from Harris et al.¹ _____ **2**
- Figure 1.2:** Barriers to ocular drug delivery. The structure of the corneal epithelium is unique. The aqueous layer above the mucin layer is relatively thick, and turnover is rapid. The cornea itself is a covered by a narrow but tightly bound epithelial cell layer. Adapted from Janagam et al.² ____ **5**
- Figure 1.3:** Drug nanocarriers. There are several different classes of polymer based nanocarriers. Drugs can be covalently or ionically coupled, or encapsulated in the core of the particle. Typical size ranges for these carriers vary widely. Adapted from Kamaledin et al.³ _____ **6**
- Figure 1.4:** Dendrimers as Flexible Delivery Vehicles. The organized branching structure of dendrimers makes many surface groups available for functionalization. The allows dendrimers to serve as drug delivery vehicles combining direct cell targeting, imaging probes, and gene delivery into a single compact vehicle. _____ **8**
- Figure 1.5:** Large scale electrospinning. The Nanospider system uses a needless spinneret to rapidly generate large quantities of nanofibers. Adapted from Niu.⁴ _____ **10**
- Figure 2.1: Dendrimer routes of ocular administration. Dendrimer based vehicles have shown pre-clinical efficacy in delivering ocular drugs through multiple routes of administration. These include 1) topical application, 2) injection into the vitreous humor, and 3) injection into the tissues around the eye. The eye structure was adapted with permission from the copyright holder of this work from <https://en.wikipedia.org/wiki/Eye>, retrieved March 1, 2017. _____ **13**
- Figure 2.2:** Dendrimer synthesis and structure. PAMAM generations 0.0-3.0, with half generations omitted. Particle size grows linearly with each full generation, but molecular weight and the number of surface groups increase exponentially. _____ **16**
- Figure 2.3:** Dendrimer gelation strategies. Dendrimers can be modified with diverse array of reactive groups to form hydrogels. Drug release from these materials can be further controlled by dendrimer type and generation, spacer length, and the mechanism of drug loading. _____ **19**

Figure 3.1: At least 20% high molecular weight polymer is necessary for stable fiber formation. Poly (ethylene oxide) (Mw 900kDa) was added to dissolved chitosan electrospinning solution in decreasing ratios. At 20% PEO solution content intermittent beading can be observed. Scale bar 10 μ m. _____ **29**

Figure 3.2: CS:PEO fibers dissolve slowly under physiologic conditions. 10mg samples of CS:PEO fiber blends (n=3) were immersed in 5ml of PBS at 37⁰C. At predetermined time points PBS was removed. Samples were then washed once with diH₂O and freeze dried overnight. Mass loss approximated PEO content (A). SEM micrographs showed no major morphological changes in fibers over the degradation period (B, scale bar represents 50 μ m). The average fiber diameter measured in these micrographs also showed no significant changes within individual fiber blends after hydration (C). (* denotes statistically significant difference between all groups p < 0.05) **31**

Figure 3.3: Polysaccharide content controls insulin release kinetics. Fiber blends of different chitosan:PEO ratios were immersed in PBS at 37⁰C. Insulin release was quantified at 15 minutes, 6 hours, and 1 day by ELISA assay. Various models were applied to fit the data. Curves corresponding to the Ritger-Peppas equation are shown. CS:PEO20 fibers show the fastest release profile, but there was no difference observed between blends at 24 hours. _____ **32**

Figure 3.4: Insulin remains bioactive after electrospun fiber fabrication. 3T3-L1 preadipocytes incubated for 10 minutes in either fresh growth medium (control), 6 hour CS:PEO20 fiber release medium, or insulin containing media (7.98 μ g/mL). Western blots of cell lysates were run for p-Akt expression then stripped and re-probed for total Akt1 as loading controls. Cells exposed to fiber release medium showed 3.5 fold higher p-Akt/Akt expression ratio than control cells. (* denotes statistically significant difference from all other groups p < 0.05) _____ **33**

Figure 3.5: Chitosan enhances buccal permeability. Insulin transport across the buccal membrane was determined using a Franz diffusion cell. Measurements of the insulin concentration of the acceptor chamber showed that membranes were largely impermeable to both dissolved insulin and the lower chitosan blend ratios, with those groups delivering less than 1% of their total protein over 6 hours. CS:PEO20 fibers however showed significantly higher insulin delivery over the other groups at all time points over 2 hours. The permeability coefficient of the buccal mucosa to each of these insulin compounds was calculated from the steady state flux region of the tests and

CS:PEO20 fibers showed around a 500 fold increase in permeability over the other fiber blends and a 16 fold increase over naked insulin. _____ 34

Figure 4.1: Graphic abstract. _____ 41

Scheme 4.1: Synthesis and fabrication of DNF and BT/DNF mats. Following the synthesis of PEGylated PAMAM dendrimer G3.0 (i.e., G3.0-mPEG), G3.0-mPEG is dissolved in HFP with high molecular weight PEO in the absence or presence of the antiglaucoma drug BT and electrospun into DNF or BT/DNF mats. _____ 44

Figure 4.2: ¹H NMR spectrum of G3.0-mPEG. Degree of PEGylation was determined by integrating proton peak j (mPEG) and comparing with integration of proton peaks a-f, h, and i (G3.0). The analysis determined around 40% of G3.0 surface groups were PEGylated. _____ 48

Figure 4.3: DNF characterization. (A) High magnification electron micrographs of DNF and BT/DNF. (B) Histograms of fiber measurements show BT caused an overall decrease in fiber diameter. (C) Uniaxial tensile testing shows BT/DNF has higher elastic modulus, peak stress, and strain at break than DNF. _____ 50

Figure 4.4: DNF cytotoxicity. NIH 3T3 fibroblasts were incubated with varying concentrations of DNF for 24 h and cell viability measured via WST-1 assay. Degassing fibers under vacuum (vacuum degassing) was shown to be more efficient in removing residual electrospinning solvent and increasing DNF cytocompatibility than degassing fibers at atmospheric pressure (ATM degassing). _____ 51

Figure 4.5: In vitro brimonidine release. BT delivery vehicles were dissolved and drug diffusion across a 3.5 kDa dialysis membrane was measured for 90 min. Unmodified dendrimers and DNF slowed initial drug diffusion in STF. DNF further slowed the rate of drug release for the entire duration of the test. _____ 52

Figure 4.6: In vivo single dose response. Brown Norway rats (n=4) received a single dose of BT via saline eye drops or DNF topically. One dose of BT/DNF and one dose BT saline eye drops are equivalently effective in reducing IOP response (* indicates significantly different, P<0.01). _ 53

Figure 4.7: In vivo 3-week daily dose response. Brown Norway rats (n=4) received a daily dose of brimonidine via saline eye drops or DNF for three weeks. IOP was recorded immediately prior to drug application. Values expressed are the difference between the experimental and contralateral

eyes after normalizing individual eyes to baseline levels. The dash lines represent the mean IOP reduction values. DNF was able to sustain reduced IOP over the test period compared to saline eye drops (# indicates significantly different, $P < 0.001$). _____ 55

Figure 4.8: Ocular histopathology of chronic DNF application. Brown Norway rats ($n=3$) received a single dose of BT via saline eye drops or DNF every 24 h for 21 days. No changes in cornea morphology could be observed between the experimental groups. Other ocular structures such as the ciliary body and retina showed the same result. _____ 56

Figure 4.9: Ocular disposition of DNF. Brown Norway rats ($n=3$) received a DNF-FITC mat topically in the right eye (experimental eye) while the left eye received no treatment (contralateral eye). Animals were euthanized at 2 or 24 h and the ocular tissues harvested and immediately processed for cryosectioning. Fluorescent imaging of sections from various ocular organs showed most dendrimers were flushed from the cornea in 24 h. Over the same time period, FITC-G3.0-mPEG accumulated in the ciliary body of the experimental eye. _____ 57

Scheme 5.1: DenTimol synthesis. (Clockwise from top right) OTM was coupled to amine-PEG-carboxyl by spontaneous ring opening reaction. OTM-PEG was coupled to G3.0 dendrimer by EDC/NHS mediated crosslinking reaction. _____ 63

Figure 5.1: HPLC of reaction products. Purified DenTimol product shows no elution peak at 3min, indicating no free prodrug present. _____ 65

Figure 5.2: DenTimol NMR spectra. OTM proton peaks at 3.79 and 3.49 ppm (h & i) were still present on the final nanoparticle NMR spectra, but were obscured by overlapping dendrimer signals. Integration of PEG peak f and dendrimer peaks a-d was used to estimate drug loading quantity. _____ 66

Figure 5.3: Corneal permeability. Permeation rates (by percentage) were equivalent for DenTimol and OTM. PEG-OTM intermediate was not able to penetrate ex vivo corneas. _____ 67

Figure 5.4: Cytotoxicity. DenTimol conjugate shows no increased toxicity over OTM prodrug at the same effective drug concentrations. Red line indicates estimated maximum therapeutic concentration. _____ 68

Figure 5.5: Single dose IOP response. DenTimol induced a significant drop in IOP at 8 hours, indicating similar bioactivity to timolol ($n=4$). _____ 70

Abbreviations

| | |
|-----------|---|
| PAMAM | Poly(amidoamine) dendrimer |
| IOP | Intra-ocular pressure |
| GI | Gastro-intestinal |
| PEG | Poly(ethylene glycol) |
| G0.0-G5.0 | Generation 0.0-generation 5.0 PAMAM dendrimer |
| DEX | Dexamethasone |
| FDA | Federal Drug Administration |
| PEO | Poly(ethylene oxide) |
| CS | Chitosan |
| INS | Insulin |
| HFP | Hexafluoroisopropanol |
| SEM | Scanning electron microscope |
| ELISA | Enzyme-linked immunosorbant assay |
| PVDF | Poly(vinylidene difluoride) |
| TBS | Tris buffered saline |
| PBS | Phosphate buffered saline |
| SSF | Simulated saliva fluid |
| DNF | Dendrimer nanofiber |

| | |
|-------|---|
| BT | Brimonidine tartrate |
| STF | Simulated tear fluid |
| HPLC | High performance liquid chromatography |
| NMR | Nuclear magnetic resonance |
| WST-1 | Water soluble tetrazolium salt |
| IACUC | Institutional animal care and use committee |
| ANOVA | Analysis of variance |
| ATM | Atmospheric pressure |
| mPEG | Methoxy-poly(ethylene glycol) |
| FITC | Fluorescein isothiocyanate |
| OTM | (S)-4-[4-(Oxiranylmethoxy)-1,2,5-thiadiazol-3-yl]morpholine |
| DCM | Dichloromethane |
| EDC | N-(3-Dimethylaminopropyl)-N'-ethylcarbodiimide |
| NHS | N-Hydroxysuccinimide |

Abstract

NANOMEDECINE DRUG DELIVERY ACROSS MUCOUS MEMBRANES

By Michael G. Lancina III

A dissertation submitted in partial fulfillment of the requirements for the degree of Doctor of Philosophy at Virginia Commonwealth University.

Virginia Commonwealth University, 2017.

Major Director: Dr. Hu Yang, Associate Professor, Chemical and Life Science Engineering

Control over the distribution of therapeutic compounds is a complex and somewhat overlooked field of pharmaceutical research. When swallowing a pill or receiving an injection, it is commonly assumed that drug will spread throughout the body in a more or less uniform concentration and find its way to wherever it is needed. In truth, drug biodistribution is highly non-uniform and dependent on a large number of factors. The development of advanced drug delivery systems to control biodistribution can produce significant advances in clinical treatments without the need to discover new therapeutic compounds. This work focuses on a number of nanostructured materials designed to improve drug delivery by direct and efficient transfer of drugs across one of the body's external mucous membranes.

Chapter 1 outlines the central concept that unites these studies: nanomaterials and cationic particles can be used to delivery therapeutic compounds across mucous membranes. Special attention is given to dendritic nanoparticles. In chapter 2, uses for dendrimers in ocular drug delivery are presented. The studies are divided into two main groups: topical and injectable formulations.

Chapter 3 does not involve dendrimers but instead another cationic particle used in transmembrane drug delivery, chitosan. Next, a dendrimer based nanofiber mat was used to deliver anti-glaucoma drugs in chapter 4. A three week in vivo efficacy trial showed dendrimer nanofiber mats outperformed traditional eye drops in terms of intra-ocular pressure decrease in a normotensive rat model. Finally, we have developed a new dendrimer based anti-glaucoma drug in chapter 5. Collectively, these studies demonstrate some of the potential applications for nanotechnology to improve transmembrane drug delivery. These particles and fibers are able to readily adhere and penetrate across epithelial cell layers. Utilizing these materials to improve drug absorption through these portals has the potential to improve the clinical treatment of wide variety of diseases.

Chapter 1

Background and Significance

1.1 Transmembrane Drug Delivery

Direct drug delivery across one of the body's mucous membranes is a very attractive route of administration for several reasons. Passing therapeutics directly through these barriers can improve both tissue specificity and access depending on the application, and it is considered less invasive than injections.⁷ Mucous membranes are found at the external surfaces of the eyes, mouth, reproductive organs, respiratory system, and gastrointestinal tract. The specific properties of these membranes vary considerably, but they share the same basic structure. (**Figure 1.1**) All of these membranes are characterized by an epithelial cell layer coated in a viscous, constantly regenerating fluid known as mucus. The mucus serves as a lubricant, but it also is a critical selective barrier against external pathogens and particulates.⁸ Since the underlying cell layer is designed for selective solute transport, it has a much higher permeability than dermal epithelia, but this is highly dependent on the compound being absorbed.⁹ This is because there are multiple processes by which drugs can cross the epithelial cell layer including transcellular and paracellular routes. Transcellular permeation, either by active transport or simple diffusion is rapid but highly selective, so it is not feasible for most compounds. Paracellular permeation through the gaps in epithelial cells is slower, unless the membrane is modified in some way to loosen these junctions.¹⁰ Inflammation naturally disrupts cell junctions, making it one way to direct site-specific absorption of drugs or drug vehicles.¹¹ Certain compounds such as detergents or chitosan are also known to temporarily disrupt cell-cell gap junctions and increase the permeability of the membrane.¹²

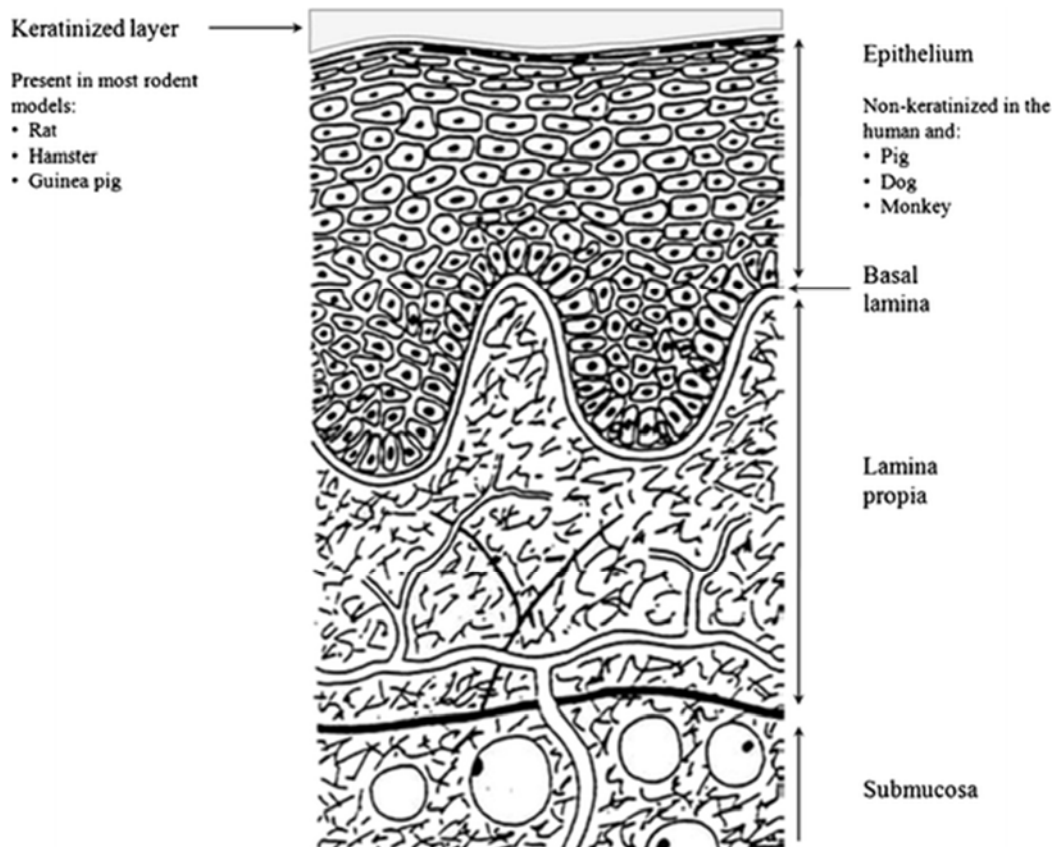


Figure 1.1: Typical mucosa structure. This schematic depicts the buccal mucosa, which lines the oral cavity, but in general all mucous membranes contain a mucous covered epithelium anchored to a basal lamina. For drugs to reach systemic circulation, they must penetrate to the vascularized lamina propia. Adapted from Harris et al.¹

Direct membrane absorption also avoids processes that can degrade or remove certain drugs, the low pH of the upper GI tract and first pass filtration through the portal system, respectively. This makes it an ideal delivery system for unstable therapeutics such as peptide drugs and genes. Non-invasive delivery of bioactive insulin has long been a target of transmembrane drug delivery, with oral and pulmonary systems showing the most promise.^{13,14} In some cases, transmembrane drug delivery can also dramatically improve target specificity. Blood perfusion is highly non-uniform, so simple systemic drug delivery results in an equally non-uniform drug distribution. For organs

such as the eye, this produces low concentrations at the desired site while concentrations in high perfusion organs such as the liver can reach dangerous levels.¹⁵

There are downsides to transmembrane drug delivery as well. The structure of both the mucous and epithelial layers are highly complex and much about their physiology remains understudied.¹⁶ Drug absorption rates can vary widely depending on individual differences and diseases states. The immune function of mucous membranes is a relatively new field of study, and there is concern that use of permeation enhancers can expose patients to risk of pathogen invasion.¹⁷ Even with these problems, cutting edge modeling and experimental studies are revolutionizing our understanding of drug kinetics at the mucosal interface.¹⁸ As these techniques become more sophisticated, the potential for transmembrane drug delivery will increase as well.

1.1.1 Ocular Drug Delivery: Transcorneal drug delivery is a unique case deserving of special consideration for a few reasons. Most importantly, it is perhaps the organ where advanced transmembrane drug delivery systems have the most potential for clinical impact.^{19,20} Existing strategies for ocular drug delivery are particularly deficient in terms of both efficiency, reliability, and safety. As mentioned above, the eye receives low blood perfusion overall in terms of volume, but in addition it is isolated by an extra selective membrane similar to the blood brain barrier. The delicate nature of the organ also makes injections problematic.²¹ All of these procedures must be performed by health care professionals, and still there can be serious complications. The pool of ocular disease patients is also massive. Glaucoma alone threatens the sight of over 60 million people worldwide, most of which administer highly inefficient eye drops several times per day.²²

Simple saline eye drops are largely ineffective because of the structure of the corneal epithelium and ocular mucosa. **(Figure 1.2)** The cornea is covered in a simple epithelium (there is only one cell type, unlike the stratified epithelium of the gut) where the cells are completely surrounded by

tight junctions.²³ In contrast with other mucous membranes, the ocular epithelium is very delicate. Corneal wounds heal slowly, so any permeation enhancers used must meet a higher standard of cytocompatibility than in other tissues.²⁴ Ocular mucous serves a similar function as other mucous layers, but it contains additional mucins to more aggressively clear particulates and pathogens which constantly barrage the eye surface.²⁵ This is the reason for the relatively rapid turnover of tear fluid. These two physiologic phenomenon combine to greatly limit drug permeation for almost all topically applied ocular drugs, but novel vehicle strategies are working to overcome this.

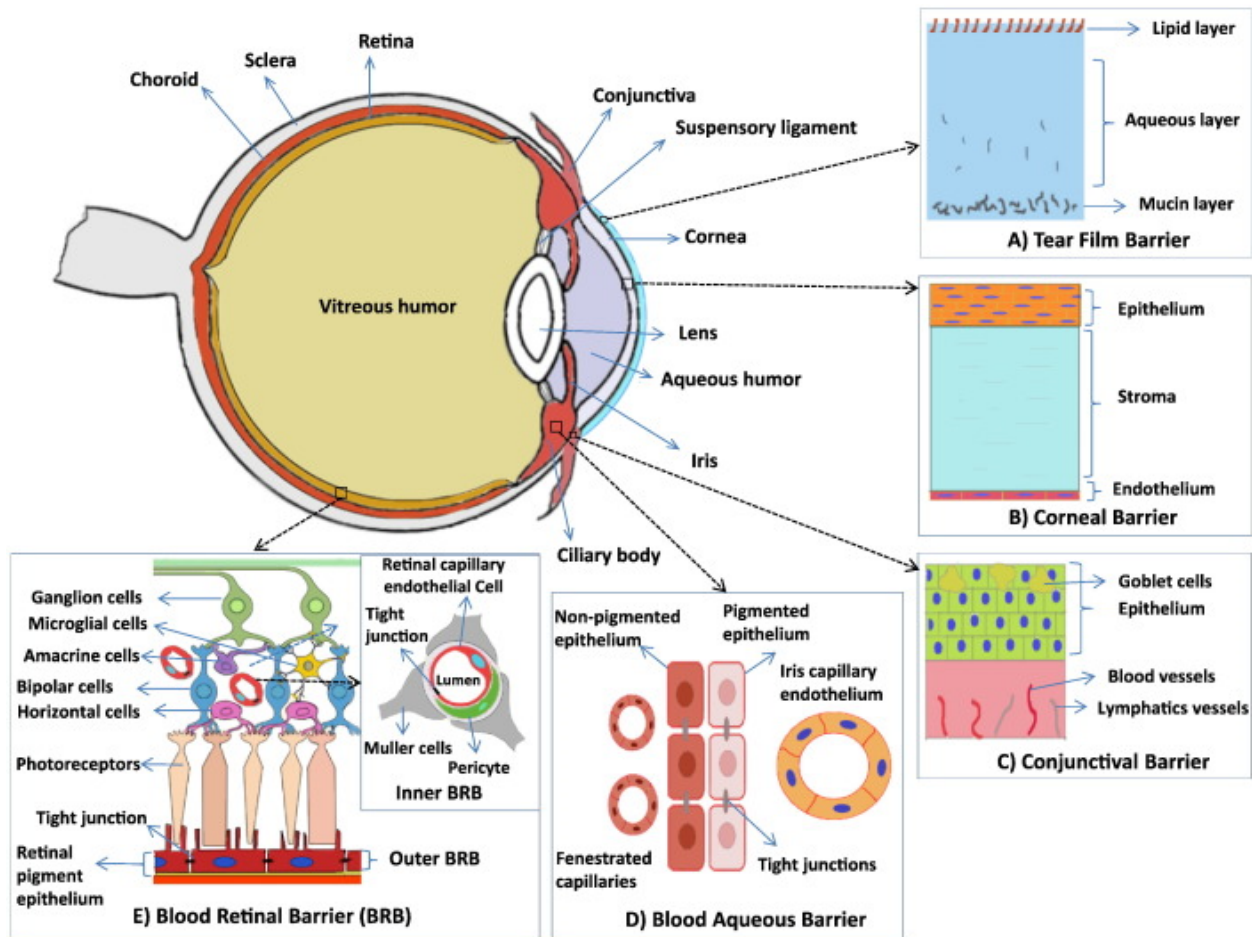


Figure 1.2: Barriers to ocular drug delivery. The structure of the corneal epithelium is unique.

The aqueous layer above the mucin layer is relatively thick, and turnover is rapid. The cornea itself is covered by a narrow but tightly bound epithelial cell layer. Adapted from Janagam et al.²

1.2 Nanoparticles

Nanoparticles have been a fundamental aspect of pharmaceutical engineering since medicine has existed, but only with the development of technologies to image and characterize sub-micron particles has their development become a deliberate science.²⁶ Much of this work is focused on using nanoparticles as drug delivery vehicles. Several classes of these nanocarriers exist including solid nanoparticles, liposomes, micelles, linear polymers, and dendrimers. (**Figure 1.3**) All of these nanocarriers can be designed to solubilize drugs at higher concentrations, control drug

distribution, and co-deliver imaging agents, depending on particle properties such as size, charge, and surface functionalization.²⁷

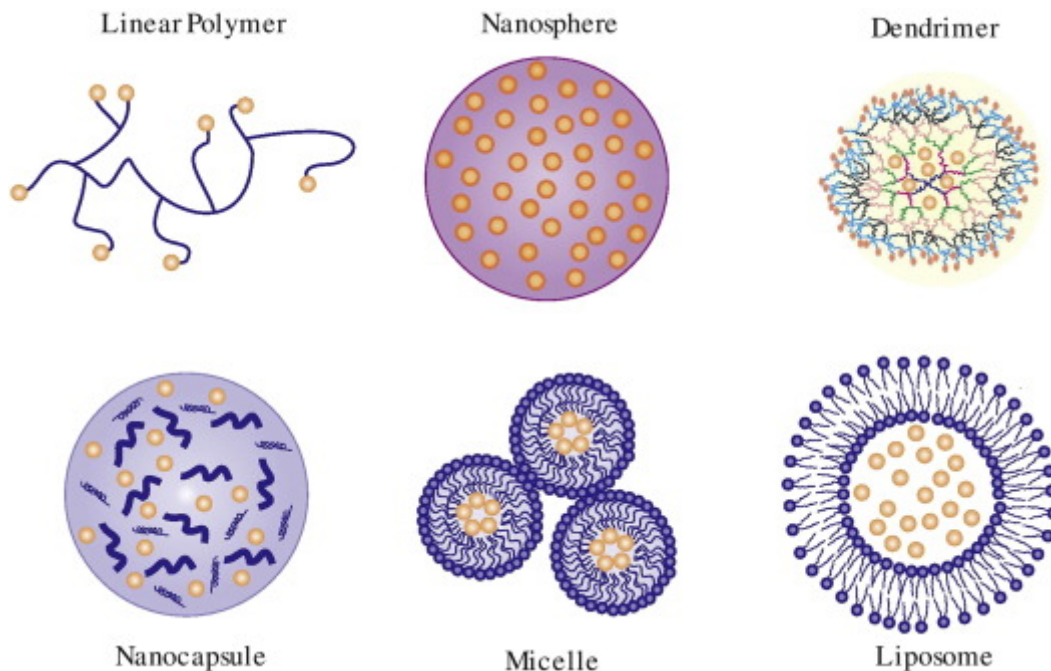


Figure 1.3: Drug nanocarriers. There are several different classes of polymer based nanocarriers. Drugs can be covalently or ionically coupled, or encapsulated in the core of the particle. Typical size ranges for these carriers vary widely. Adapted from Kamaledin et al.³

Particle size and charge have the largest influence over carrier distribution. In terms of size nanocarriers can be divided into three basic categories, small particles less than 100nm, medium particles between 100 and 200nm, and large particles over 200nm. In general small particles are able to diffuse away from their site of application faster.²⁸ 100nm is used as a critical cutoff because carriers under this size can pass through the capillary endothelium, meaning they can enter and exit circulation and possibly be used for targeted delivery vehicles. Medium sized particles are not able to readily cross normal endothelium, but can pass through the larger pores that open up during inflammation. This means they can be used as passively targeted vehicles, as they will only exit circulation in areas of active inflammation or tumor growth. Large particles over 200 nm are

recognized by the immune system and aggressively removed by phagocytotic cells, so they have a short circulation time.²⁹ Still they can be useful in some applications depending on the target.

Surface charge is also a critical parameter to consider when trying to design nanocarriers. Changing the net charge of a particle while holding other properties constant will have a dramatic effect on how the carrier interacts with biologic membranes and extracellular matrix proteins. Cell membranes carry a net negative charge, so positively charged nanoparticles will more readily penetrate into cells and across selective membranes.³⁰ However, these strongly charged particles also tend to be toxic, and can be subject to renal clearance. Passivating polymers like poly(ethylene) glycol (PEG) neutralize the charge and increase the circulation time and biocompatibility of these particles so they can be used safely *in vivo*.³¹ Anionic particles avoid strong interaction with most extracellular components, but the presence of the negative charge enables them to form complexes with cationic drugs or other compounds.

Surface functionalization with direct cell binding ligands is a way to produce even more targeted nanocarrier distributions. There is an incredibly variety in the types of cell binding groups now used for these approaches. They can be highly specific targets such as monoclonal antibodies, selectively metabolized compounds such as folate, or entirely synthetic systems like aptamers. Clinical use of these vehicles is complicated by factors such as target specificity, carrier stability, and the immune system, but these vehicles have the potential to revolutionize the delivery of things like chemotherapeutics or siRNA in the near future.

1.2.1 Dendrimers: Dendrimers are a unique class of polymeric nanoparticles characterized by a highly organized branching structure. Synthesis of dendrimers involves sequential attachment of alternating branching units, resulting in a linear increase in the size of the particles but an exponential increase in their molecular weight and surface groups. (**Figure 1.4**) In contrast with

linear polymers this synthesis results in a much more dense structure, with a very high number of available terminal groups relative to the particle size. This makes dendrimers extremely flexible nanocarriers, able to simultaneously delivery drugs, imaging agents, targeting moieties, and even nucleic acids through both covalent attachments and ionic complexing. They also deliver these therapeutics at comparatively high payloads while maintaining a small enough size to utilize multiple cell entry or bypass pathways depending on the surface modifications or generations used.

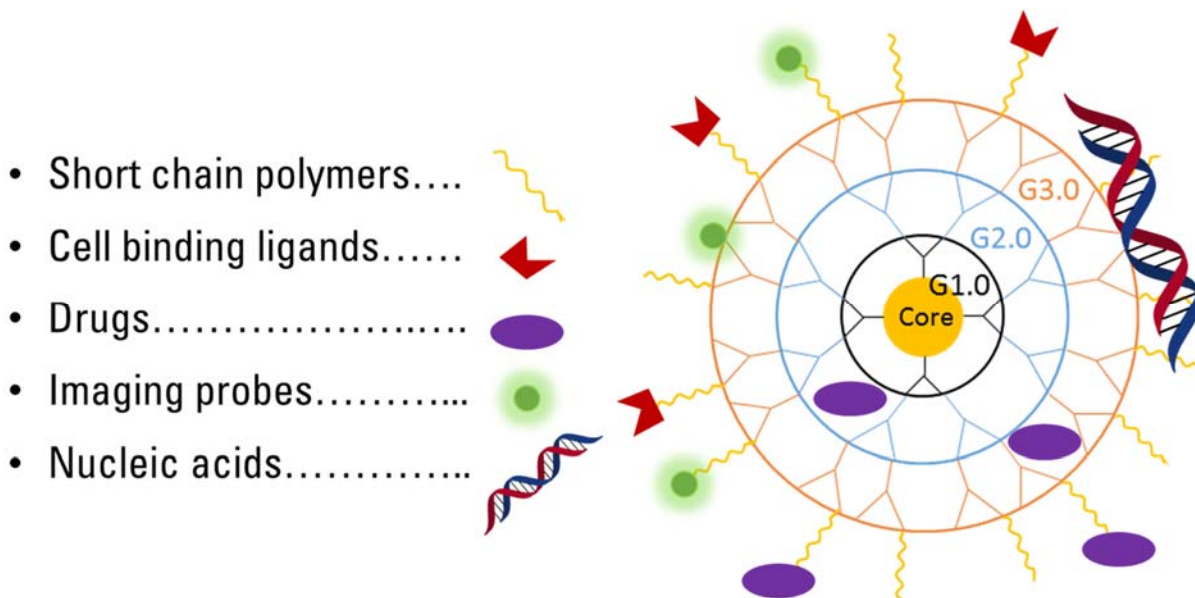


Figure 1.4: Dendrimers as Flexible Delivery Vehicles. The organized branching structure of dendrimers makes many surface groups available for functionalization. The allows dendrimers to serve as drug delivery vehicles combining direct cell targeting, imaging probes, and gene delivery into a single compact vehicle.

There is a large and growing number of dendritic polymers, but poly(amidoamine) (PAMAM) dendrimers are the most well studied and commercialized family. For successful trans-membrane delivery, the most beneficial properties of these materials are their variable surface charge and dense structure. The small size and cationic character of full generation (amine terminated)

PAMAM dendrimers allow them to bind to extracellular mucins and penetrate through the epithelial cell layer through both transcellular and paracellular routes.

1.3 Electrospun Nanofibers

Electrospinning is simple and versatile technique for fabricating sub-micron fibers. The process is analogous to mechanical fiber pulling techniques, but a DC electric field is used pull polymers in solution towards a grounded collecting surface. If conditions are right, the polymer solution is drawn into a narrow but continuous stream. The solvent dries as the stream travels through the air and a dry fiber of entangled polymer molecules is deposited. Changing electrospinning parameters such as the strength of the electric field, air gap distance, and solution concentration can be used to modulate properties of the fibers such as size, density and alignment. The same process can also be used to fabricate electrosprayed nanoparticles if chain entanglements do not occur.

These nanofiber mats have been investigated extensively as tissue engineering scaffolds, but they can also be utilized as drug delivery vehicles when therapeutic agents are incorporated into the electrospinning solution. The primary advantage of nanofibers as drug delivery vehicles is their high surface area to volume ratio. Nanofibers dissolve or release dissolved drugs faster than simple solution cast films of the same materials. For certain applications where immediate dissolution is desirable, electrospun nanofibers can be an improvement over existing formulations. Another aspect of nanocarrier drug delivery sometimes overlooked is storage stability. Many targeted nanocarrier vehicles are not stable for long periods of time at physiologic pH and room temperature. This can result in major changes in drug potency if the carrier must be delivered in solution. Reliable storage of these vehicles is critical for clinical use, particularly when bioactive groups are integrated. Nanofiber formulations offer the superior long term stability of other dry dosage forms such as powders, but they are easier to handle and measure.

Research into electrospun nanofibers as drug delivery vehicles is fairly new, but has steadily progressed over the last decade to include a broad range of therapeutic agents and applications. Over the same period, parallel experimental and theoretical studies have revolutionized our knowledge of the electrospinning process, and how to control parameters to produce desired fiber morphologies. Considerable hardware advancements have occurred as well, in terms of both complexity and efficiency of the machines. Coaxial needles can produce core-shell fibers with different polymers, possibly for tailored drug release rates. Rapid electrospinning machines with multiple spinnerets or even spinneret less systems produce large volumes of nanofibers in less time, opening the door for commercial scale up. **(Figure 1.5)** Taken together, these studies suggest electrospun nanofibers may see clinical application in the near future.

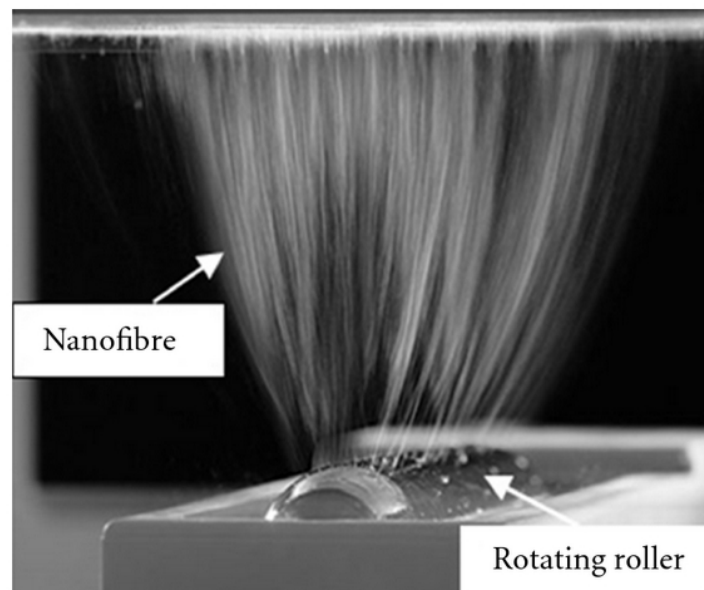


Figure 1.5: Large scale electrospinning. The Nanospider system uses a needleless spinneret to rapidly generate large quantities of nanofibers. Adapted from Niu.⁴

Chapter 2

Dendrimer Application in Ocular Drug Delivery – A Literature Review⁵

2.1 Abstract

Existing methods of administering ocular drugs are limited in either their safety or efficiency. Nanomedicine therapies have the potential to address this deficiency by creating vehicles that can control drug biodistribution. Dendrimers are synthetic polymeric nanoparticles with a unique highly organized branching structure. In recent years, promising results using dendrimer vehicles to deliver ocular drugs through different routes of administration have been reported. In this review, we briefly summarize these results with emphasis on the dendrimer modifications used to target different ocular structures.

Keywords: dendrimer; ocular drug delivery; nanomedicine

2.2 Introduction

Delivery of therapeutic compounds to the eye remains one of the largest unmet needs in advanced drug delivery research. The massive market for ocular drugs, and the deficiencies of current delivery methods create a tremendous opportunity for developing novel materials to improve patient outcomes and reduce costs.^{20,22,32} Existing treatments are generally inadequate because both the structure and the function of the eye create significant hurdles to delivering therapeutic compounds safely and efficiently. Delivery through systemic circulation would be the simplest method for patients to self-administer, but drug transport to most ocular structures is very low or isolated by specialized selective barriers.¹⁵ Topical delivery is straightforward and safe, but the combined effects of low corneal permeability and washout by tear fluid make this route highly inefficient as well.³³ More invasive approaches such as direct intravitreal or periocular injections are efficient, but unattractive from a safety and cost perspective. Finally, poor solubility and

systemic side effects are problems with many ocular drugs independent of route of administration.³⁴

Despite the clear need for improved vehicles, an ideal solution has yet to be developed. Nanoparticle-based drug delivery systems have been theorized and investigated for decades, but only recent years have seen rapid growth in the application of these systems.^{35,36} Nanoparticles fabricated from a wide range of materials including polymers (natural and synthetic), liposomes, and polysaccharides have shown enhanced delivery of ocular therapeutics.^{19,26,37,38} Alternative strategies such as in-situ polymerizing hydrogels and erodible inserts have been developed.³⁹⁻⁴² The biodistribution of these nanomaterials in ocular tissues allows them to serve as vehicles that compared to simple drug solutions: 1) increase quantity of drug that reaches the target organ, 2) increase the length of time the drug remains at the target organ, 3) reduce the quantity of drug in off-target tissues.⁴³

One class of polymers that has shown particular promise in ocular applications are dendrimers.^{44,45} These uniquely structured polymeric nanoparticles provide versatile platforms capable of delivering the complete array of ocular therapeutics³⁰. Dendrimer science is still in its infancy, with the first synthetic molecules being synthesized in the mid 1980s⁴⁶. Still, by this point some level of study has been conducted using dendrimers with all available routes of ocular administration (**Fig 2.1**). This review briefly discusses the key considerations when designing dendrimers for ocular drug delivery as well as recent developments in the field. It also briefly outlines possible future directions for dendrimer-based materials and the possible regulatory hurdles that need to overcome.

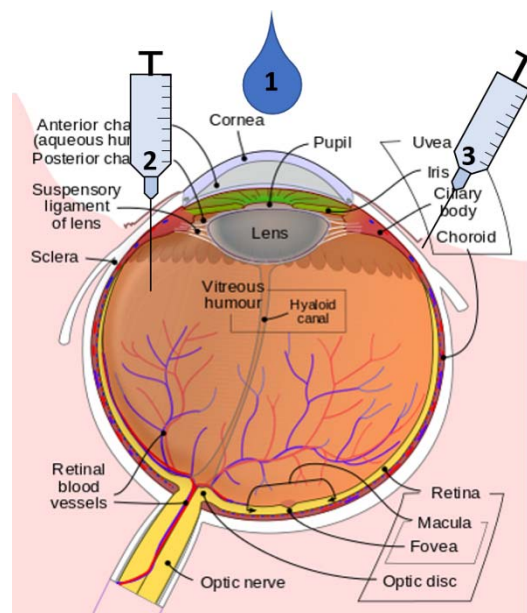


Figure 2.1: Dendrimer routes of ocular administration. Dendrimer based vehicles have shown pre-clinical efficacy in delivering ocular drugs through multiple routes of administration. These include 1) topical application, 2) injection into the vitreous humor, and 3) injection into the tissues around the eye. The eye structure was adapted with permission from the copyright holder of this work from <https://en.wikipedia.org/wiki/Eye>, retrieved March 1, 2017.

2.3 Anatomy and Physiology of the Eye

Both the underlying structure and ongoing physiologic processes in the eye create major barriers to ocular drug delivery.⁴⁷ The eye is divided into two major chambers—the anterior and posterior segments. The anterior segment of the eye contains everything between the lens and the cornea and is filled with a continuously circulating aqueous fluid. The posterior segment of the eye is the portion between the lens and the choroid and it is filled with a more gelatinous fluid called the vitreous humor. Anterior segment diseases such as corneal wounds, glaucoma, and conjunctivitis are generally targeted with topical eye drops.⁴⁸ Posterior segment diseases such as macular degeneration and retinopathy cannot currently be treated with topical vehicles and require more invasive techniques such as direct injections or surgical interventions.^{49,50}

2.4 Routes of Administration

2.4.1 Topical delivery: Topical delivery of ocular drugs, virtually always in the form of saline eye drops applied directly to the cornea, has the advantage of being the simplest route of administration. For drugs directed at anterior segment diseases, such as intra-ocular pressure lowering agents, these drops are a safe and cost-effective treatment option. However, these therapies suffer from notoriously poor patient compliance due ultimately to the poor delivery efficiency of eye drops.⁵¹⁻⁵³ Even under ideal conditions, only around 5% of the drug placed on the eye reaches the anterior chamber.⁵⁴ Permeation through the tightly packed epithelium of the cornea and sclera is slow for anything but the smallest, most lipophilic compounds.²³ At the same time, tear turnover is relatively rapid, with virtually all of the eye drop drained from the ocular surface within 15 minutes after instillation.⁴⁸ To counter poor delivery efficiency, eye drops must either utilize higher drug concentrations or a more frequent dosing schedule. Both are burdensome on patients in the form of even greater quantities of the drug in off-target tissues, often resulting in side effects. Successful topical ocular drug delivery vehicles must then either increase the permeation rate of their material across the cornea or prolong the residence time of the drug on the ocular surface.^{40,55,56}

2.4.2 Systemic administration: Systemic administration is not commonly used with ocular drug therapies. Although it would solve some of the patient compliance problems of topical delivery while remaining simple and inexpensive, efficiencies are even lower. In the anterior segment, blood perfusion rate is incredibly low, even relative to the size of the tissue. The posterior segment does have significant vascularization, but almost all of it is concentrated in the choroid and separated from direct access to the retina by the blood-retina-barrier.⁵⁷ While some compounds can be delivered to the eye through systemic administration, the concentrations needed to achieve

therapeutic efficacy often result in many of the same side effects observed with topical administration.

2.4.3 Injections: The only highly efficient route of administering ocular drugs currently in practice are intravitreal and periocular injections. Both of these methods deliver high doses of drug in a tightly targeted manner, but they come with significant drawbacks. Intravitreal injections are the most direct possible route to deliver drugs to the interior ocular structures, but they also carry the greatest risk of damage to the eye because the needle tip is hidden during the procedure.^{21,58} Injections into the surrounding structures such as the periocular tendons minimize most of these risks, but they are still highly invasive and expensive.⁵⁹ Critically, these methods are not viable for managing chronic diseases like glaucoma. Serious risk factors associated with an individual injection are slight, but their chance of occurring rises greatly when injections are used repeatedly and frequently. Strategies to improve ocular drug delivery injections focus mainly on building extended release mechanisms that can act as long term drug reservoirs *in situ* and minimize the necessary dosing regimen.

2.5 Dendrimers

The term ‘dendrimer’ refers to any polymer composed of repeating, regularly branching units. A large number of chemically distinct dendrimer families have been synthesized, but very few have been studied in depth. Only one, polyamidoamine (PAMAM) dendrimers have been commercialized.⁴⁶ The synthesis of PAMAM dendrimers begins with a central core molecule and ‘generations’ of branches are added in a series of sequential reactions (**Fig 2.2**). This reaction scheme produces highly monodisperse, spherical nanoparticles. With each successive generation, the radius of the particle increases linearly, while the number of terminal groups and molecular weight grow exponentially.

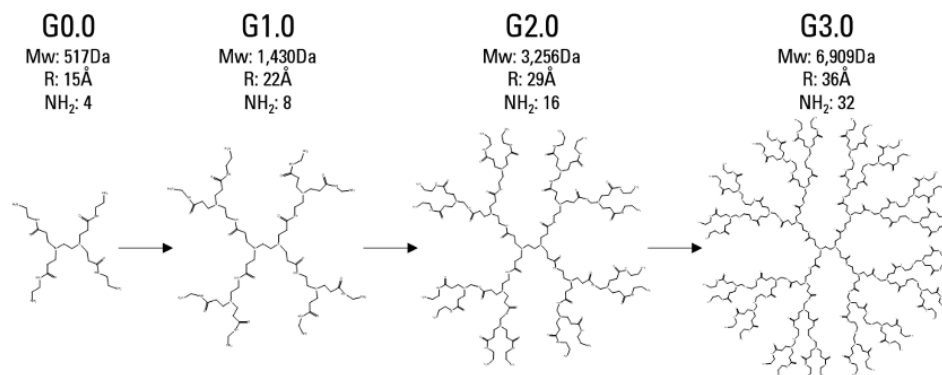


Figure 2.2: Dendrimer synthesis and structure. PAMAM generations 0.0-3.0, with half generations omitted. Particle size grows linearly with each full generation, but molecular weight and the number of surface groups increase exponentially.

This unique structure gives dendrimers a number of useful properties for drug delivery not shared by linear polymers.⁶⁰ Primarily, their well-defined core-shell architecture and narrow polydispersity make bio-distribution more predictable and easier to control through modifications to the terminal groups.⁶¹ Also, drugs and other therapeutics can be loaded onto the nanoparticle through multiple modalities, such as direct conjugation, ionic interactions, or trapping in the core of the particle.⁶² This versatility makes dendrimers highly adaptable platforms that can be designed to carry a wide range of therapeutics to a wide range of targets.⁶³ In ocular drug delivery research groups have utilized this versatility to develop dendrimer based strategies for multiple routes of administration (**Table 2.1**). While this review is focused primarily on PAMAM dendrimers because they are the closest to clinical translation, it is important to recognize the growing body of research on alternative dendrimer particles in ocular drug delivery. These include phosphorous, carbosilane, and peptide based dendritic nanoparticles.⁶⁴⁻⁶⁷ As the science matures, these novel structures may represent the future of dendrimer nanoparticle drug delivery vehicles.

2.5.1 Topical formulations: Topical application, being the most direct and simplest method of ocular drug delivery, was the first route investigated with dendrimer-based vehicles.⁶⁸ Cationic

nanoparticles have shown efficacy as permeation enhancers for transepithelial drug delivery.^{18,69,70} PAMAM dendrimers are strongly cationic on the full generations when amine terminated (G3.0, G4.0, G5.0, etc.), so logically they should increase corneal permeability when applied in aqueous solution. Vandamme et al. undertook systematic studies on the corneal residence time of PAMAM dendrimers with an *in vivo* rabbit model.⁷¹ They found residence time was highly dependent on the generation and terminal groups on the particle. In general, larger and hydroxyl terminated dendrimers showed increased corneal residence time and drug delivery efficacy in these tests. The authors hypothesized this effect was dominated by the dendrimers interaction with ocular mucins, which impede washout of the drug. *Ex vivo* corneal permeation experiments by Yao et al. several years later also found improved drug delivery efficacy with increasing dendrimer generation, but they attributed this instead to greater disruption of corneal epithelial tight junctions by the larger (and more cationic) particles.⁷² Likely, both phenomena are at work and represent important aspects of dendrimer based ocular drug delivery.⁷³⁻⁷⁵

Table 2.1: Preclinical ocular drug delivery studies utilizing dendrimer vehicles.

| Dendrimer | Drug | Reference |
|----------------------------------|---------------------------|----------------------------------|
| Topical Application | | |
| PAMAM (G1.5-4.0) | Pilocarpine & Tropicamide | Vandamme et al. ⁷¹ |
| PAMAM (G3.5-5.0) | Puerarin | Yao et al. ⁷⁶ |
| Carbosilane (G1.0-3.0) | Acetazolamide | Bravo-Osuna et al. ⁶⁵ |
| PAMAM (divalent) | Sulfonamide | Richichi et al. ⁷⁷ |
| PPI | Acetazolamide | Mishra et al. ⁷⁸ |
| PAMAM (G3.0 gel) | Timolol & Brimonidine | Holden et al. ⁷⁹ |
| Intravitreal Injection | | |
| PAMAM (G4.0-OH) | Fluocinolone Acetonide | Iezzi et al. ⁸⁰ |
| PAMAM core micelle | S1R agonist | Zhao et al. ⁸¹ |
| PAMAM (G4.0-OH) | Triamcinolone Acetonide | Kambhampati et al. ⁸² |
| Subconjunctival Injection | | |
| PAMAM (G3.5) | Carboplatin | Kang et al. ⁸³ |
| PAMAM (G3.5, 4.5) | Dexamethasone | Yavuz et al. ⁸⁴ |
| PAMAM (G4.0-OH) | Dexamethasone | Soiberman et al. ⁸⁵ |

A similar but distinct strategy for utilizing topically applied dendrimers is to incorporate them into *in situ* polymerizing gels. This approach relies on the same principle that prolonging corneal residence time can improve drug delivery efficiency, given most drops are rapidly drained from the ocular surface. Dendrimers are highly versatile gel forming agents (**Fig. 2.3**).⁸⁶ There are several potential strategies for fabricating mucoadhesive ocular hydrogels from PAMAM dendrimers alone.^{24,87,88} The properties of these materials can be easily tuned by modifying parameters such as the concentration of polymer in solution or the number of reactive groups present. This is critical to controlling the drug release kinetics and total residence time of the gel. Photocurable dendrimer-poly(lactic-co-glycolic) acid hydrogels were first developed and tested in

2012 by Holden et al.⁷⁹ During UV initiated polymerization, the loose network trapped nanoparticles containing anti-glaucoma drugs, and slowly released them over a four day period. Because the gel network was completely independent of the drug nanoparticles, this material could easily be adapted to deliver different ocular therapeutics.

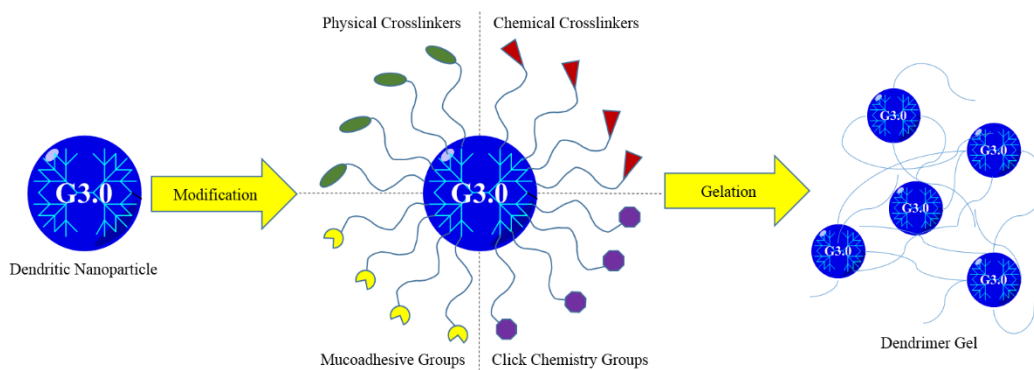


Figure 2.3: Dendrimer gelation strategies. Dendrimers can be modified with diverse array of reactive groups to form hydrogels. Drug release from these materials can be further controlled by dendrimer type and generation, spacer length, and the mechanism of drug loading.

2.5.2 Injectable formulations: Intravitreal injection has become an increasingly common method of ocular drug delivery over the last 15 years.⁸⁹ Several physiochemical properties of PAMAM dendrimers can be modified to give them a very long residence time in the vitreous cavity. Dendrimers of varying generations and drug conjugations have been studied utilizing this route by several groups.^{11,80,84} Kambhampati et al. injected G4 PAMAM dendrimers conjugated with an anti-inflammatory drug and showed the conjugates selectively migrated to cells in the retinal pigmented epithelium and activated microglial cells.⁸² These conjugates took advantage of phagocytosis by activated inflammatory cells to prolong nanoparticle residence time, but in theory other dendrimer properties could be used to develop long term vitreal drug reservoirs. *Ex vivo* modeling studies have shown diffusion through the vitreous humor for nanoparticles the size of dendrimers (<10nm) is dependent entirely on the surface charge of the particle.⁹⁰⁻⁹² Highly cationic

dendrimers should associate strongly with the anionic glycans of the vitreous humor, but the cytotoxicity of these particles needs to be reduced with a passivating polymer such as poly(ethylene glycol).⁹³

Periocular injections offer many of the same potential benefits as intravitreal injections in terms of highly efficient extended drug delivery, but with a less delicate injection site. To date studies on periocular dendrimer injections have focused on subconjunctival delivery. This delivery site protects the nanoparticles from washout by tear drainage, but still requires trans-scleral permeation.⁹⁴ Dendrimers in this application can be used to solubilize hydrophobic drugs and provide a sustained release depot adjacent to the sclera.^{85,94,95} Sustained delivery vehicles have many advantages from a patient compliance standpoint, but they can also make existing therapeutics more effective. Kang et al. used PAMAM based aggregates to deliver the chemotherapeutic carboplatin over a three-week period following a single subconjunctival injection.⁸³ The presence of the dendrimer network dramatically reduced the toxicity of the drug, allowing for the use of an increased therapeutic concentration and corresponding reduction in tumor volume.

Dexamethasone (DEX) is a particularly important ocular therapeutic with limited bioavailability.^{96,97} While this glucocorticoid has been shown to effectively reduce inflammation following eye injury, it is also rapidly cleared from both chambers.⁴¹ Recent studies by Yavuz et al. and Soiberman et al. have utilized hydroxyl terminated PAMAM dendrimers to sustain DEX delivery after subconjunctival injection.^{85,98} In the former, DEX delivery was directed toward the posterior segment. In the latter, corneal inflammation was the target. Both studies showed increased DEX delivery efficiency and longer residence time compared to simple solution

injection. These two studies highlight the potential of dendrimer based injection systems as promising strategies to treat both anterior and posterior segment diseases.

2.6 Conclusions & Future Directions

Even with a growing body of promising research, commercialization of dendrimer based drug delivery systems remains slow. Dendrimers exist in a unique space where they are much larger than traditional small molecule drugs and much smaller than traditional polymeric particles but have biological properties similar to both. This has created a number of barriers to clinical approval that industry and the regulatory agencies have yet to work out.⁹⁹ First, the long-term safety of dendrimers is a primary concern.¹⁰⁰ Dendrimers are small enough (in most formulations) that they will ultimately end up entering systemic circulation regardless of their initial route of administration.^{15,28} This makes overall safety an incredibly complicated area of study because the local biodistribution, toxicity, and complete biological activity of the vehicle must be determined in many different tissues at many different time points.¹⁰¹ Even for unmodified PAMAM dendrimers, there is a tremendous amount of work left to be completed. When you consider that a principle advantage of dendrimers is how easy they are to modify with additional groups to control biodistribution, it is not surprising that creation of novel conjugates has outpaced deep study of their systemic safety. The reliability and purity of commercial sources (or lack thereof), is another bottleneck. Scale up for production and purification of complex conjugates is going to require novel processes that are usually outside of the purview of the labs developing these technologies.¹⁰² There are also purely bureaucratic questions that remain unresolved. Chiefly, are dendrimer-drug conjugates considered novel drugs or medical devices by the FDA? It would appear that most dendrimer vehicles would classify as combination devices, but even in such cases the lead center of the FDA is not clear. It seems these questions may continue until one PAMAM based vehicle

breaks through to clinical approval and establishes precedent. Regulatory approval has been swifter in Europe, where OcuSeal™, a dendrimer based cornea sealant was approved for human use in 2009.

Despite these challenges, it is clear from recent research that dendrimers hold tremendous potential as ocular drug delivery vehicles. Research groups around the world have been able to develop dendrimer based materials which have shown improved drug delivery efficacy when applied directly to the cornea as solutions or gels, as well as intravitreal, or subconjunctival injections. The common theme throughout all these projects is that the unique structure of the nanoparticles make them extremely versatile platforms for innovative scientists to adapt to overcome very different barriers. As our understanding of the pharmacokinetics of the eye increase, the ways for dendrimers and dendrimer based materials to improve drug delivery to this singularly complex organ will inevitably increase as well.

Acknowledgements

This work was supported by the National Institutes of Health (R01EY024072).

Chapter 3

Chitosan Nanofibers for Oral Insulin Delivery

3.1 Abstract

Purpose: In this work, we aimed at producing chitosan based nanofiber mats capable of delivering insulin via the buccal mucosa. **Methods:** Chitosan was electrospun into nanofibers using poly(ethylene oxide) (PEO) as a carrier molecule in various feed ratios. The mechanical properties and degradation kinetics of the fibers were measured. Insulin release rates were determined in vitro using an ELISA assay. The bioactivity of released insulin was measured in terms of Akt activation in pre-adipocytes. Insulin permeation across the buccal mucosa was measured in an ex-vivo porcine transbuccal model. **Results:** Fiber morphology, mechanical properties, and in vitro stability were dependent on PEO feed ratio. Lower PEO content blends produced smaller diameter fibers with significantly faster insulin release kinetics. Insulin showed no reduction in bioactivity due to electrospinning. Buccal permeation of insulin facilitated by high chitosan content blends was significantly higher than that of free insulin. **Conclusions:** Taken together, our work demonstrates chitosan based nanofibers have the potential to serve as a transbuccal insulin delivery vehicle.

Keywords: electrospun fiber, chitosan, insulin, transbuccal delivery

3.2 Introduction

Diabetes and other metabolic diseases are one of the most significant and growing health problems in developed nations. As of 2011 almost 6 million Americans were already using exogenous insulin to manage their diabetes, and of these patients almost all administer insulin through invasive means, usually subcutaneous injection or infusion pump.¹⁰³ Injections and pumps however both have numerous associated side effects including but not limited to allergic reactions

and lipohypertrophy.¹⁰⁴ Importantly, neither is an optimal solution for pediatric patients, a rapidly growing group.^{105,106} These problems and the poor patient compliance associated with them has driven considerable research into alternative delivery methods, including oral, nasal, and rectal therapies.¹³ There are obvious advantages of oral insulin delivery compared to injections, but enzymatic and chemical processes in the GI tract limit the bioavailability of orally delivered insulin to a degree where traditional drug delivery materials and methods are not viable.¹⁴ One possible solution to this problem is to bypass the GI tract and hepatic portal system by absorbing insulin through the oral mucus membranes.¹⁰⁷⁻¹¹⁰ A material capable of enhancing rapid uptake of insulin across the buccal mucosa would be able to combine the rapid and predictable dosing of subcutaneous injection with the patient comfort of a pill.

The buccal mucosa itself is comprised of a layer of epithelial cells around 40-50 cells thick that make up the inner lining of the cheeks.¹¹¹ Besides its ready accessibility, several other aspects of this tissue make it an attractive drug delivery route. The buccal mucosa is estimated to be as much as 4000 times more permeable than skin epithelium.¹¹² The area is highly vascularized, so absorbed materials reach the systemic circulation rapidly. Also, cell turnover is very rapid, with complete turnover every 5-8 days, limiting any acute cytotoxic effects caused by high drug concentrations at the delivery site.¹¹² Despite these advantages, hydrophilic drugs and especially peptides do not usually diffuse across the mucosa fast enough to overcome the effects of continuous saliva flux washing them out of the oral cavity. Mucoadhesive polymers are capable of holding the peptide at high local concentrations long enough to allow diffusion to take place, but very few materials meet the level of biocompatibility necessary to be used for long term insulin therapy.

Chitosan (CS), is one such material. Chitosan is the partially N-deacetylated derivative of chitin, the major structural component of crustacean and insect shells. In addition to excellent

biocompatibility comparable to similar structural polysaccharides, chitin is extremely naturally abundant and therefore low in cost. For the most part though, it is chitin's unique cationic character that have make it an attractive research target in a number of biomedical applications; but this work is hindered by chitin's insolubility in most solvents. Despite this, processing into CS and nanofabrication methods such as electrospinning can produce solid scaffolds for potential drug delivery applications.¹¹³ CS based nanoparticles have been investigated for oral insulin delivery,^{12,114-119} but there are physical limitations to handling and packaging nanoparticles. Electrospun fibers on the other hand have many of the advantageous physical properties of polymeric films and textiles while maintaining the high surface area to volume ratios of nanoparticles.

In this work we have developed electrospun chitosan fibers using different amounts of poly(ethylene oxide). The fiber diameter, mechanical properties, degradation rates, and insulin release kinetics of these fiber blends were first measured and compared. To ensure insulin entrapped in the fibers remains bioactive during the electrospinning process Akt-1 phosphorylation in preadipocytes exposed to CS fiber scaffolds was quantified. An ex-vivo porcine model was used to measure the buccal permeability of insulin released from each fiber blend. We believe this material has the potential to serve as a cost effective platform for transbuccal insulin delivery.

3.3 Materials and Methods

3.3.1 Materials: Chitosan (CS, product#448869, batch#SLBH5874V), poly(Ethylene Oxide) (PEO, Mw 900kDa, product#189456 batch#0741DD), and human insulin (INS, product#I2643, batch#SIBK6641V) were purchased from Sigma Aldrich (St. Louis, MO). , 1,1,3,3,3-hexafluoro-2-propanol (HFP) was purchased from Oakwood Chemicals (Estill, SC). Insulin ELISA assay kit was purchased from Calbiotech (Spring Valley, CA).

3.3.2 Electrospun fiber production: CS and PEO were dissolved in HFP at the concentrations indicated in **table 3.1**. This solution was stirred for 72 hours at room temperature, allowing all solid components to completely dissolve. INS was then added at 0.4 mg/ml and the solution stirred for an additional 48 hours. The solution was electrospun into solid fiber mats with the following conditions: 15 kV DC offset, 17 cm airgap, 18 ga. blunted needle, and 3 ml/hr flowrate. A typical spinning run used 5 ml of solution and a round collecting mandrel (6.5 mm diameter). Scaffolds were dried under vacuum 3 hours to remove residual solvent before any further testing.

Table 3.1: Electrospinning solutions content and final INS content.

| Blend Ratio | CS conc. (mg/mL) | PEO conc. (mg/mL) | INS conc. (mg/mL) |
|-------------|------------------|-------------------|-------------------|
| CS:PEO20 | 8 | 2 | 0.4 |
| CS:PEO33 | 8 | 4 | 0.4 |
| CS:PEO50 | 8 | 8 | 0.4 |

3.3.3 Mechanical tests: Uniaxial tensile testing of electrospun scaffolds was performed as previously described.^{120,121} Briefly, dog bone shaped punches of all fiber blends were taken longitudinally oriented with the predominant fiber alignment. Scaffold thickness over the gauge length was measured with precision calipers and the samples were loaded into a MTS Bionix 200 testing frame. Samples were uniaxially extended at 10mm/min until failure.

3.3.4 In vitro stability: Fiber stability under physiologic conditions was assessed quantitatively by mass loss and qualitatively by SEM imaging. 10 mg fiber samples were incubated in 1 ml of PBS at 37°C. At predetermined time points samples (n = 3) were spun down, and the degradation media was removed. Scaffolds were then washed briefly in diH₂O, lyophilized and weighed. One sample from each time point was then mounted and gold coated for SEM imaging. SEM images were taken on a JEOL LV-5610 scanning electron microscope in the Nanomaterials Core

Characterization facility at Virginia Commonwealth University. The diameters of fabricated fibers were analyzed using ImageJ software, manually measuring at least 150 randomly chosen fibers in each SEM image as previously reported.¹²²

3.3.5 In vitro insulin release: 8mm punches of each fiber blend were weighed and hydrated in 10 ml of phosphate buffered saline at 37°C. At specified time points the tubes were vortex stirred briefly and 100 µL samples taken of the release medium. A sandwich ELISA assay was then used to quantify insulin concentrations.

3.3.6 Insulin bioactivity: To ensure insulin was not denatured during electrospinning Akt phosphorylation of cells exposed to fiber release media was measured by western blot. 3T3-L1 preadipocyte cells were seeded in 6-well tissue culture plates and allowed to reach confluence. Growth medium was removed and replaced with either fresh growth medium, insulin containing medium (200 µIU/ml), or fiber release medium (CS:PEO20 0.15mg/mL for 6 hours). After incubating for 10 minutes at room temperature, cells were lysed and western blot analysis was performed as previously described.¹²¹ Briefly, cell lysates were separated on an SDS-PAGE gel (10% w/v) and transferred onto a PVDF membrane using Bio-Rad Mini-Blot transfer apparatus. The membrane was blocked for 2 h in Tris-buffered saline (TBS) containing non-fat dried milk (5% w/v). Phosphorylated Akt-1 on the membrane was determined by incubating with a primary antibody overnight at 4 °C with shaking. The membrane was washed and then incubated in a 1:3000 dilution of a secondary antibody at room temperature for 1 hour in washing buffer (TBS containing 0.5% w/v Tween 20). The specific antigen-antibody interactions were detected using enhanced chemiluminescence. The membranes were then stripped and re-probed for total expression of Akt-1 to use as the loading control.

3.3.7 Trans-buccal permeation: Fresh porcine heads were purchased from Animal Biotech Industries (Danboro, PA). Immediately upon arrival buccal membranes were removed and cleaned of any loose connective or adipose tissue to a thickness of approximately 1mm. Buccal membranes were loaded into a Franz diffusion cell (PermeGear, Cranford, NJ) with the epithelial side facing the donor chamber. The acceptor chamber was filled with 5.2 ml of PBS and maintained at 37°C. A 10mm fiber sample was placed on the buccal tissue in the donor chamber and 0.5 ml of simulated salival fluid (SSF) was added.¹²³ At predetermined time points 100 µl samples were taken from the acceptor chamber and the fluid was replaced with fresh PBS. The insulin concentration in the acceptor chamber fluid was measured using ELISA assay as previously described. The permeability coefficient, P , of the membranes was calculated using the following equation:

$$P = \frac{dQ/dt}{AC}$$

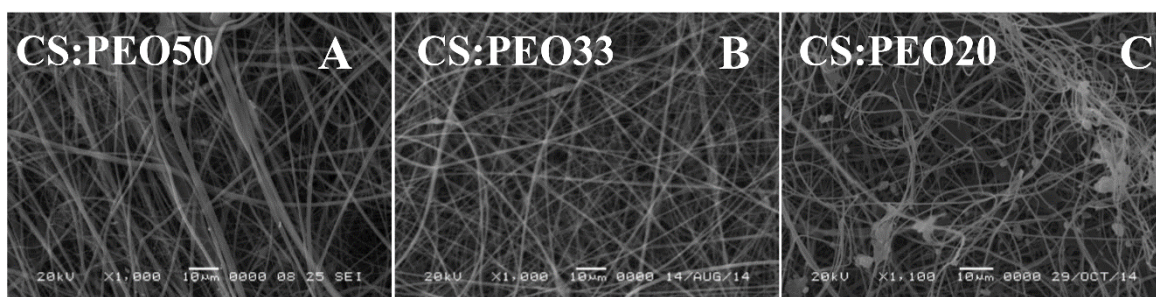
where dQ/dt is the steady-state slope of a cumulative flux curve, C is the loading concentration of free insulin or sIPN GIF in the donor chamber, and A is the effective cross-sectional area (0.785 cm²) available for diffusion.¹¹⁸

3.4 Results

3.4.1 Electrospun fiber production: Electrospinning of neat chitosan was not successful due to the lack of sufficient chain entanglements.¹²⁴ The addition of PEO enabled production of smooth fibers, but mixed beading due to fiber rupture was observed at polymer concentrations less than 20% (wt/wt). A mixed population of sub-micron (~200 nm) and larger (1-2 µm) fibers were seen under SEM for high PEO content blends (**figure 3.1**). Mandrel shape was found to have a significant impact on the distribution of insulin in the fiber scaffolds. Early experiments using a flat rectangular mandrel showed wide variability in both the thickness of fibers deposited and the

weight ratio of insulin trapped within the fibers. Both of these problems were corrected by switching to a cylindrical collecting mandrel. Mechanical tests confirmed mechanical properties of the fibers changed predictably with the composite ratios of CS and PEO. High CS content fibers showed a significantly higher maximum stress but also reduced strain at failure compared to the more ductile high PEO blends (**table 3.2**).

Figure 3.1. At least 20% high molecular weight polymer is necessary for stable fiber formation.



formation. Poly (ethylene oxide) (Mw 900kDa) was added to dissolved chitosan electrospinning solution in decreasing ratios. At 20% PEO solution content intermittent beading can be observed. Scale bar 10µm.

Table 3.2: CS:PEO fiber mechanical properties.

| Blend Ratio | Peak Stress (Mpa) | Strain at Break (%) |
|-------------|-------------------|---------------------|
| CS:PEO20 | 1.03±0.15 | 24.8±1.5 |
| CS:PEO33 | 1.14±0.15 | 18.3±1.3 |
| CS:PEO50 | 2.59±0.21 | 13.7±2.3 |

3.4.2 Physiologic stability: Mass measurements and SEM micrographs were used to evaluate how fiber mats degraded when hydrated. These experiments showed CS:PEO fiber solubility in physiologic conditions can be predicted by blend ratio (**figure 3.2A**). When hydrated fibers lose most of their bulk mass of PEO within 15 minutes, but show no significant mass loss over the next

6 hours. SEM images were consistent with these measurements, with significant changes in fiber diameter from 0 to 15 minutes, but no changes for the duration of the degradation period (**figure 3.2B&C**).

3.4.3 In vitro insulin release: Short and long term insulin release under physiologic conditions was measured for all fiber blends. Insulin release kinetics were highly dependent on the polysaccharide content of electrospun fiber mats (**figure 3.3**). Higher chitosan content blends released insulin significantly faster than lower chitosan content blends. By six hours CS:PEO20 and CS:PEO33 blends showed no significant difference and by 24 hours all fibers showed the same level of insulin release.

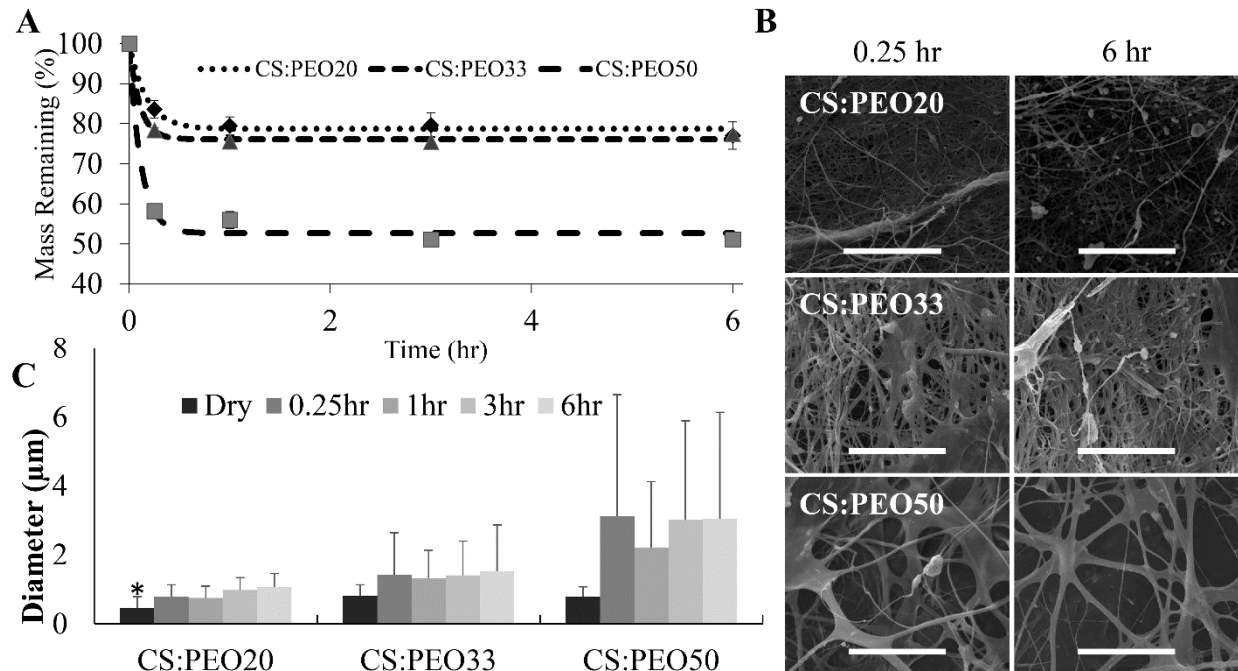


Figure 3.2. CS:PEO fibers dissolve slowly under physiologic conditions. 10mg samples of CS:PEO fiber blends (n=3) were immersed in 5ml of PBS at 37°C. At predetermined time points PBS was removed. Samples were then washed once with diH₂O and freeze dried overnight. Mass loss approximated PEO content (A). SEM micrographs showed no major morphological changes in fibers over the degradation period (B, scale bar represents 50 µm). The average fiber diameter measured in these micrographs also showed no significant changes within individual fiber blends after hydration (C). (* denotes statistically significant difference between all groups p < 0.05)

3.4.4 Insulin bioactivity: 3T3L-1 preadipocytes treated with 6 hour release medium showed significantly greater ratio of activated Akt than both negative (culture medium) and positive (insulin containing) controls (**figure 3.4**). This indicates there is no loss of insulin bioactivity

caused by dissolution in HFP, electrospinning, or dry storage at room temperature for several weeks.

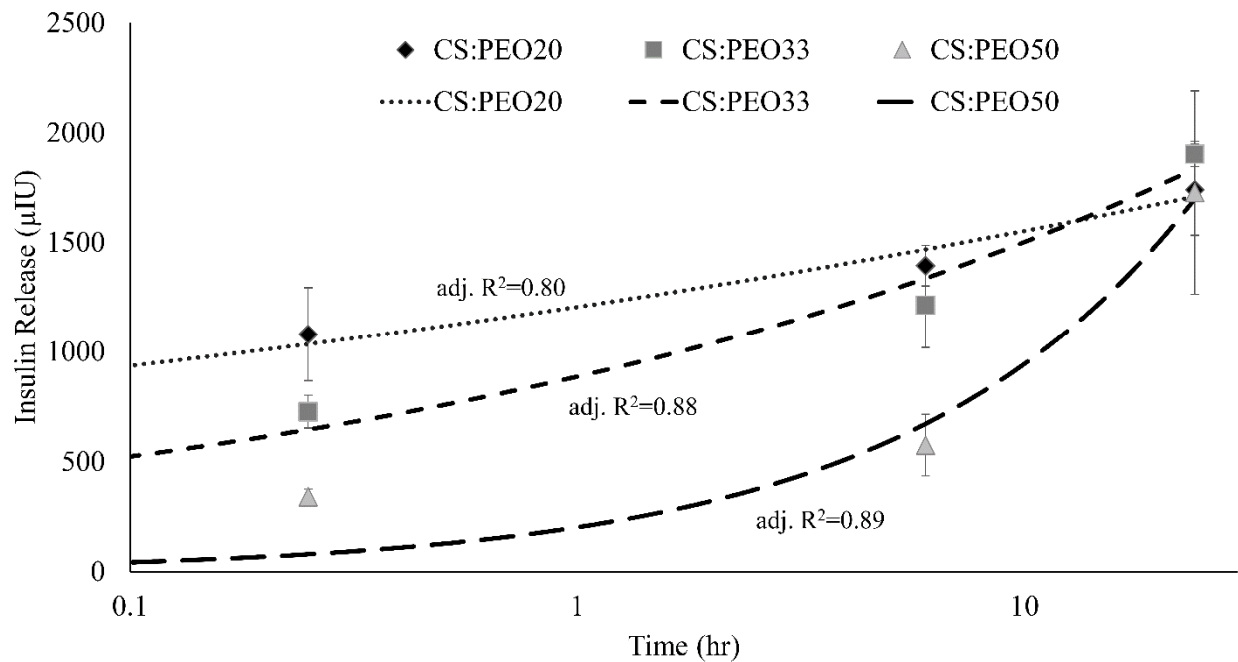


Figure 3.3. Polysaccharide content controls insulin release kinetics. Fiber blends of different chitosan:PEO ratios were immersed in PBS at 37°C. Insulin release was quantified at 15 minutes, 6 hours, and 1 day by ELISA assay. Various models were applied to fit the data. Curves corresponding to the Ritger-Peppas equation are shown. CS:PEO20 fibers show the fastest release profile, but there was no difference observed between blends at 24 hours.

3.4.5 Buccal permeation: High chitosan content is needed to induce trans-buccal insulin delivery. Lower chitosan content blends CS:PEO50 and CS:PEO33 did not outperform dissolved insulin in the 6 hour test, although all three groups saw negligible concentrations of trans-buccal insulin (less than 1% of the total) (**figure 3.5**). CS:PEO20 fibers on the other hand delivered on average around 1/3 of their total insulin into the acceptor chamber after 6 hours. Permeability coefficients for the lower chitosan content blends were 5 and 10 fold lower than naked insulin respectively while CS:PEO20 fibers had a permeability coefficient over 10 fold higher than the same control (**table 3.3**).

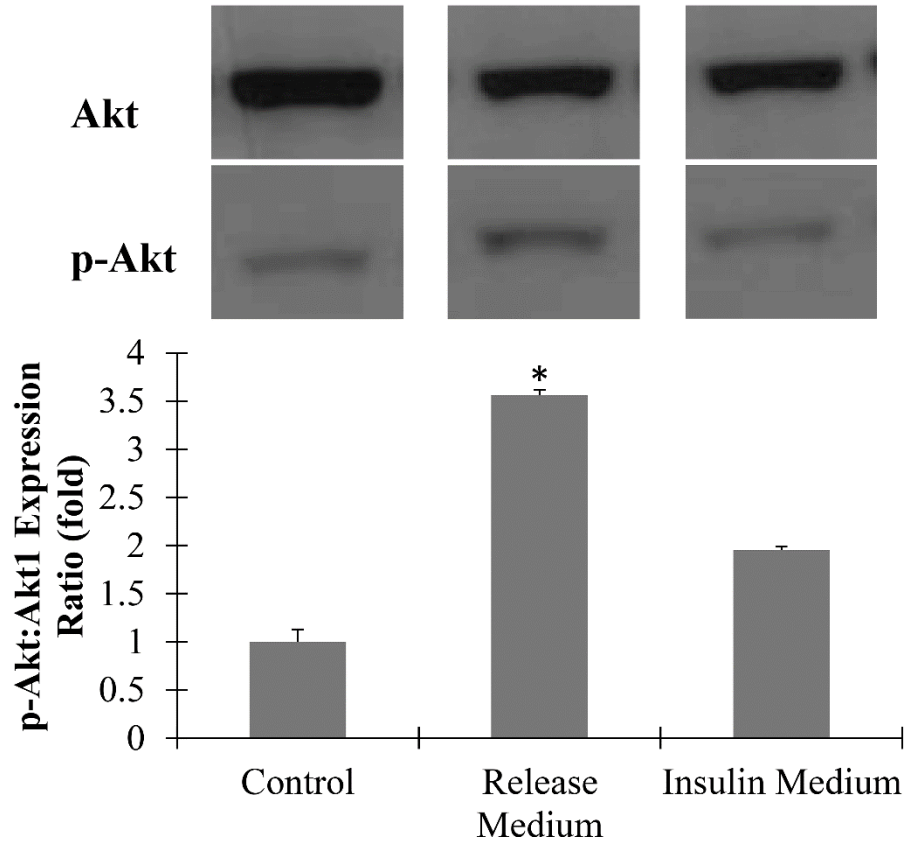


Figure 3.4. Insulin remains bioactive after electrospun fiber fabrication. 3T3-L1 preadipocytes incubated for 10 minutes in either fresh growth medium (control), 6 hour CS:PEO20 fiber release medium, or insulin containing media (7.98 $\mu\text{g}/\text{mL}$). Western blots of cell lysates were run for p-Akt expression then stripped and re-probed for total Akt1 as loading controls. Cells exposed to fiber release medium showed 3.5 fold higher p-Akt/Akt expression ratio than control cells. (* denotes statistically significant difference from all other groups $p < 0.05$)

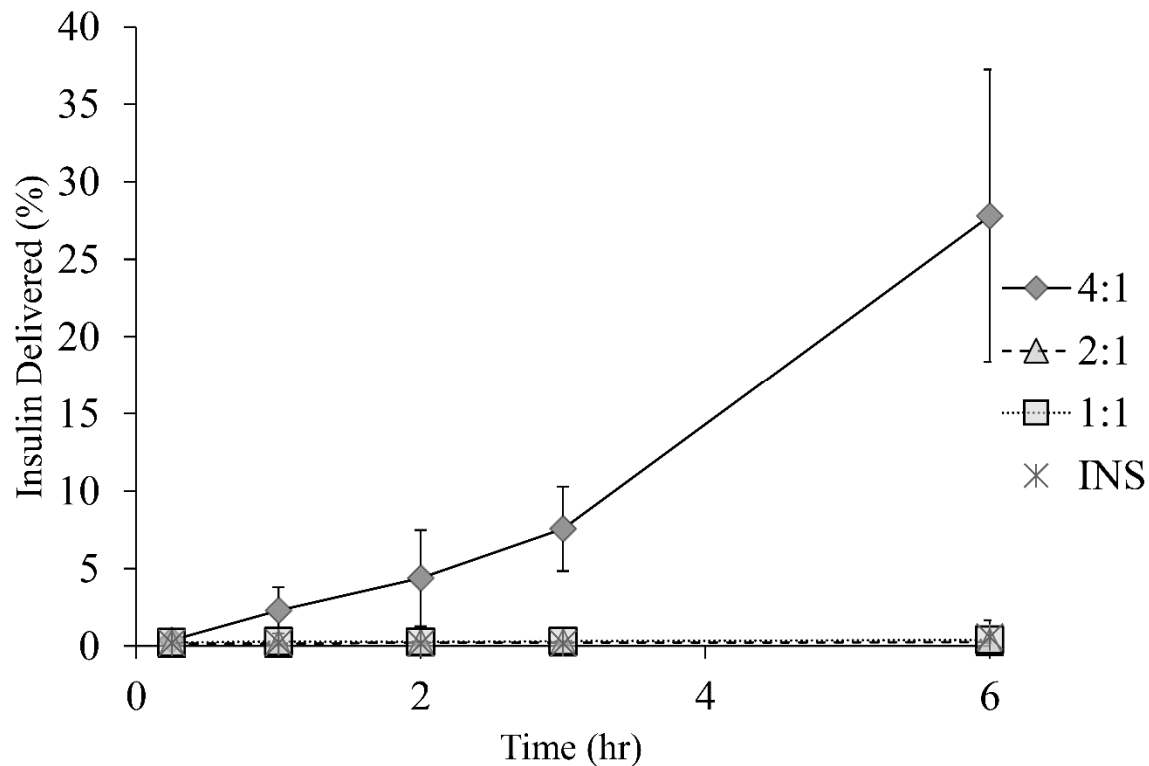


Figure 3.5. Chitosan enhances buccal permeability. Insulin transport across the buccal membrane was determined using a Franz diffusion cell. Measurements of the insulin concentration of the acceptor chamber showed that membranes were largely impermeable to both dissolved insulin and the lower chitosan blend ratios, with those groups delivering less than 1% of their total protein over 6 hours. CS:PEO20 fibers however showed significantly higher insulin delivery over the other groups at all time points over 2 hours. The permeability coefficient of the buccal mucosa to each of these insulin compounds was calculated from the steady state flux region of the tests and CS:PEO20 fibers showed around a 500 fold increase in permeability over the other fiber blends and a 16 fold increase over naked insulin.

Table 3.3: The insulin permeability coefficient and R² of the cumulative flux curve for CS:PEO fiber blends and naked insulin.

| Blend Ratio | Permeability (10⁻⁵cm/s) | Q-R² |
|--------------------|---|------------------------|
| CS:PEO20 | 0.255 | 0.74 |
| CS:PEO33 | 0.127 | 0.61 |
| CS:PEO50 | 21.5 | 0.97 |
| INS | 1.27 | 0.76 |

3.5 Discussion

3.5.1 Synthesis: In this work we developed chitosan based electrospun fiber scaffolds for oral insulin delivery. Chitosan nanoparticles have shown promise in a number of trans-buccal drug delivery applications, but there are drawbacks to producing and utilizing nanoparticles in a clinical setting. Electrospun fiber mats overcome many of these physical limitations, combining the rapid production and workability of polymer films with the high surface area of nanoparticles. The structure of chitosan however presents several problems for electrospinning. Solubility was the first hurdle, as the solvent system used needed to efficiently dissolve chitosan without denaturing insulin. A number of solvent systems have been investigated for electrospinning pure chitosan, most commonly dilute acetic acid solutions but insulin is known to rapidly lose bioactivity at low pH.¹²⁵ Highly polar fluorinated solvents, such as HFP had previously been shown to readily dissolve chitin and chitosan, as well as insulin without permanent structural changes.^{121,126} Neat chitosan solutions in HFP can be readily electrospayed into nanoparticles, but the rigid, charged polysaccharide molecules do not readily form the chain entanglements that are needed for stable fiber formation.¹²⁷ High Mw PEO is readily electrospun, has excellent biocompatibility, and has

been theorized to form hydrogen bonds with the amine groups on chitosan.¹²⁴ These hydrogen bonds encourage the chain entanglement that improve the overall spinning efficiency of the polymer solution, but also significantly increases the fiber diameter of the final composite fiber material. Preliminary work then focused on finding the minimum amount of PEO needed to reliably form composite fiber scaffolds, and characterizing the material properties of different CS:PEO blend ratios. 1:1 and 2:1 CS:PEO blends efficiently produced mats of continuous fibers (**figure 3.1A&B**) as previously reported.¹²⁸ At blend ratios greater than 4:1 fibers ruptured before solidifying, a phenomenon known as beading. Beading was intermittent at 4:1 but could be minimized by adjusting spinning parameters slightly (**figure 3.1C**).

Mechanical tests confirmed the composition of deposited fiber scaffolds matched that of the initial spinning solution, and neither component was disproportionately lost during fiber formation. As expected, increasing polysaccharide concentration in the spinning solution resulted in more brittle fiber scaffolds, with an increased peak stress and decreased strain at failure (**table 3.2**).

3.5.2 In vitro stability and insulin release: For this work, it was desirable for fibers to adhere, swell, and release loaded insulin but not to degrade significantly over the 3-6 hours they will be attached to the application site. While both components of the scaffolds have very good biocompatible properties it is always still preferable to limit the amount of polymer delivered into the circulation in case there are any unknown tissue specific effects or unanticipated drug interactions. Degradation experiments show when hydrated the different CS:PEO blends lose approximately 15, 20, and 50% of their bulk mass rapidly depending on the blend ratio, but there is no significant mass loss over the next 6 hours (**figure 3.2A**). This suggests the majority of PEO incorporated into the fiber mats dissolves rapidly leaving behind primarily chitosan fibers. Chitosan is stable enough in aqueous solvents that no significant amount dissolves under the remainder of the test period and

the fiber morphology remains constant (**figure 3.2B**), with no significant change in average fiber diameter (**figure 3.2C**).

After material characterization, the insulin release kinetics of the fibers needed to be measured. Although there are applications for long-acting insulin, for oral delivery it is not realistic to expect a material to stay in place for more than a few hours. This makes it critical for a trans-buccal delivery vehicle to have quick, predictable insulin release. With no significant degradation occurring over the test period, the only possible mechanism of insulin release was diffusion out of the fibers. Drug release by diffusion is directly proportional to surface area, so it was expected that insulin release kinetics would be more rapid in mats with smaller fibers and this is what was measured (**figure 3.3**). Measurements of SEM micrographs showed that while the average fiber diameter within a group did not change over the degradation period, there were significant differences between the groups at all points, with higher chitosan content in the initial spinning solution resulting in smaller fiber diameters. At 15 minutes for example, this would have an equally significant impact on the available surface area of the fiber mats since the volume of all samples was the same. This process physically encapsulated insulin within the material, as opposed to a surface binding technique, so a large surface area is critical to provide enough area for diffusion out of the hydrated fibers to take place at a sufficient rate.

3.5.3 Bioactivity: The other major concern apart from the rate of insulin delivery was the bioactivity of the insulin delivered. Dissolution in HFP, electrospinning, or dry storage could all potentially affect the signaling potential of insulin by degrading or denaturing the protein. While there are several major targets of the insulin signaling pathway that could have been measured, one of the largest upstream targets of the insulin signaling cascade is protein kinase B (Akt1) phosphorylation. Insulin causes Akt activation through insulin receptor substrate 1 (IRS1)

phosphorylation, which activates phosphoinositide-3 kinase (PI3K). PI3K activates Akt1, which in turn is responsible for many of the metabolic and mitogenic cellular responses to insulin stimulation. For this reason cells exposed to bioactive insulin should contain a higher ratio of phosphorylated Akt (S473) to total Akt compared to cells exposed to standard culture medium. Adipocytes and preadipocytes in particular show a robust response to insulin, given their role as the body's major long term energy store. The response of the preadipocytes used in this study showed that insulin dissolved in HFP and electrospun into chitosan fibers undergoes no significant decrease in its bioactivity (**figure 3.4**).

3.5.4 Buccal permeability: Buccal permeability was the only property of these fibers tested that did not show a dose-dependent relationship with polysaccharide content. In vitro experiments suggested that the 4:1 CS:PEO fibers would have the highest short term insulin transport across the buccal mucosa simply by diffusion. While this was observed, the trend did not hold true for the other fiber blends. 2:1 and 1:1 CS:PEO fibers greatly underperformed the level of insulin delivery expected following the in vitro experiments (**figure 3.5**). Hydrophilic compounds must cross the epithelium via the paracellular route through tight junctions between cells. Chitosan is known to enhance the permeability of membranes by transiently disrupting binding between tight junction proteins.¹⁷ Furthermore, mucoadhesive materials hold dissolved compounds in much higher concentrations directly adjacent to the epithelium, encouraging diffusion across the membrane. While 4:1 CS:PEO fibers were able to deliver promising levels of insulin across the buccal mucosa, the variation between samples was sub-optimal. It is possible this is a function of the tissues samples used and not the fibers themselves. Permeability of the buccal mucosa is known to vary widely throughout the mouth and in ex-vivo studies it can be problematic to keep

application sites constant.¹¹¹ Future work will need to confirm this result in a more reproducible way by measuring the ability of CS:PEO fibers to lower blood sugar in a suitable animal model.

3.6 Conclusion

In this work we have developed electrospun Chitosan scaffolds designed for oral insulin delivery. Poly(ethylene oxide) was added in different ratios to control fiber morphology and physical properties. Degradation studies showed PEO dissolves rapidly under physiologic conditions but fiber diameter does not change. Higher Chitosan:PEO ratio when spinning results in smaller fibers and more rapid insulin release. Insulin released from electrospun fiber mats shows no impaired bioactivity. 4:1 CS:PEO fibers have 16 times higher buccal permeability compared to free insulin. Taken as whole, the results of this study suggest electrospun chitosan nanofibers can function as a viable vehicle for oral insulin delivery deserving of further study.

Chapter 4

Fast Dissolving Dendrimer Nanofiber (DNF) Mats as Alternative to Eye Drops for Antiglaucoma Drug Delivery

4.1 Abstract

PAMAM dendrimers have been investigated as a potential platform for a number of ocular drugs, but they are unstable when stored in aqueous solution. In this work we have developed dendrimer based nanofibers (DNF) as a topical delivery vehicle for the glaucoma drug brimonidine tartrate (BT). The safety and drug release kinetics of these nanofiber mats were evaluated in vitro and in vivo using a normotensive rat model. DNF caused no toxicity at therapeutic levels in cultured cells or ocular irritation in animal tests. Intra-ocular pressure response was equivalent between DNF and BT solution in single dose tests, but DNF showed improved efficacy with daily dosing. This study indicates electrospun nanofibers are a viable alternative to aqueous solutions as a method of applying dendrimer drug vehicles to mucous membranes.

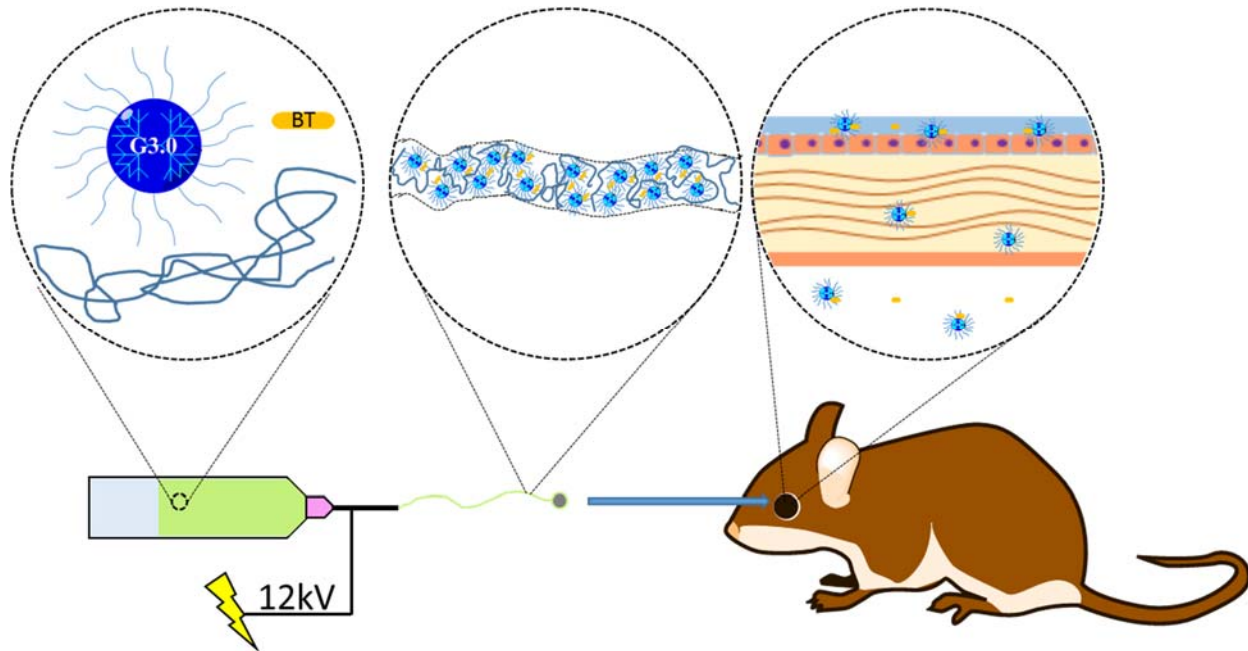


Figure 4.1: Graphic abstract.

4.2 Introduction

Among the available routes of administration for ocular drugs, topical application is considered the most desirable due to its combination of good tissue specificity and minimal invasiveness.¹²⁹ However, delivery of drugs using conventional saline eye drops is severely limited by anatomical and physiologic factors unique to the eye. Following administration, the entire drop is drained into the systemic circulation in a matter of minutes, typically resulting in less than 5% of the drug reaching the desired tissue.¹³⁰ This increases costs and creates the risk of off-target effects. Patient non-compliance is a major issue for glaucoma medications because most eye drops must be applied at least two or three times per day, and they are difficult to administer. Combined, these drawbacks lead many glaucoma patients to skip doses or even stop medication treatment.^{51,131} Estimates of patient non-compliance vary, but electronic monitoring studies have consistently shown that a major portion of glaucoma patients struggle to adhere to this dosing regimen for more than a few weeks.⁵² For these patients, long-term treatment of high intraocular pressure (IOP) then relies on

more invasive therapies such as surgical intervention. Despite the clear benefits of a more efficient topically applied ocular drug delivery vehicle, significant research investment has so far borne no optimal solution.^{39,132-134}

A true replacement for saline eye drops would increase the bioavailability of therapeutic compounds and reduce the dosing frequency while still having a simple application procedure and minimal invasiveness. While conventional materials have failed to deliver these features, novel nanocarriers such as dendrimers may offer new opportunities.^{73,79,87,135,136} Dendrimers are a class of polymers with a well-defined branching structure. Each branch has a terminal end group that can be functionalized with solubilizing polymers, targeting domains, imaging molecules, or therapeutic compounds.¹³⁶ The ability to incorporate these agents into a single nanoparticle make dendrimers extremely flexible drug delivery platforms.¹³⁷

Polyamidoamine (PAMAM) dendrimers have already demonstrated promise as vehicles for a number of ocular drugs, although IOP lowering agents have not yet been studied.^{76,78,84,138} These previous studies have delivered drug loaded dendrimers as nanoparticles in solution, where they rely solely on the mucoadhesive properties of the polymer to extend residence time on the corneal surface, but solid dosage forms such as erodible inserts extend corneal residence time using mechanisms independent of particle charge.³⁹ We also believe solid dendrimer based materials will have other advantages over dendrimers in solution including superior storage ability and a more reliable application procedure.

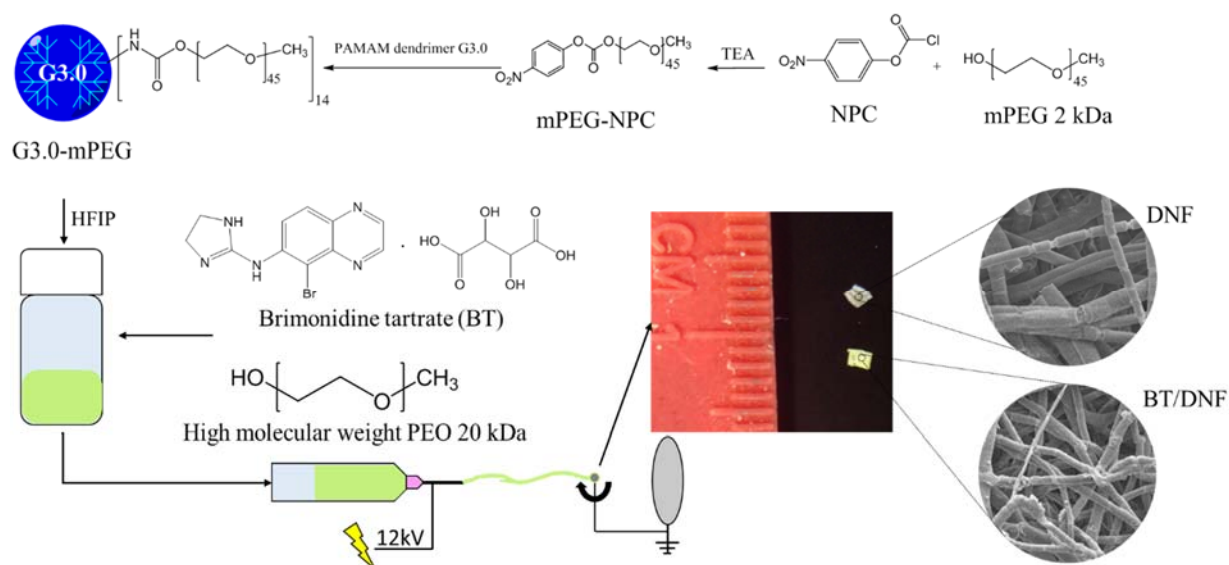
Previously, this lab has developed dendrimer based nanofibers.¹³⁸ In this work, we sought to further develop this material platform as well as investigate it as an ocular drug delivery vehicle. To this end, modified PAMAM dendrimers were co-spun with polyethylene oxide and brimonidine tartrate into nanofiber mats. The drug release kinetics of these fiber mats and the permeability of

the drug across live corneas was quantified. The in vivo efficacy and biocompatibility of these nanofibers was evaluated in a normotensive rat model by intra-ocular pressure measurement and examination over a three-week trial. Disposition of dissolved dendrimers in various ocular organs was determined by using fluorescently labeled nanofibers. Success of using these fiber mats for glaucoma medications has been demonstrated by their ability to match or exceed the performance of conventional saline eye drops in each of these tests.

4.3 Materials and Methods

4.3.1 Materials: All reagents were purchased from Sigma-Aldrich (St. Louis, MO) unless otherwise stated. PAMAM dendrimers (G3.0) were purchased from Dendritech (Midland, MI). Hexafluoroisopropanol (HFP) was purchased from Oakwood Chemicals (Estill, South Carolina). Cellulose dialysis membranes were purchased from Spectrum Labs (Rancho Dominguez, California). Fresh rabbit eyes were purchased from Pel-Freeze Biologicals (Rogers, Arkansas).

4.3.2 G3.0-mPEG synthesis: PAMAM dendrimers generation 3.0 were conjugated with methoxy polyethylene glycol (mPEG) ($M_n=2$ kDa) as previously described (**Scheme 4.1**).¹³⁹ Briefly, mPEG (1 equiv) was dissolved in tetrahydrofuran, followed by addition of 4-nitrophenol chloroformate (NPC) (1.5 equiv) and triethylamine (TEA) (20 equiv). The reaction was run for 24 h at room temperature and the salt was filtered off. The resulting mPEG-NPC was collected by precipitation in diethyl ether and vacuum dried. PAMAM dendrimer G3.0 and mPEG-NPC were dissolved in DMSO separately. The mPEG-NPC solution was added dropwise to the dendrimer solution at a feed molar ratio of 16:1 for mPEG-NPC:G3.0. After 72 h, the solvent was removed under vacuum. The resulting product G3.0-mPEG was purified via dialysis in deionized water using a 7000 MWCO dialysis membrane.



Scheme 4.1: Synthesis and fabrication of DNF and BT/DNF mats. Following the synthesis of PEGylated PAMAM dendrimer G3.0 (i.e., G3.0-mPEG), G3.0-mPEG is dissolved in HFIP with high molecular weight PEO in the absence or presence of the antiglaucoma drug BT and electrospun into DNF or BT/DNF mats.

4.3.3 Electrospinning: HFIP electrospinning solution containing G3.0-mPEG (120 mg/mL) and polyethylene oxide (PEO) ($M_n = 90$ kDa, 20 mg/mL) was prepared. Brimonidine tartrate (BT) was added to the electrospinning solution at the final concentration of 20 mg/mL prior to electrospinning. One mL of electrospinning solution (with or without BT) was loaded into a custom electrospinning machine and spun onto a rectangular aluminum mandrel using the following parameters: 12 kV DC offset, 20 cm airgap distance, and a 1.5 mL/h solvent flow rate. The obtained dendrimer nanofibers (DNF) and BT-containing DNF (i.e., BT/DNF) were degassed overnight at atmospheric pressure (i.e., ATM degassing) and removed from the mandrel. Any residual solvent was further removed under vacuum for 1 h (i.e., vacuum degassing).

4.3.4 Fiber characterization: To assess fiber morphology, the samples of electrospun fiber mats were mounted and platinum sputter coated for imaging using a Hiatachi SU-70 scanning electron

microscope. Fiber mechanical properties were measured by using uniaxial tensile testing. “Dogbone” punches (19.0×3.2 mm) were taken and deformed at a 10 %/min strain rate until failure using an MTS Bionix 200 Mechanical Testing System.

4.3.5 In vitro drug release: Cellulose dialysis membranes (MWCO 3.5 kDa) were sealed on one end and filled with 10 mg BT/DNF dissolved in 100 μ L simulated tear fluid (STF).¹²³ The tube was placed in 2 mL of STF in a quartz cuvette. The concentration of the drug in the bulk solution was quantified using absorbance of 320 nm light at 5 min intervals for 90 min. This procedure was repeated for neat brimonidine solution (40 μ g) and unmodified dendrimers mixed with an equivalent drug amount.

4.3.6 Cornea permeability: Brimonidine transport across live corneas was measured using Franz diffusion cells (PermeGear, Hellertown, PA). Corneas from fresh rabbit eyes were excised and placed immediately into diffusion cells with the endothelial surface facing the acceptor chamber and the epithelial surface facing the donor chamber. The acceptor chamber was filled with 5 mL of glutathione buffered Ringer’s solution and the donor chamber with 100 μ L of solution containing 40 μ g of the drug. The entire cell was placed in a water bath at 37 °C. At various time points 250 μ L samples were taken from the acceptor chamber solution and drug concentration was measured using a reverse phase HPLC equipped with a UV detector (96v:4v water:acetonitrile mobile phase, 50×150 mm C18 column with 5 μ m pore size).

4.3.7 In vitro cytocompatibility: NIH 3T3 fibroblasts were seeded into 96 well plates at a density of 5000 cells/well and allowed to attach overnight. The cells were incubated with DNF at various concentrations (on the basis of dendrimer) for an additional 24 h and assessed for viability using WST-1 viability assay.

4.3.8 IOP measurement: Normotensive adult brown Norway rats (Charles River Labs, Wilmington MA) were used for all animal experiments in this study. They were housed under proper conditions at Virginia Commonwealth University (VCU) and Medical University of South Carolina (MUSC). The rats were kept under a cycle of 12-h light and 12-h dark for all the studies. All animal procedures were approved by the VCU and MUSC IACUC. Rat IOP measurements were taken with a TonoLab rebound tonometer (iCare, Finland) as described earlier.¹⁴⁰ No anesthetics or artificial restraints were employed during measurement. All measurements were taken by the same operator at the same location using the hand corresponding to that eye. Time 0 for all experiments (and baseline IOP readings) occurred at approximately 10 a.m. All IOP values reported represent the average of at minimum 18 and maximum 30 individual instrument readings of each eye.

4.3.9 In vivo single dose response: Rats (n=4) were conditioned for at least 1 week to establish baseline IOP. On the day of the experiment the animals had either 5 μ L BT solution (40 μ g), or an equivalent dose of BT/DNF placed in the right eye (experimental eye). At time points 2, 4, 6, and 24 h post-dosing the IOP in both the experimental and contralateral eye was measured. Animals were closely monitored for irritation and inflammation for the duration of the test.

4.3.10 Chronic use safety and efficacy: Normotensive rats (n=3) received 40 μ g BT delivered via saline solution or BT/DNF mat in the right eye (experimental eye) daily. IOP was measured daily in both eyes immediately prior to drug administration. After 21 d, the animals were euthanized and the eyes enucleated. Eyes were immediately fixed with Davidson's solution and 5 μ m sections prepared. Sections were stained with hematoxylin and eosin and imaged.

4.3.11 Ocular disposition: Fluorescently tagged nanofiber mats were synthesized by covalently linking fluorescein isothiocyanate (FITC) to G3.0-mPEG prior to electrospinning. Normotensive rats (n=3) had fluorescently tagged nanofiber mats (without drug) applied to the right eye. At

various time points, the animals were euthanized by carbon dioxide asphyxiation and the ocular tissues harvested. Ocular globes were fixed in 4% paraformaldehyde, perfused with glucose, and frozen for cryosectioning. Nanoparticle contents in the cornea, ciliary body, and retina were visualized using fluorescence imaging.

4.3.12 Statistical analysis: The data are expressed as mean \pm standard deviation. The single dose response data were analyzed using one-way analysis of variance (ANOVA) for multiple comparisons versus control group (time point zero) (Holm-Sidak method) in each treatment. T-test was used for comparison of 3-week IOP reduction effect between BT saline solution and BT/DNF. A p value <0.05 is considered statistically significant.

4.4 Results and Discussion

4.4.1 Synthesis and fabrication: The ^1H NMR spectrum confirms that the partial modification of G3.0 PAMAM dendrimers with mPEG was successful (**Fig. 4.2**). Integration of the peak at 3.72 ppm, the methane protons on PEG, and 2.4-3.5 ppm, assorted dendrimer peaks, showed the 16:1 molar feed ratio mPEG:G3.0 resulted in a final dendrimer surface coverage of approximately 40%. PEG modification of PAMAM dendrimers has been widely studied by our lab and others, and has a major impact on the physical and chemical properties of the nanoparticles.^{31,60} A higher degree of PEGylation (the percentage of surface groups modified) results in easier electrospinning by lowering the charge density and breaking up the highly compact structure of dendrimers. Both of these changes help encourage the polymer chain entanglements that differentiate electrospinning nanofibers from electrospaying nanoparticles.¹⁴¹ These property changes also greatly increase the biocompatibility of PAMAM dendrimers, which are cytotoxic in their unmodified form. However, for drug delivery applications full PEGylation is not desirable as it neutralizes the dendrimers' charge to a degree where cell permeation is inhibited, and it leaves no remaining surface groups

for later modification.⁶⁹ Approximately half PEGylation was selected for this project to balance efficient nanofiber production and leave sufficient available groups to later adapt the material to delivery alternate therapeutic compounds, targeting moieties, or imaging tags.

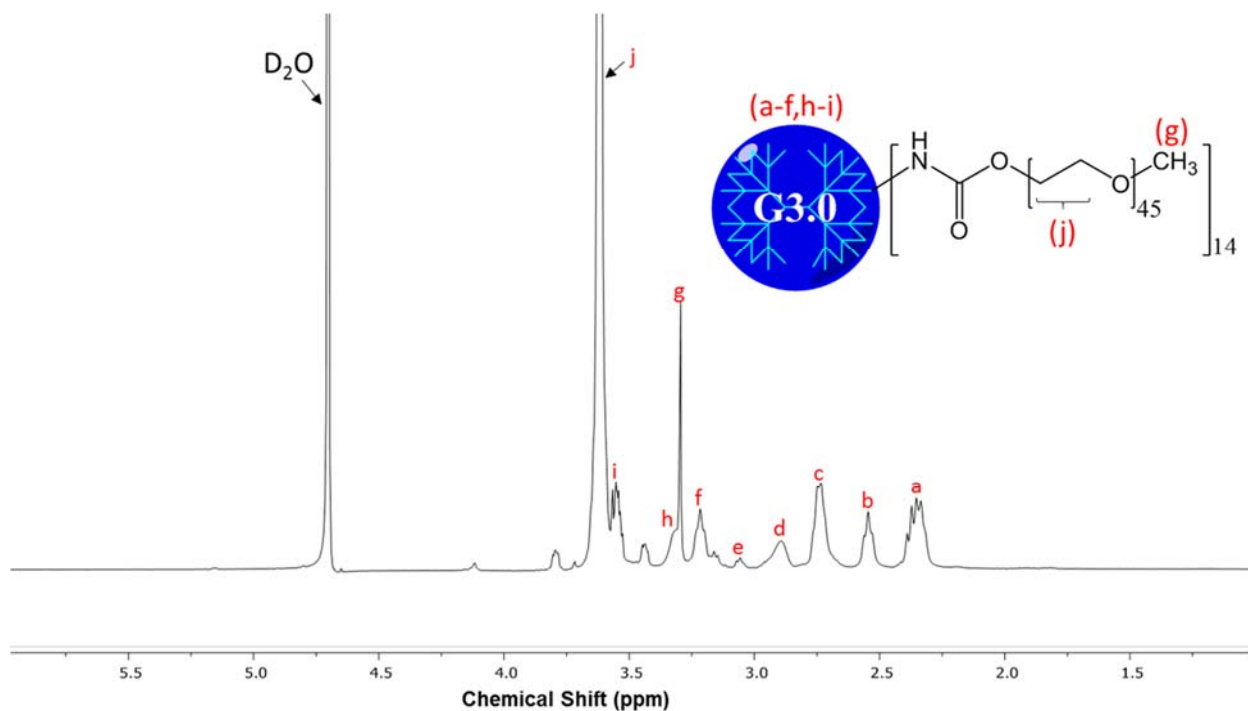


Figure 4.2: ¹H NMR spectrum of G3.0-mPEG. Degree of PEGylation was determined by integrating proton peak j (mPEG) and comparing with integration of proton peaks a-f, h, and i (G3.0). The analysis determined around 40% of G3.0 surface groups were PEGylated.

Electrospinning parameters were designed to optimize efficiency while still producing dry nanofibers. The most significant determining factor of fiber yield and morphology was expected to be the quantity of high molecular weight PEO added to the electrospinning solution.¹⁴² While 1% wt/vol was sufficient to produce fibers a higher quantity of 2% was selected to ensure the final material would dissolve rapidly when placed onto the ocular surface. Parameters such as flow rate, mandrel speed, and DC offset were minimized at the given air gap distance to maintain a stable pull of fibers. No preferred fiber morphology was directed with this approach. SEM imaging

showed DNF mats had a low degree of alignment (**Fig. 4.3A&B**). The median fiber diameter was around 2 μm for plain DNF with the distribution skewed toward smaller fibers (**Fig. 4.3C**). The addition of BT decreased median fiber diameter to less than 1.5 μm and balanced the distribution. Mechanical properties were not robust, with a modulus of just 1.81 and 4.97 MPa for DNF and BT/DNF respectively, but these values were sufficient to cut and manipulate the mats without breakage (**Fig 4.3D**).

4.4.2 In vitro assessment: Conversion of the tetrazolium salt WST-1 to formazan was used as an indirect measure of cytotoxicity by quantifying the metabolic activity of viable cells. As the fibers are not expected to have an impact on the mitochondrial activity of cells, this can be used to approximate the number of living cells quickly. Preliminary experiments on fibroblasts showed a 50% reduction in cell viability at a concentration of 32.5 μM (IC₅₀). To determine if this was caused by residual electrospinning solvent another batch of fibers were dried by vacuum oven prior to testing. It's IC₅₀ increased by 67% to 54.2 μM (**Fig. 4.4**). This is well above the expected maximum concentration in vivo (~ 30 μM), given the BT loading concentration and approximate volume of rat tear fluid. Because of this finding, all samples later used in animal experiments were first vacuum dried.

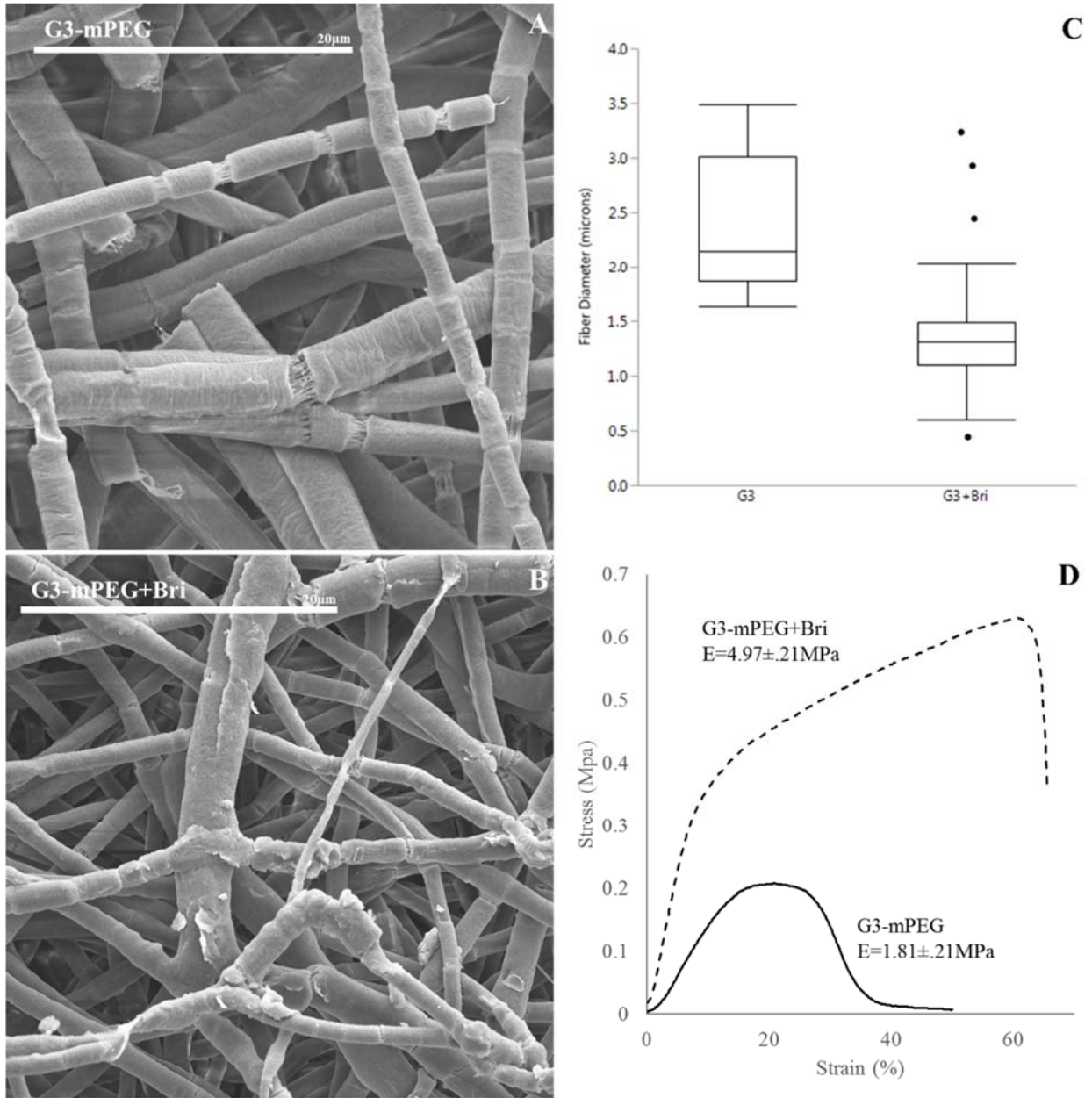


Figure 4.3: DNF characterization. (A) High magnification electron micrographs of DNF and BT/DNF. (B) Histograms of fiber measurements show BT caused an overall decrease in fiber diameter. (C) Uniaxial tensile testing shows BT/DNF has higher elastic modulus, peak stress, and strain at break than DNF.

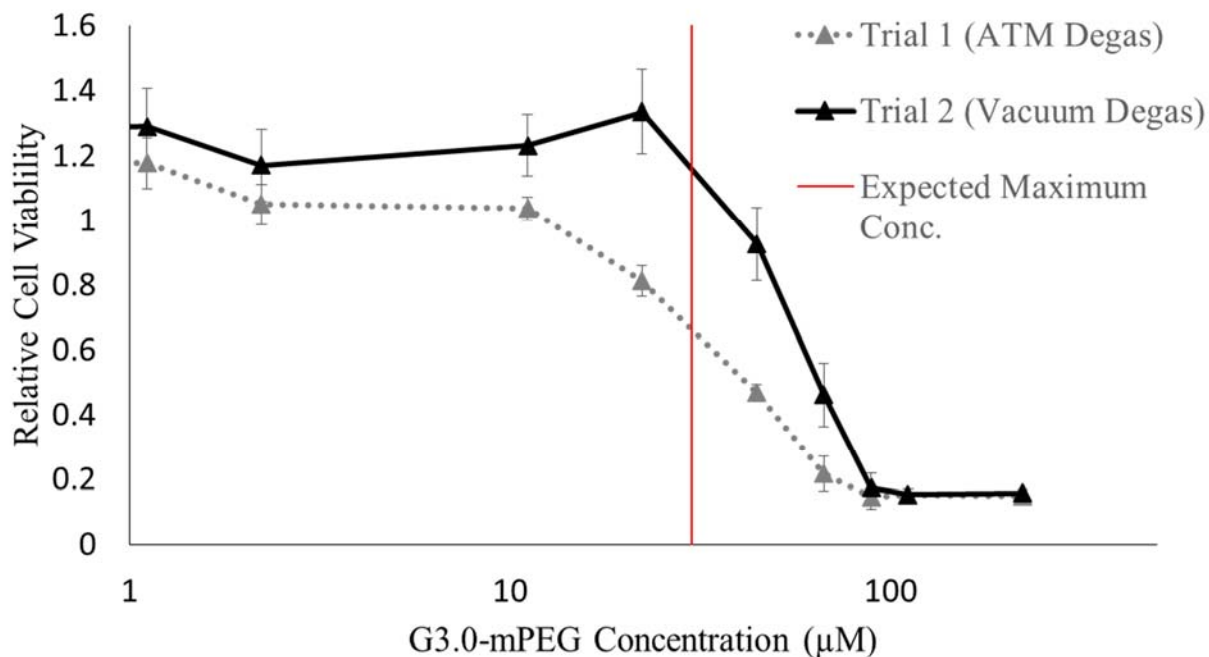


Figure 4.4. DNF cytotoxicity. NIH 3T3 fibroblasts were incubated with varying concentrations of DNF for 24 h and cell viability measured via WST-1 assay. Degassing fibers under vacuum (vacuum degassing) was shown to be more efficient in removing residual electrospinning solvent and increasing DNF cytocompatibility than degassing fibers at atmospheric pressure (ATM degassing).

As proof of concept before animal testing, the release kinetics of BT from DNF mats was evaluated under static in vitro conditions, as well as permeation using ex vivo rabbit corneas. Static BT release due to diffusion was determined by the interaction of the drug with G3.0-mPEG in solution. Release was significantly slower from G3.0-mPEG fibers compared to both neat BT solution and unmodified G3.0 dendrimers (**Fig. 4.5**). Due to the number of constituents present, there are several mechanisms which may be responsible for this result. Slowed drug release in the G3.0 group indicates there is some interaction between PAMAM dendrimers and BT in solution. This

may be with the terminal or core groups on the polymer. More importantly, the PEGylation of the dendrimers and the addition of PEO to the fibers appear to form a loose network in solution.

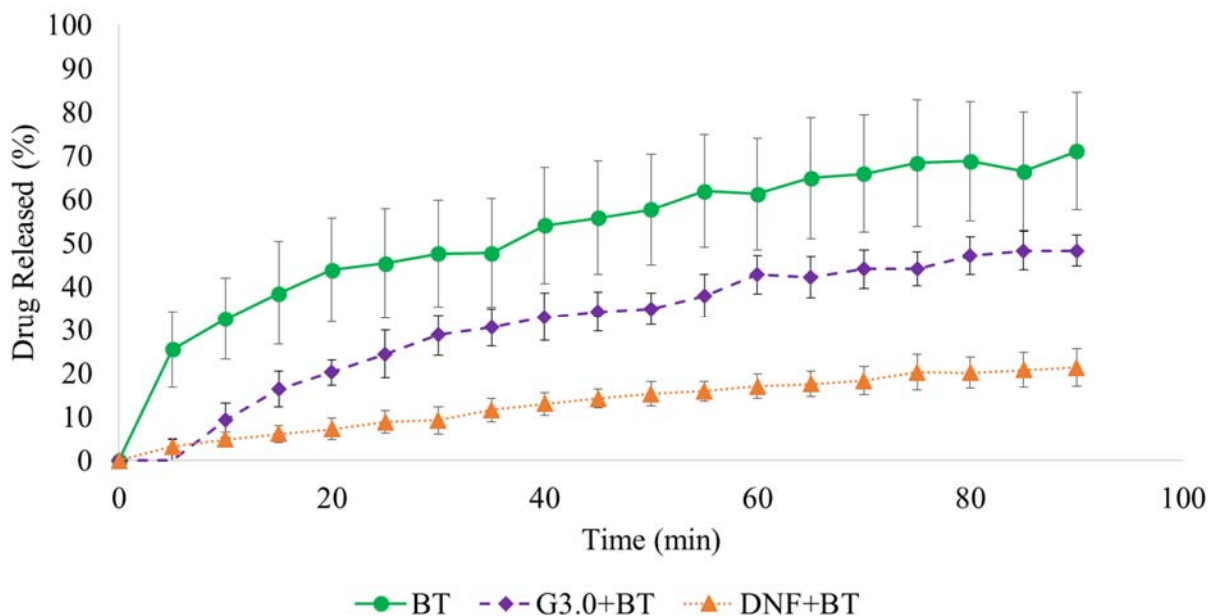


Figure 4.5: In vitro brimonidine release. BT delivery vehicles were dissolved and drug diffusion across a 3.5 kDa dialysis membrane was measured for 90 min. Unmodified dendrimers and DNF slowed initial drug diffusion in STF. DNF further slowed the rate of drug release for the entire duration of the test.

Corneal permeability was investigated in an ex vivo rabbit model. Dendrimers have previously been shown to increase permeability of epithelial cell layers, but BT eye drops have a relatively high corneal permeability compared to most ocular drugs.⁷⁰ Typical permeability coefficients for brimonidine range between 2.1×10^{-7} and 3.6×10^{-7} cm/s.²³ At the doses used in our tests G3.0-mPEG fibers had no difference in permeability compared to brimonidine solution and all groups agreed with the literature values for live rabbit corneas (**Table 4.1**). While increased permeability would be beneficial to drug delivery efficiency, it is also known to cause numerous potential problems, most commonly irritation.⁵⁵ The fact that DNF did not affect corneal permeability

indicates that they are not disrupting the structure of the native epithelium, an important consideration for the long term biocompatibility of the material.^{74,143}

Table 4.1: Permeability coefficient of rabbit corneas to brimonidine.

| Formulation | P (10 ⁻⁶ cm/s) | Q-R ² |
|-------------|---------------------------|------------------|
| BT solution | 6.90 | 0.93 |
| BT/G3.0 | 7.77 | 0.97 |
| BT/DNF | 6.43 | 0.91 |

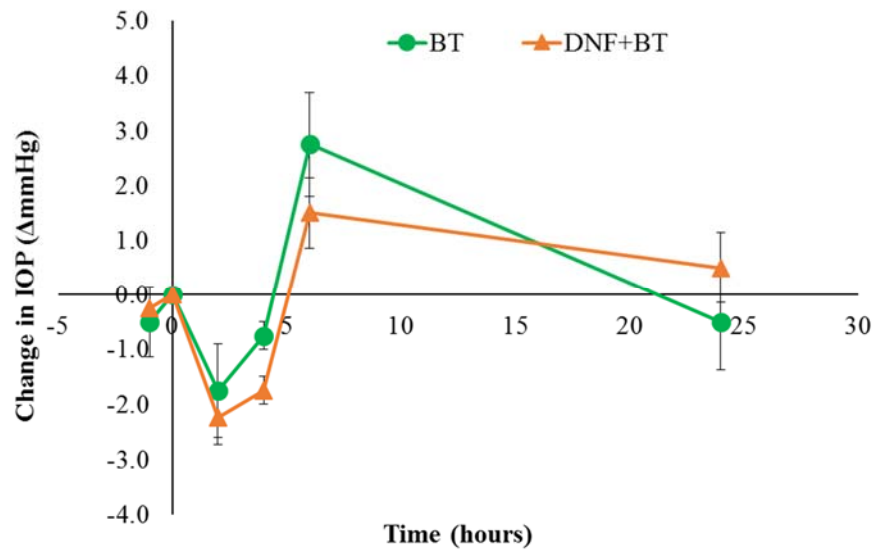


Figure 4.6: In vivo single dose response. Brown Norway rats (n=4) received a single dose of BT via saline eye drops or DNF topically. One dose of BT/DNF and one dose BT saline eye drops are equivalently effective in reducing IOP response (* indicates significantly different, P<0.01).

4.4.3 In vivo efficacy and safety: In vivo experiments indicate BT drug delivery efficiency may be improved by DNF, but the effect is difficult to capture in normotensive animals. Drug efficacy was equivalent between DNF and saline eye drops in terms of single dose IOP response (**Fig. 4.6**). In those tests, both formulations induced an approximately 2 mmHg (~15%) drop in IOP at 2 h,

followed by a rebound above baseline at 6 h, and finally a return to baseline values by 24 h. While DNF values were slightly lower than eye drops at all these time points, the difference was not significant. It took several days of repeated application to achieve a differential effect with DNF. The nature of IOP measurement on fully conscious animals produces considerable noise, but over the three-week test period DNF experimental eyes recorded significantly lower average pressure values than conventional eye drops. This result held when measurements were normalized to the contralateral eye, individual eye baseline IOP, or both (**Fig. 4.7**). Taken together, these results suggest DNF mats deliver BT with a similar efficiency to conventional eye drops with each individual dose, but over repeated applications they build an additive effect, and are able to achieve a significant drop in IOP using a sub-therapeutic drug dosage.

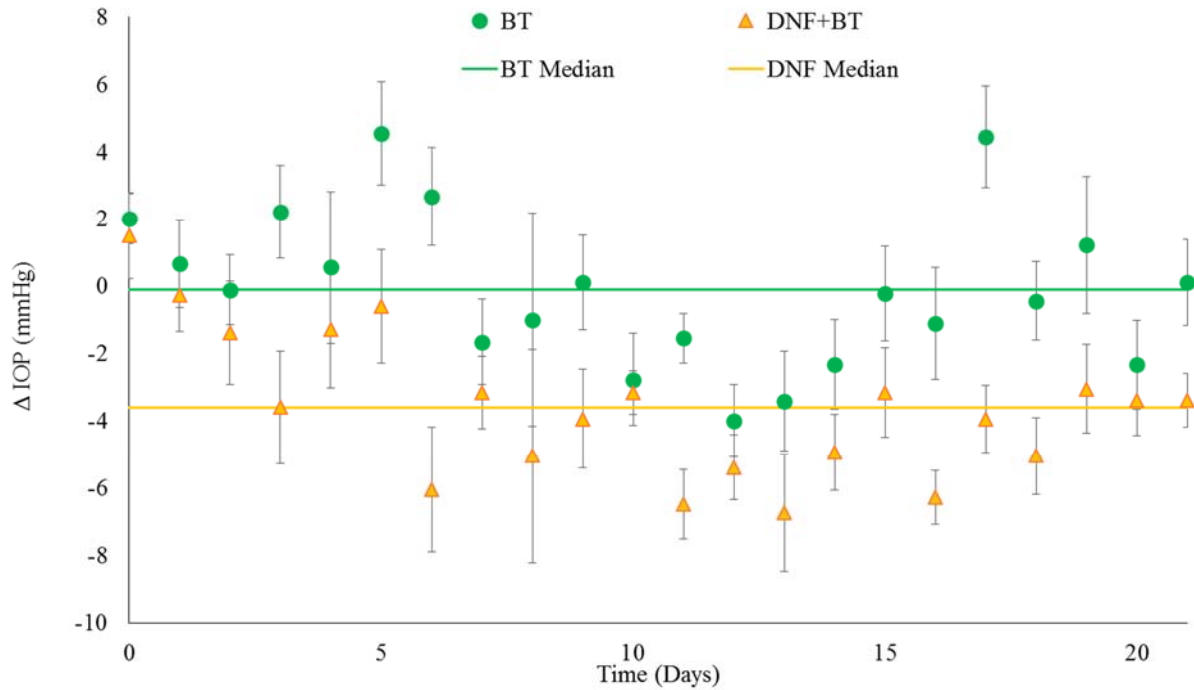


Figure 4.7: In vivo 3-week daily dose response. Brown Norway rats (n=4) received a daily dose of brimonidine via saline eye drops or DNF for three weeks. IOP was recorded immediately prior to drug application. Values expressed are the difference between the experimental and contralateral eyes after normalizing individual eyes to baseline levels. The dash lines represent the mean IOP reduction values. DNF was able to sustain reduced IOP over the test period compared to saline eye drops (# indicates significantly different, $P < 0.001$).

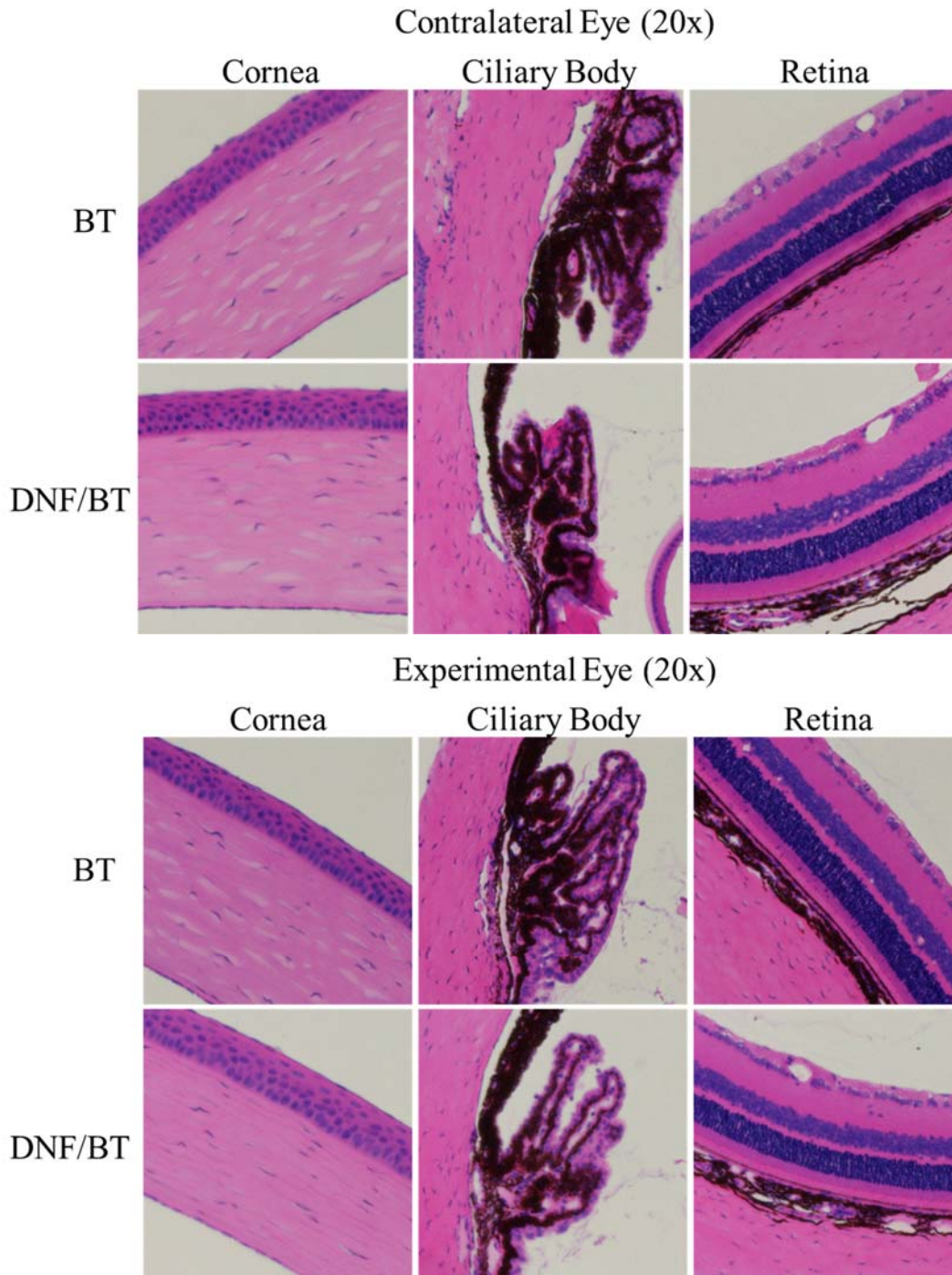


Figure 4.8: Ocular histopathology of chronic DNF application. Brown Norway rats (n=3) received a single dose of BT via saline eye drops or DNF every 24 h for 21 days. No changes in cornea morphology could be observed between the experimental groups. Other ocular structures such as the ciliary body and retina showed the same result.

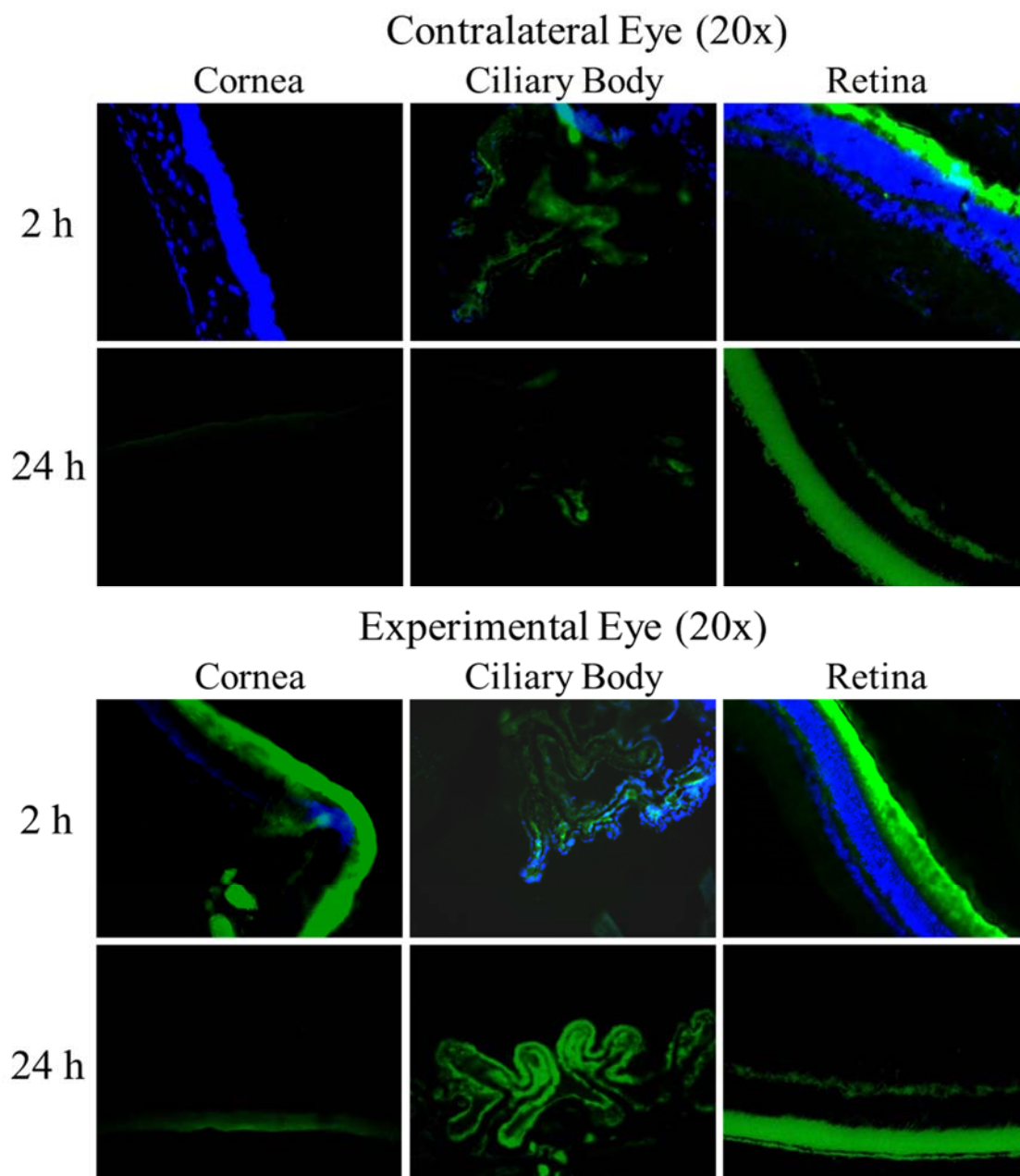


Figure 4.9: Ocular disposition of DNF. Brown Norway rats (n=3) received a DNF-FITC mat topically in the right eye (experimental eye) while the left eye received no treatment (contralateral eye). Animals were euthanized at 2 or 24 h and the ocular tissues harvested and immediately processed for cryosectioning. Fluorescent imaging of sections from various ocular organs showed most dendrimers were flushed from the cornea in 24 h. Over the same time period, FITC-G3.0-mPEG accumulated in the ciliary body of the experimental eye.

In vivo ocular tolerance of DNF was excellent. DNF dissolve virtually instantly (<1s by video analysis) Animals reacted noticeably less to direct DNF application than BT solution. No outwardly visible signs of irritation or inflammation, such as redness, excessive blinking, or ocular discharge were observed in any animals in the single dose response experiments. During the chronic use trial several of the animals exhibited known side effects of BT in the experimental eye by the second week, namely redness of the surrounding skin. Histopathology of these eyes showed no gross morphological changes in the eyes exposed to either BT solution or DNF (**Fig. 4.8**). Taken together, DNF appears to be a safe material for ocular applications.

A potential mechanism for this additive effect can be found in the results of the disposition experiments. Fluorescence images indicated that while few dendrimers could still be observed in the cornea 24 h after fiber application, quantities in the ciliary body had noticeably increased compared to eyes harvested just 2 h after fiber application (**Fig. 4.9**). This means in the chronic use trial, some of the previous day's dendrimers were still present in the target organ when that day's BT was at its peak concentration. If these latent dendrimers were able to increase the residence time of that next dose of BT, it could account for the gradual increase and plateau in potency that we observed. It also agrees with the response of the contralateral eye, which saw a slight IOP drop from baseline in the eye drop group, but no change with DNF. If the dendrimers are holding the drug closer to the site of application, then they may be able to reduce the bleed-over effects common with BT.

Other phenomenon could also be responsible for the result. The ocular bioactivity of topically applied PAMAM dendrimers themselves is somewhat unknown, but no strong effect has been detected in the limited studies conducted to this point.^{68,71,77,144} It could also be that fiber application is simply more reliable. Great care was taken to ensure that drug dosage was consistent

between the groups (as confirmed by HPLC), but eye drop instillation is prone to inaccuracy in both animals and humans. Since the fibers are applied dry it is easy to ensure that all of the material successfully makes it into the eye, where it is not uncommon for some amount of a drop to spill onto the face of the animal. This could point to a possible pediatric or veterinarian use for the material, where topical drops problematic not just for their low efficiency, but also their awkward application procedure. Other groups have seen similar improved efficacy with solid dosage forms in veterinary glaucoma treatment.¹³⁴

4.5 Conclusion

In this work, electrospun dendrimer based fibers have been developed as a novel vehicle for topical administration of therapeutic compounds to the eye. The drug delivery efficacy and ocular tolerance of the material has been evaluated in vitro, ex vivo, and in vivo using a model ocular drug, brimonidine tartrate. Results were equivalent between DNF and saline eye drops in terms of safety and single dose drug delivery efficacy, but DNF outperformed the control when applied daily. Disposition experiments showed dendrimer accumulation in the anterior chamber, suggesting the platform can function as a powerful ocular drug delivery vehicle with further study and development. The studies suggest that drug loaded dendrimer nanofiber mats can be a promising alternative to drug saline eye drops.

Acknowledgements

This work was supported by the National Institutes of Health (R01EY024072). Tissue sectioning and H& E staining services in support of the research project were generated by the VCU Massey Cancer Center Cancer Mouse Model Shared Resource, supported, in part, with funding from NIH-NCI Cancer Center Support Grant P30CA016059.

Chapter 5

PAMAM Dendrimers for Improved Timolol Delivery

5.1 Abstract

Anti-glaucoma drugs suffer from poor bioavailability due to low solubility and corneal permeability. In this work we have sought to improve these properties of the beta-blocker timolol by direct coupling of the active group on timolol to a generation 3.0 PAMAM dendrimer via a PEG spacer to form dendritic timolol (DenTimol). Preliminary animal tests indicate that DenTimol retains bioactivity similar to timolol after grafting. Ongoing experiments are evaluating the corneal permeability and ocular disposition of this material. Future experiments will focus on further characterizing the PK/PD profile of this coupled drug.

5.2 Introduction

Ocular hypertension, or elevated intra-ocular pressure (IOP) is a chronic condition that can lead to degenerative and irreparable vision loss. There are multiple causes of ocular hypertension, but in all cases the immediate aim of treatment is to lower IOP back to normal levels and prevent further progression of the disease. Pharmacologic therapies are usually the first treatment option employed, because they are considerably cheaper and less invasive than surgical intervention options. Beta-adrenergic antagonists, colloquially referred to as β -blockers, reduce IOP by slowing production of aqueous humor. Timolol maleate is a β -blocker developed in the 1970s.¹⁴⁵ It selectively binds to adrenergic receptors in the ciliary body, making it a more potent IOP lowering drug than other β -blockers.¹⁴⁶

Despite the existence of these potent IOP lowering drugs, glaucoma remains the second leading cause of preventable blindness worldwide.²² This is because the impact of current treatments are severely limited by inefficient drug delivery systems. For example, when timolol is delivered as a

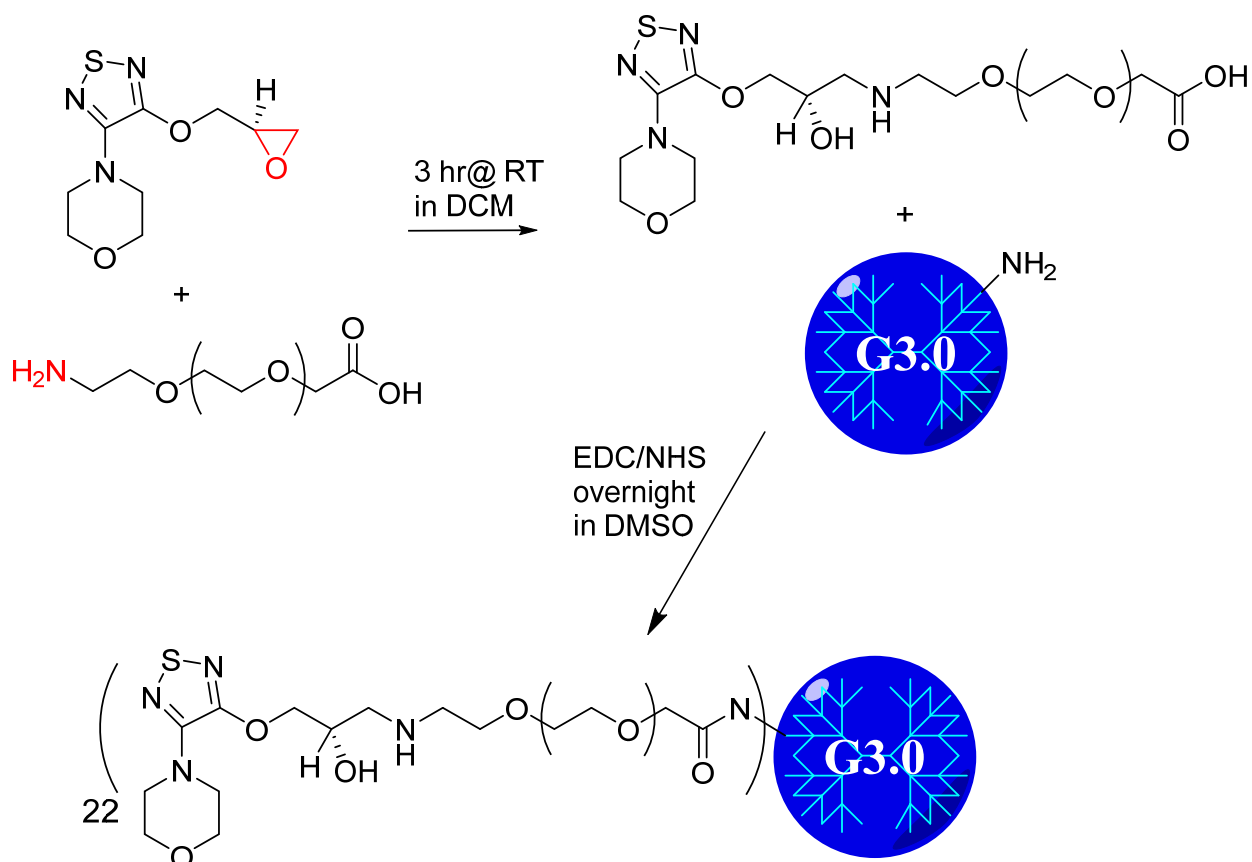
topical solution, only about 5% of the total drug at best makes it to the target organ with each dose.⁴⁸ Because of this, the period of time after a dose where the drug is within its therapeutic concentration window in the anterior chamber is narrow, between 4-5 hours.^{147,148} The remaining volume is flushed into systemic circulation where it can cause cardiovascular side effects of varying severity.^{33,149,150} Vehicles that can improve the delivery efficiency of this drug could reduce either the necessary concentration or dosing regimen, representing a significant improvement in the clinical management of glaucoma.

The study of nanoparticle vehicles to improve the bioavailability of topical ocular drugs has received considerable research interest over the last decade.^{35,36,56} Most drug loss from eye drops occurs due to pre-corneal mechanisms.⁴⁸ Generally, most drugs penetrate the corneal epithelium slowly relative to the rate of tear drainage and turnover.¹⁵¹ Poly(amidoamine) (PAMAM) dendrimers are polymeric nanoparticles with the potential to overcome these factors because they have appropriate size and mucoadhesive character to both slow washout and increase cornea permeability.^{30,152} PAMAM dendrimers have been complexed with other ocular therapeutics, resulting in improved drug deliver efficacy, but these methods rely on the formation of metastable dendrimer-drug complexes.^{76,78,82,98} To date, studies using directly coupled dendrimer-drug conjugates have not been carried out with ocular therapeutics, but the technique has shown promise in the field of targeted chemotherapy.¹⁵³

The purpose of this study is to modify dendrimers with a prodrug of the IOP lowering drug timolol in order to increase the bioavailability of the compound. The safety and efficacy of this material will be measured relative to conventional timolol eye drops.

5.3 Methods and Materials

5.3.1 Synthesis: (S)-4-[4-(Oxiranylmethoxy)-1,2,5-thiadiazol-3-yl]morpholine (OTM, Toronto Research Chemicals, Toronto ON, cat#O847080) was dissolved in DCM and reacted with an equimolar amount of 5kDa Amine-poly(ethylene glycol)-carboxyl (PEG, JenKem, Plano TX) for 3 hours at room temperature. The product was recovered by rotary evaporation and purified by dialysis in water with a 3.5kDa dialysis membrane and lyophilized. OTM-PEG was then coupled to Generation 3.0 poly(amidoamine) dendrimers (G3.0, Dendritech, Midland MI) by dissolving in DMSO and reacting overnight in the presence of a large molar excess of N-(3-Dimethylaminopropyl)-N'-ethylcarbodiimide hydrochloride and N-Hydroxysuccinimide (EDC/NHS). The product was purified by dialysis with a 7.5 kDa dialysis membrane for 48 hours and lyophilized (**Scheme 5.1**).



Scheme 5.1: DenTimol synthesis. (Clockwise from top right) OTM was coupled to amine-PEG-carboxyl by spontaneous ring opening reaction. OTM-PEG was coupled to G3.0 dendrimer by EDC/NHS mediated crosslinking reaction.

5.3.2 NMR spectra: ^1H NMR was performed using a Bruker 400 MHz NMR to verify successful conjugation. OTM spectra was obtained in deuterated methanol. OTM-PEG and G3-PEG-OTM spectra were obtained in D_2O .

5.3.3 HPLC analysis: Reaction products were separated using a Waters reverse phase HPLC system equipped with a UV detector (50v:50v water:acetonitrile mobile phase, 50×150 mm C18 column with 5 μm pore size). UV absorbance was monitored at 220 and 300nm.

5.3.4 Ex vivo permeability: Corneal permeability was determined using Franz diffusion cells (PermeGear, Hellertown, PA). Corneas from fresh rabbit eyes were excised and placed

immediately into diffusion cells with the endothelial surface facing the acceptor chamber and the epithelial surface facing the donor chamber. The acceptor chamber was filled with 5 mL of glutathione buffered Ringer's solution and the donor chamber with 100 μ L of solution containing 1 mg G3-PEG-OTM or and equimolar amount of OTM and OTM-PEG intermediate. The entire cell was placed in a water bath at 37 °C. At various time points 250 μ L samples were taken from the acceptor chamber solution and drug concentration was measured using reverse phase HPLC as described in section 5.3.3.

5.3.5 In vitro cytotoxicity: NIH 3T3 fibroblasts were seeded in a 96 well plate at 5000 cells per well and allowed 24 hours to attach. OTM, PEG-OTM, and G3-PEG-OTM solutions of various concentrations were added and incubated for 24 hours. A WST-1 formazan conversion assay (Roche BioTech, cat#05015944001) was run according to the manufacturer's protocol to quantify viable cell numbers.

5.3.6 In vivo efficacy: Rat IOP measurements were taken with a TonoLab rebound tonometer (ICare, Finland) as described earlier. No anesthetics or artificial restraints were employed during measurement. All measurements were taken by the same operator at the same location using the hand corresponding to that eye. Time 0 for all experiments (and baseline IOP readings) occurred at approximately 10 a.m. All IOP values reported represent the average of at minimum 18 and maximum 30 individual instrument readings of each eye.

Drug efficacy was measured *in vivo* by dosing brown Norway rats (n=4) in the left eye with 10 μ L timolol solution or equivalent G3-PEG-OTM solution. IOP was measured using a TonoLab rebound tonometer (Icare, Finland) at various time points in both eyes. Change in IOP was referenced to the contralateral (right) eye. A one-way t-test was performed to determine significant decreases in IOP ($\alpha \leq 0.05$).

5.4 Results and Discussion

5.4.1 Synthesis & characterization: ^1H NMR spectra indicated that OTM coupling to PEG was successful due to the presence of peaks at 3.79 and 3.54 ppm. HPLC of the raw product from this reaction produced multiple elution peaks, but dialysis removed free drug successfully (**Fig 5.1**). HPLC output after purification showed a single DenTimol elution peak about 1 minute after injection, indicating the absence of free drug in the final conjugate. Analysis of the final nanoparticle spectra determined a PEG:G3.0 ratio of approximately 22:1, or 61% surface coverage (**Fig 5.2**). While OTM specific peaks cannot be resolved on the full DenTimol H+NMR spectra due to the relatively large mass of dendrimer and PEG present, is assumed at this time that no loss of drug has occurred during the PEG:G3.0 coupling step. More detailed mass spectrometry testing will be needed to verify this assumption.

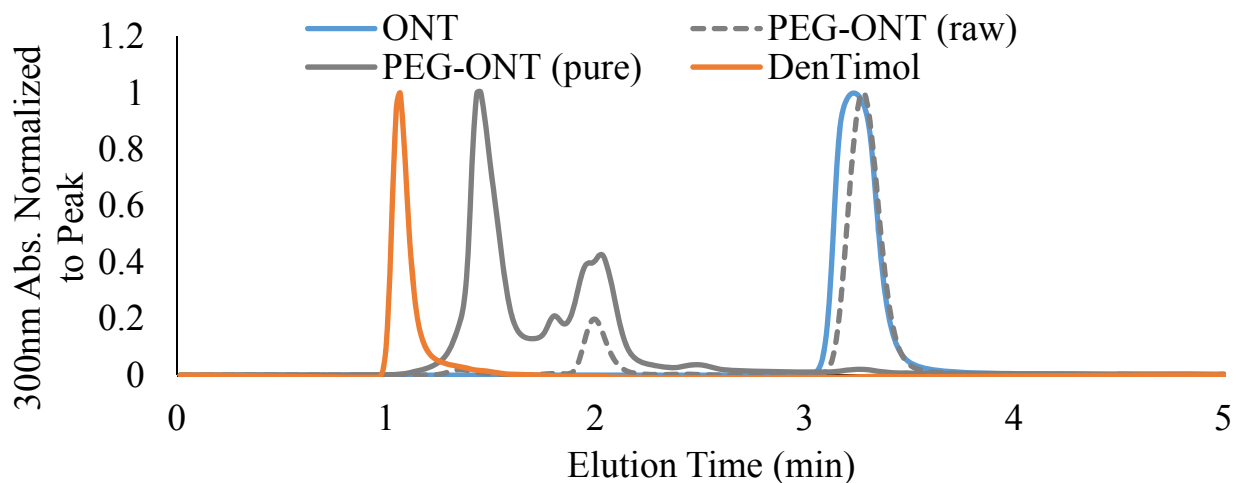


Figure 5.1: HPLC of reaction products. Purified DenTimol product shows no elution peak at 3min, indicating no free prodrug present.

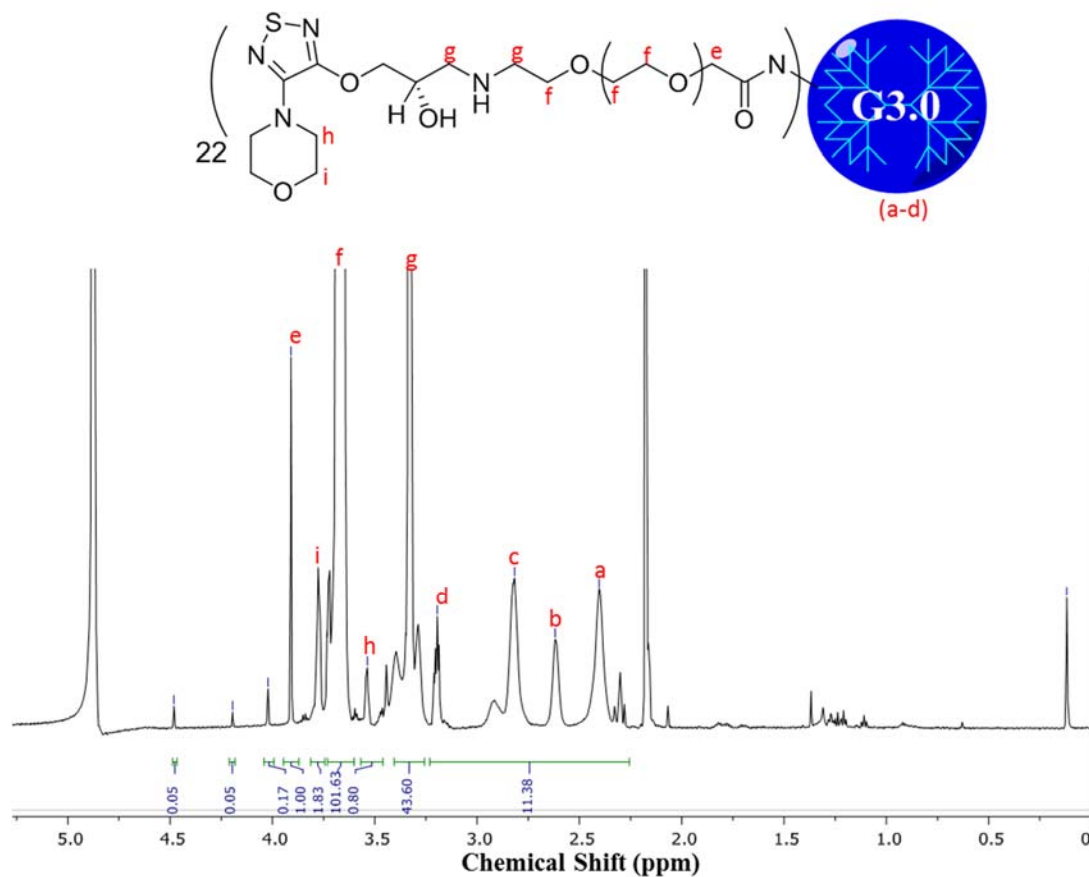


Figure 5.2: DenTimol NMR spectra. OTM proton peaks at 3.79 and 3.49 ppm (h & i) were still present on the final nanoparticle NMR spectra, but were obscured by overlapping dendrimer signals. Integration of PEG peak f and dendrimer peaks a-d was used to estimate drug loading quantity.

5.4.2 In vitro assessment: OTM has similar bioactivity to timolol and is non-toxic, but it is hydrophobic, with even lower ocular bioavailability than timolol maleate.¹⁵⁴ Coupling to a linear hydrophilic polymer such as PEG, can solubilize the compound, but as our corneal permeability results show this structure does not readily penetrate the cornea (**Fig 5.3**). PAMAM dendrimers are also highly hydrophilic, but they are also compact and strongly cationic. This unique architecture allows them to penetrate the cornea relatively easily even when covered with drug moieties. Direct coupling of OTM to dendrimer without a spacer is theoretically possible, and would likely result in an even higher level of bioavailability.¹⁵⁵ However, without the flexibility provided by the polymeric linker it is likely bioactivity of each prodrug moiety would be reduced, either due to steric hindrance from the dendrimer, or folding in of the dendrimer end groups towards the core of the molecule.⁶²

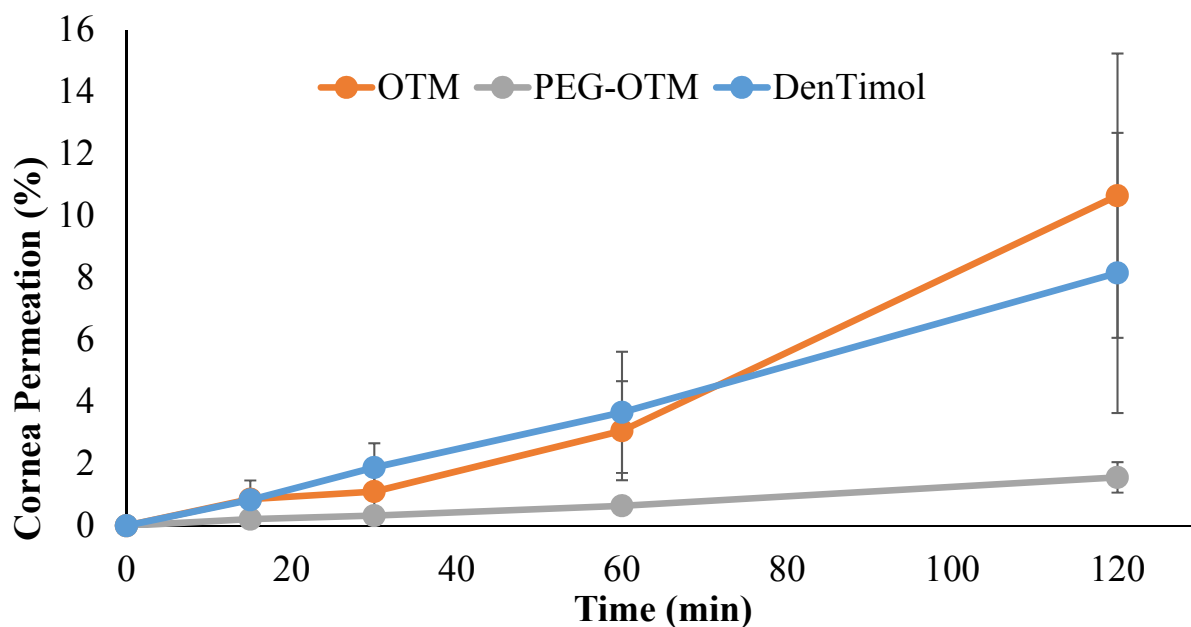


Figure 5.3: Corneal permeability. Permeation rates (by percentage) were equivalent for DenTimol and OTM. PEG-OTM intermediate was not able to penetrate ex vivo corneas.

Use of the spacer also has another benefit. PAMAM dendrimers are known to be cytotoxic at micromolar concentrations, but covering a large portion of the particle's surface with PEG chains

erases most of this effect.³¹ Indeed, our cytotoxicity results indicate that DenTimol particles show no signs of cytotoxicity up to 10 μ M, but due to the high drug payload per dendrimer this is many times higher than the effective drug concentration necessary to match therapeutic timolol concentrations (**Fig 5.4**). This suggests drug payload may be able to be reduced somewhat without hurting the safety of the particle. A lower degree of PEGylation would increase the charge of the particle and presumably the corneal permeability.

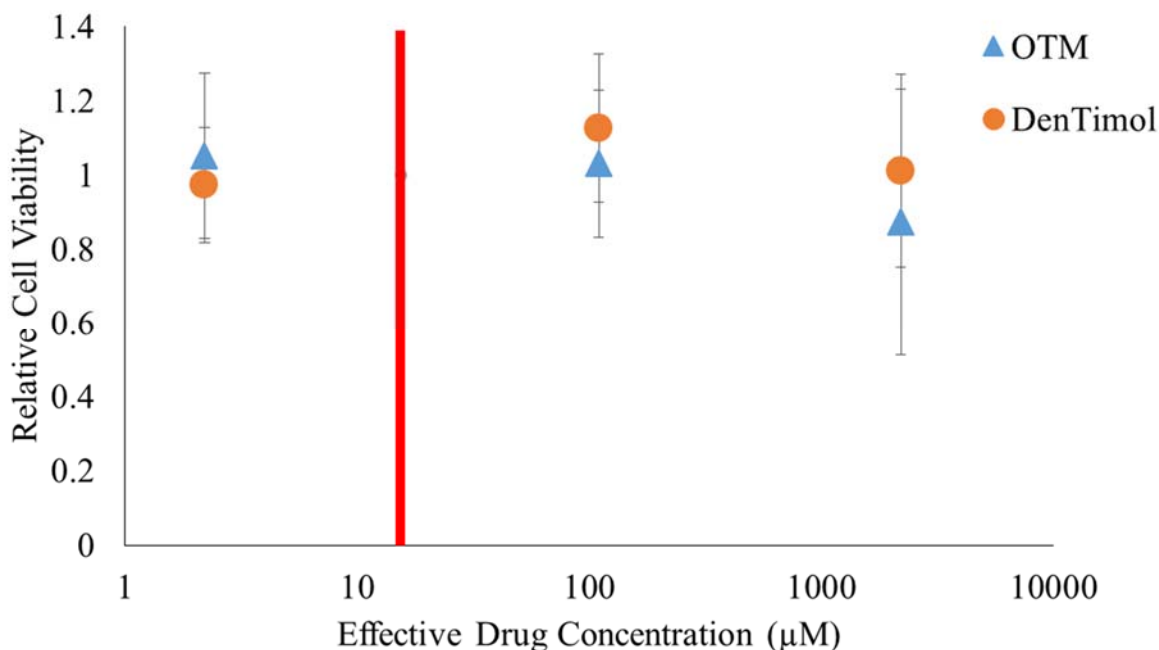


Figure 5.4: Cytotoxicity. DenTimol conjugate shows no increased toxicity over OTM prodrug at the same effective drug concentrations. Red line indicates estimated maximum therapeutic concentration.

5.4.3 In vivo safety and efficacy: Animal tests showed that G3-PEG-OTM lowers IOP when administered in a topical drop. IOP in the experimental eye dropped by an average of 7.3 mmHg (~30%) (**Fig 5.5**). Unfortunately, while the use of fully awake animals provides a more physiologically relevant model, it also produces more noise in the measurement of pressures by rebound tonometry. This noise makes it unclear at this point if potency is increased over timolol.

The IOP response profile observed for DenTimol is roughly equivalent to literature reported values for timolol in rodents.¹⁵⁶ The effect of chronic application has also not yet been studied. Clinical IOP lowering treatments rely on an additive effect of repeated drug dosing. We expect, at minimum, for this phenomenon to be present with DenTimol treatment, if not greater due to the mucoadhesive quality of the particles. Ongoing and future work is also focused on building a more complete pharmacokinetic profile for the compound. We believe this material can extend the therapeutic window for timolol sufficiently to reduce dosing frequency to once a day or less. If this is not achieved with the current synthesis strategy, there are numerous options for further dendrimer modifications including changes to dendrimer generation, PEGylation density, and even active targeting ligands with mucin selectivity.²⁵

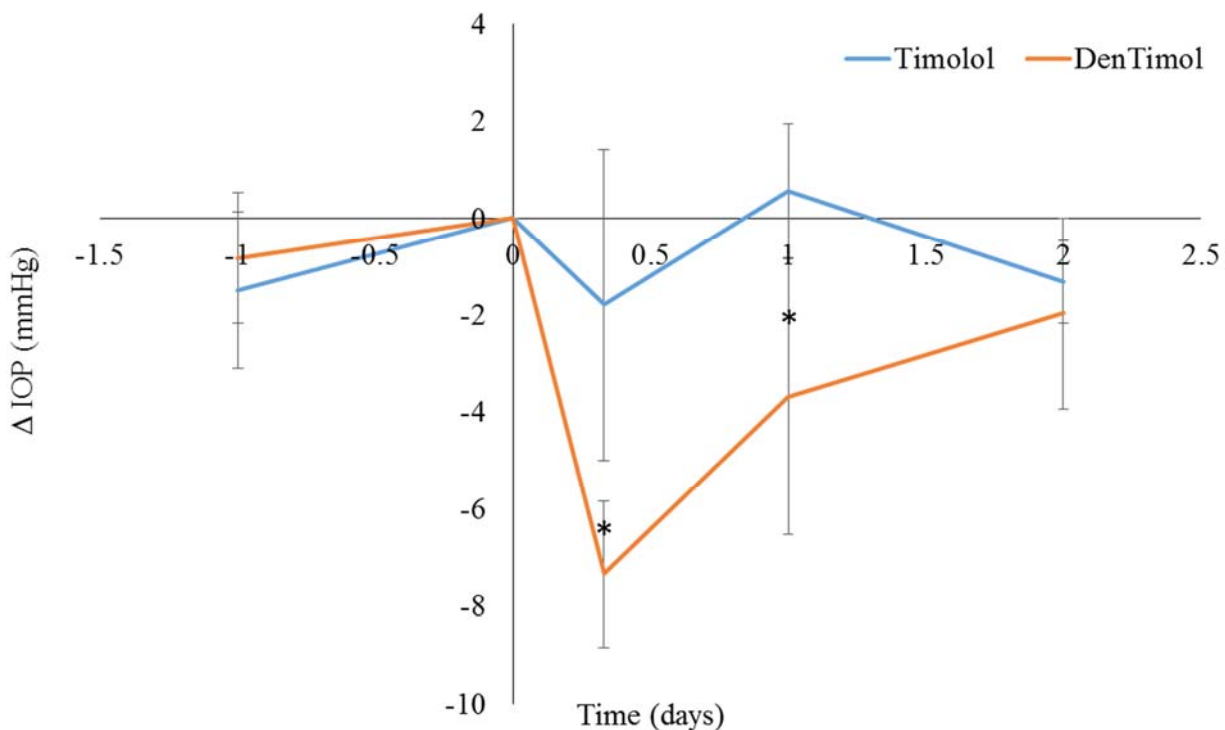


Figure 5.5: Single dose IOP response. DenTimol induced a significant drop in IOP at 8 hours, indicating similar bioactivity to timolol (n=4). (* indicates statistically significant decrease in experimental eye IOP $p \leq 0.05$)

5.5 Conclusions

In this work, we have coupled a prodrug of the selective β -blocker timolol to a PAMAM dendrimer via a flexible spacer. This new conjugate is highly water soluble and shows no signs of toxicity or ocular irritation *in vitro* or *in vivo*. Administration of the conjugate to normotensive rats results in a mean 30% decrease in IOP at 8 hours compared to the contralateral eye. Optimization of drug loading and spacer length may be able to further improve this response. Detailed pharmacokinetic work is ongoing.

Acknowledgements

This work was supported by the National Institutes of Health (R01EY024072).

Chapter 6

Conclusions and Future Directions

6.1 Summary

The background and significance of transmembrane drug delivery were discussed in chapter 1. The body possesses mucous covered membranes at several external sites, including the eyes, mouth, nose, and reproductive organs. Drugs can be delivered directly across these membranes to avoid clearance mechanisms in the liver and kidneys, but there are special considerations to ensure that drug permeation is quick, efficient, and safe. After application, liquid flow flushes drug away from the desired site before they can penetrate the epithelial cell layer that makes up these membranes. The cornea is a site where topical drug delivery is particularly inhibited by these processes, but it is also a location where transmembrane drug delivery can have the biggest clinical impact.

Nanotechnology approaches to improving transmembrane drug delivery were the next topic covered. Nanocarriers, which are particles less than a micron in diameter, can be used as drug delivery vehicles that change drug biodistribution to concentrate it at the desired site of action. Many classes of these carriers with unique structures are under investigation, but in general properties like size, charge, and functional groups are used to direct vehicle distribution. Dendrimer based vehicles are the major focus of this work. Dendrimers are spherical polymeric nanoparticles with an organized branching structure. Because they are compact and easy to functionalize, they are an ideal vehicle for transmembrane drug delivery.

Most of these nanocarriers are usually delivered as particles in solution, but solid formulations have some special utility. Generally, solid materials have superior storage stability to solutions under ambient conditions and are easier for patients to apply reliably. In these studies,

electrospinning was used to turn particle nanocarriers into dry nanofiber mats. These fibers hydrate very quickly due to their large surface area. When compared to simple films of the same materials, this increases drug release rate and decreases dissolution time.

Literature examples of dendrimers being used in ocular drug delivery were documented and discussed in chapter 2. Broadly, these approaches were divided into topical and injectable formulations. Topically applied dendrimer based ocular drug delivery vehicles included simple approaches such as the one taken by Yao et al. where dendrimers of various generations were added to a drug solution and applied to the eye.⁷⁶ They also include more complex strategies such as the one employed by Holden et al. where dendrimers used to form an *in situ* polymerizing gel on the corneal surface.⁷⁹ Both of these approaches resulted in increased corneal residence time for the drug, and ultimately enhanced efficacy. Injectable formulations used a similar variety in strategies, but one notable result was obtained by Kambhampati et al., who used hydroxyl terminated dendrimers to selectively target areas of active retinal inflammation. The breadth of these projects and the diverse array of ocular therapeutics delivered shows the flexibility of dendrimers as a drug delivery platform that can be adapted for ocular drug delivery.

Chapters 3, 4, and 5 focused on nanocarrier materials developed at this lab for transmembrane drug delivery. The chitosan nanofibers developed in chapter 3 were an extension of earlier work completed by Aduba et al. on gelatin based nanofibers.¹²⁰ In that study, nanofiber patches were used to deliver insulin across the buccal mucosa. However, the material dissolved too quickly to be clinically viable. Xu et al. improved this solubility by using a synthetic crosslinker to stabilize the fiber network.¹²¹ This crosslinker was potentially toxic though, so in the present study, we produced insulin containing nanofibers from the insoluble polysaccharide chitosan.⁶ Drug release kinetics from these fibers illustrated a key advantage of using nanofibers as drug vehicles. High

chitosan content blends produced fibers with a smaller average diameter. These materials therefore contained a larger effective surface area and released insulin faster. While permeation studies showed improvement over previous insulin delivery nanofiber patches, delivery rates are still too slow for clinical use.

Chapters 4 and 5 are closely related dendrimer based ocular drug delivery projects. In chapter 4, we demonstrated that dendrimer based nanofibers could function as a viable ocular drug delivery platform, with modest improvement in IOP reduction over traditional eye drops in a normotensive rat model. It is not yet clear if this result was due to the chemistry of the nanofiber mats or their physical form. *Ex vivo* and single response data suggested that DNF improved drug delivery efficiency very little relative to eye drops, but when applied daily they produced an additive effect, plateauing after about 4 days. This may be due to the relative difficulty and inaccuracy of instilling drug solutions into the eyes of conscious, unrestrained rodents. If true, this points to possible application for nanofiber based materials as veterinary or pediatric ocular drug delivery vehicles.

Chapter 5 extended dendrimer based delivery of anti-glaucoma drugs to direct covalent conjugation. A prodrug of the β -blocker timolol was attached via flexible spacer to a generation 3.0 PAMAM dendrimer. This novel conjugate retained the bioactivity of the prodrug while increasing the solubility of the compound dramatically. Initial animal tests showed a dramatic and prolonged reduction in IOP after just one dose. Ongoing experiments are determining the chronic IOP response and safety of this conjugate. Initial attempts to electrospun this compound have been unsuccessful, but further modifications are being attempted.

6.2 Discussion

6.2.1 Nanofiber patches as transmembrane drug delivery vehicles: The preceding studies have focused largely on the pharmacokinetic benefits of topically applied drug delivery films, but thin

films offer many benefits for patient comfort and compliance as well. Rapidly dissolving dosage forms have a long history of success as an alternative option for pediatric patients, but recent developments have spurred interest in the technology for general use. They are easier to apply, produce no choking hazard, and do not require water.¹⁵⁷ It is also easier to scale down dosage than with capsules or tablets, a critical feature for pediatric or veterinary use where patient weight can vary widely. For these reasons and others, advanced thin film systems have seen increased research interest and clinical application. The bulk of this work is for oral and dermal drug delivery, but examples of ocular devices can be found as well.¹⁵⁸⁻¹⁶⁰

Drug release kinetics from these films can be very complex, depending on the properties of the materials used. Layer by layer assemblies are commonly used to tailor release rates.¹⁶⁰ For transmembrane patches, the addition of extra layers can also be used direct drug release in the direction of the epithelium. Especially for sites where mucous flow is very rapid, as in the case in both the oral and ocular membranes, these devices can overcome one of the main limiting factors to drug delivery, by isolating the permeation site from any washout. For example, the rate of tear washout under a contact lens is estimated to be as low as 3%/min, compared to 16%/min for a normal eye.¹⁶¹

6.2.2 Difficulties of Transmembrane Drug Delivery Models: A major hurdle to overcome when developing thin film or semisolid drug delivery vehicles is the difficulty in developing relevant *in vitro* and *in vivo* membrane models. Even though tremendous advancements have been made in cell culture techniques, including liquid air interface systems, culture of epithelial cells into intact membranes is difficult, and even the best constructs lack critical physiologic mechanisms. *Ex vivo* systems fare better from a cell structure, but are highly dependent on sample quality and condition as well as the particular test setup. For example, *ex vivo* cornea permeability experiments are a

vital tool for exploring drug transport mechanisms, but the effect of tear flow are usually completely absent. Given tear drainage is often the major limiting factor preventing drug absorption, the ability of these models to predict clinical efficacy is debatable.¹⁶² New microfluidic systems are attempting to improve on the conventional test setup, but their development is still in the early stages.¹⁶³

Animal experiments are the natural answer to these limitations, but they present their own problems. Inter-species differences between animal models are an issue in all forms of biomedical research, but there are special considerations with pharmaceutical research. The size of the organism is a primary concern for pharmacokinetic experiments. As an example, mouse eyes are too small to reliably quantify drug content in the aqueous humor for many therapeutics. For this reason, larger rodent models such as rabbits are usually employed, but even still aqueous humor volume may not be sufficient to measure some drugs. In addition to size, membrane anatomy and physiology is very different in some animal species compared to humans. Rodents possess a keratinized epithelium in their buccal membranes because they store food in tough cheek pouches. The permeability of these membranes is many times lower than in mammals with a non-keratinized buccal epithelium, so they are inappropriate model for trans-buccal drug delivery research. The need to jump right to pre-clinical testing in large animal models such as pigs creates a significant cost hurdle to developing these technologies.

Another, and perhaps the biggest difficulty in developing transmembrane drug delivery vehicles, is the amount of unknown information on membrane physiology. Just in the last two years, it was discovered that nanoparticle transport across the intestinal mucosa was highly dependent on food intake.¹⁶⁴ For years, these were thought of as mostly passive tissues, but increasingly science is showing that these membranes are active barriers, responding to their environment. Until these

kinds of active responses are better studied, they cannot be accounted for in drug delivery studies, but nanocarriers may play a role in that as well. In October 2016, Henry et al. used fluorescently tagged polystyrene nanoparticles to monitor nanoparticle diffusion through the vaginal mucosa in real time.¹⁶⁵ This study showed that anti-PEG antibodies could recognize and immobilize particles through interactions with mucin chains. Not only is this an important discovery on an understudied mechanism our bodies use to trap pathogens in mucous membranes, it could point toward new techniques to develop mucoadhesive materials.

6.3 Future Directions

6.3.1 Layer-by-layer assemblies: As mentioned above, backing layers are one of the most common methods used to improve transmembrane drug delivery devices, usually by preventing drug diffusion in the apical direction and shielding the site of permeation from mucous flow and washout. In chapters 3 and 4, electrospinning was used to fabricate nanofiber patches designed for direct membrane application. In these studies fibers were deposited on a stainless steel collecting surface until the mat was thick enough to be removed, but this does not necessarily have to be the case. Rigid or flexible substrates can be affixed to the mandrel and used as a collecting surface for nanofibers. This technique is commonly employed in tissue engineering applications where thin or single layers of nanofibers are desirable.¹⁶⁶ Drug delivery efficacy would likely be improved in both of these materials by spinning onto impermeable supports. For chitosan insulin fibers, deposition onto a backing film would be a simple method of improving drug delivery efficiency.¹⁶⁷ With chitosan present as the mucoadhesive layer, this film need only to be impermeable to insulin. For DNF, deposition onto disposable contact lenses is the most promising approach. Drug delivery via contact lenses is not a novel idea, but applying a layer of quick dissolving nanofibers to only

the basal side of the lens has not yet been applied. Eventually, it is likely that DenTimol delivery could also be improved by this method.

6.3.2 Alternative ocular therapeutics: These vehicles are not limited only to the drugs covered thus far. DNF in particular have the potential to serve as a broad delivery platform for a wide array of ocular therapeutic compounds, from antibiotics to genes. Ocular inflammation in children is more likely to be caused by infectious agents than inflammation in adults.¹⁶⁸ Without early intervention, these infections can have long term effects on the child's vision. With younger children the risk of permanent vision loss rises sharply,¹⁶⁸ but so does the difficulty of administering eye drops. DNF could serve as more comfortable antibiotic dosage form for these patients, analogous to chewable oral tablets commonly prescribed for children. Specific to ocular pathogens, DNF have the added benefit of the known anti-microbial properties of the dendrimers themselves.¹⁶⁹

This is not to imply that electrospinning alternative therapeutic compounds is a trivial process. As seen in the morphology differences between DNF and DNF+BT additives to the electrospinning solution, even in small amounts, can have a big effect on the fiber formation process. Surface tension in particular is critical to fiber stability, so any drugs that impact surface tension may cause fiber rupture, or dramatically increase the working voltage (reducing spinning efficiency).¹⁷⁰ Compounds may also disassociate with the polymer during drying, forming crystals.¹⁷¹ Lastly, strong electrospinning solvents such as HFP are not compatible with all therapeutics. Bioactivity of more complex compounds such as peptides and genes cannot be assumed after electrospinning and requires additional testing.

6.3.3 Targeted dendrimer vehicles as nanofiber patches: In chapter 2, we proposed the ability to easily modify dendrimers with cell targeting ligands as a major advantage of the platform. In chapter 4 we developed a dendrimer based nanofiber material that outperformed traditional eye

drops in terms of ease of application. In chapter 5 we synthesized a novel dendrimer nanoparticle conjugate with potent IOP lowering bioactivity. The natural extension of this work is to combine these ideas together into a single material. Electrospinning of G3-PEG-OTM is the most immediate improvement that can be made. At least some of the variability observed in the animal IOP response to these particles can be accounted for by the loss of drug during eye drop delivery. More importantly, the long term storage stability of the dendrimer-prodrug linkage is not yet understood, but there is reason to think it will not be robust (in the lab, these particles are stored as lyophilized powder at 4°C and only hydrated immediately before use). Initial tests at electrospinning these conjugates have not yet been successful. Electrospun fiber formation requires chain entanglements, but dense cationic particles such as this favor disassociation in solution. Additional additives or modifications will be needed to pull stable fibers.

Two approaches can be taken to improve the spin ability of this compound, changes to the electrospinning parameters or changes to the vehicle. Modification of the electrospinning parameters is likely the more desirable path as the work on bioactivity and safety will not have to be re-done. At this time only attempts at varying electrospinning voltage, air gap distance, and solution concentration have been tried. PEO concentration should be systematically investigated next, as higher PEO concentrations may produce sufficient chain entanglements to form fibers, but also because a more thorough understanding of PEO's impact as a carrier polymer would benefit the fundamental study of electrospinning overall. Humidity is another critical parameter neglected in these studies that is known to have a major influence on fiber formation and efficiency.¹²² Unfortunately, our current electrospinning machine does not have humidity control, but it would be a useful addition in future upgrades. If changes to the nanoparticle structure are made, reducing

particle density and charge will increase the rate of chain entanglements, and therefore electrospinning efficiency.

References

1. Harris D, Robinson JR. Drug delivery via the mucous membranes of the oral cavity. *J Pharm Sci* 1992;81(1):1-10.
2. Janagam DR, Wu L, Lowe TL. Nanoparticles for drug delivery to the anterior segment of the eye. *Adv Drug Deliv Rev* 2017.
3. Kamaledin MA. Nano-ophthalmology: Applications and considerations. *Nanomedicine* 2017.
4. Niu H, Lin T. Fiber Generators in Needleless Electrospinning. *Journal of Nanomaterials* 2012.
5. Lancina III M, Yang H. Dendrimers for Ocular Drug Delivery. *Canadian Journal of Chemistry* 2017;0(ja).
6. Lancina MG, Shankar RK, Yang H. Chitosan nanofibers for transbuccal insulin delivery. *J Biomed Mater Res A* 2017;105(5):1252-1259.
7. Harvey RJ, Schlosser RJ. Local drug delivery. *Otolaryngol Clin North Am* 2009;42(5):829-45, ix.
8. Khutoryanskiy VV. Advances in mucoadhesion and mucoadhesive polymers. *Macromol Biosci* 2011;11(6):748-64.
9. Mrsny RJ, Brayden DJ. Introduction for the special issue on recent advances in drug delivery across tissue barriers. *Tissue Barriers* 2016;4(2):e1187981.
10. Netsomboon K, Bernkop-Schnürch A. Mucoadhesive vs. mucopenetrating particulate drug delivery. *Eur J Pharm Biopharm* 2016;98:76-89.
11. Lajavardi L, Bochot A, Camelo S, Goldenberg B, Naud M-C, Behar-Cohen F, Fattal E, de Kozak Y. Downregulation of endotoxin-induced uveitis by intravitreal injection of vasoactive intestinal peptide encapsulated in liposomes. *Investigative ophthalmology & visual science* 2007;48(7):3230.
12. Bowman K, Leong KW. Chitosan nanoparticles for oral drug and gene delivery. *International journal of nanomedicine* 2006;1(2):117.
13. Soares S, Costa A, Sarmiento B. Novel non-invasive methods of insulin delivery. *Expert opinion on drug delivery* 2012;9(12):1539.

14. Khafagy E-S, Morishita M, Onuki Y, Takayama K. Current challenges in non-invasive insulin delivery systems: a comparative review. *Advanced Drug Delivery Reviews* 2007;59(15):1521.
15. Vellonen KS, Soini EM, del Amo EM, Urtti A. Prediction of Ocular Drug Distribution from Systemic Blood Circulation. *Molecular Pharmaceutics* 2016;13(9):2906-2911.
16. France MM, Turner JR. The mucosal barrier at a glance. *J Cell Sci* 2017;130(2):307-314.
17. Rosenthal R, Günzel D, Finger C, Krug SM, Richter JF, Schulzke J-D, Fromm M, Amasheh S. The effect of chitosan on transcellular and paracellular mechanisms in the intestinal epithelial barrier. *Biomaterials* 2012;33(9):2791.
18. El-Sayed M, Ginski M, Rhodes C, Ghandehari H. Transepithelial transport of poly(amidoamine) dendrimers across Caco-2 cell monolayers. *J Control Release* 2002;81(3):355-65.
19. Patel A, Cholkar K, Agrahari V, Mitra AK. Ocular drug delivery systems: An overview. *World journal of pharmacology* 2013;2(2):47.
20. Rein DB. Vision problems are a leading source of modifiable health expenditures. *Invest Ophthalmol Vis Sci* 2013;54(14):ORSF18-22.
21. Willekens K, Reyns G, Diricx M, Vanhove M, Noppen B, Coudyzer W, Ni Y, Feyen JH, Stalmans P. Intravitreally Injected Fluid Dispersion: Importance of Injection Technique. *Invest Ophthalmol Vis Sci* 2017;58(3):1434-1441.
22. Quigley HA, Broman AT. The number of people with glaucoma worldwide in 2010 and 2020. *British journal of ophthalmology* 2006;90(3):262.
23. Prausnitz MR, Noonan JS. Permeability of cornea, sclera, and conjunctiva: a literature analysis for drug delivery to the eye. *Journal of pharmaceutical sciences* 1998;87(12):1479.
24. Grinstaff MW. Designing hydrogel adhesives for corneal wound repair. *Biomaterials* 2007;28(35):5205-14.
25. Ablamowicz AF, Nichols JJ. Ocular Surface Membrane-Associated Mucins. *Ocul Surf* 2016;14(3):331-41.

26. Jóhannesson G, Stefánsson E, Loftsson T. Microspheres and Nanotechnology for Drug Delivery. *Dev Ophthalmol* 2016;55:93-103.
27. Alexis F, Pridgen E, Molnar LK, Farokhzad OC. Factors affecting the clearance and biodistribution of polymeric nanoparticles. *Molecular pharmaceutics* 2008;5(4):505.
28. Amrite AC, Edelhauser HF, Singh SR, Kompella UB. Effect of circulation on the disposition and ocular tissue distribution of 20 nm nanoparticles after periocular administration. *Mol Vis* 2008;14:150-60.
29. Suk JS, Xu Q, Kim N, Hanes J, Ensign LM. PEGylation as a strategy for improving nanoparticle-based drug and gene delivery. *Adv Drug Deliv Rev* 2016;99(Pt A):28-51.
30. Kannan R, Nance E, Kannan S, Tomalia D. Emerging concepts in dendrimer-based nanomedicine: from design principles to clinical applications. *Journal of Internal Medicine* 2014;276(6):579-617.
31. Wang W, Xiong W, Wan J, Sun X, Xu H, Yang X. The decrease of PAMAM dendrimer-induced cytotoxicity by PEGylation via attenuation of oxidative stress. *Nanotechnology* 2009;20(10):105103.
32. Aref AA. Sustained drug delivery for glaucoma: current data and future trends. *Curr Opin Ophthalmol* 2017;28(2):169-174.
33. Korte J-M, Kaila T, Saari MK. Systemic bioavailability and cardiopulmonary effects of 0.5% timolol eyedrops. *Graefe's archive for clinical and experimental ophthalmology* 2002;240(6):430.
34. Urtti A. Challenges and obstacles of ocular pharmacokinetics and drug delivery. *Advanced Drug Delivery Reviews* 2006;58(11):1131.
35. Diebold Y, Calonge M. Applications of nanoparticles in ophthalmology. *Progress in retinal and eye research* 2010;29(6):596.
36. Zimmer A, Kreuter J. Microspheres and nanoparticles used in ocular delivery systems. *Advanced Drug Delivery Reviews* 1995;16(1):61.
37. Bravo-Osuna I, Andrés-Guerrero V, Pastoriza Abal P, Molina-Martínez IT, Herrero-Vanrell R. Pharmaceutical microscale and nanoscale approaches for efficient treatment of ocular diseases. *Drug Deliv Transl Res* 2016;6(6):686-707.

38. Ban J, Zhang Y, Huang X, Deng G, Hou D, Chen Y, Lu Z. Corneal permeation properties of a charged lipid nanoparticle carrier containing dexamethasone. *Int J Nanomedicine* 2017;12:1329-1339.
39. Di Colo G, Zambito Y. A study of release mechanisms of different ophthalmic drugs from erodible ocular inserts based on poly (ethylene oxide). *European journal of pharmaceutics and biopharmaceutics* 2002;54(2):193.
40. Yellepeddi VK, Palakurthi S. Recent Advances in Topical Ocular Drug Delivery. *Journal of Ocular Pharmacology and Therapeutics* 2015.
41. Acharya G. The dexamethasone nanowafer: A novel method of drug delivery for dry eye disease. 2015.
42. Da Silva GR, Lima TH, Oréfice RL, Fernandes-Cunha GM, Silva-Cunha A, Zhao M, Behar-Cohen F. In vitro and in vivo ocular biocompatibility of electrospun poly (ϵ -caprolactone) nanofibers. *European Journal of Pharmaceutical Sciences* 2015;73:9.
43. Joseph RR, Venkatraman SS. Drug delivery to the eye: what benefits do nanocarriers offer? *Nanomedicine (Lond)* 2017;12(6):683-702.
44. Kambhampati SP, Kannan RM. Dendrimer nanoparticles for ocular drug delivery. *Journal of Ocular Pharmacology and Therapeutics* 2013;29(2):151.
45. Spataro G, Malecaze F, Turrin C-O, Soler V, Duhayon C, Elena P-P, Majoral J-P, Caminade A-M. Designing dendrimers for ocular drug delivery. *European journal of medicinal chemistry* 2010;45(1):326.
46. Tomalia D, Baker H, Dewald J, Hall M, Kallos G, Martin S, Roeck J, RYDER J, SMITH P. DENDRITIC MACROMOLECULES - SYNTHESIS OF STARBURST DENDRIMERS. *Macromolecules* 1986;19(9):2466-2468.
47. Sultana Y, Jain R, Aqil M, Ali A. Review of ocular drug delivery. *Current drug delivery* 2006;3(2):207.
48. Davies NM. Biopharmaceutical considerations in topical ocular drug delivery. *Clinical and experimental pharmacology and physiology* 2000;27(7):558.
49. Joseph M, Trinh HM, Cholkar K, Pal D, Mitra AK. Recent perspectives on the delivery of biologics to back of the eye. *Expert Opin Drug Deliv* 2016:1-15.

50. Duvvuri S, Majumdar S, Mitra AK. Drug delivery to the retina: challenges and opportunities. *Expert opinion on biological therapy* 2003;3(1):45.
51. Sleath B, Blalock S, Covert D, Stone JL, Skinner AC, Muir K, Robin AL. The relationship between glaucoma medication adherence, eye drop technique, and visual field defect severity. *Ophthalmology* 2011;118(12):2398.
52. Sayner R, Carpenter DM, Blalock SJ, Robin AL, Muir KW, Hartnett ME, Giangiacomo AL, Tudor G, Sleath B. Accuracy of Patient-reported Adherence to Glaucoma Medications on a Visual Analog Scale Compared With Electronic Monitors. *Clinical therapeutics* 2015;37(9):1975.
53. Shaya FT, Mullins CD, Wong W, Cho J. Discontinuation rates of topical glaucoma medications in a managed care population. *American Journal of Managed Care* 2002;8(10; SUPP):S271.
54. Lee VHL, Robinson JR. Topical ocular drug delivery: recent developments and future challenges. *Journal of ocular pharmacology and therapeutics* 1986;2(1):67.
55. Kaur IP, Smitha R. Penetration enhancers and ocular bioadhesives: two new avenues for ophthalmic drug delivery. *Drug development and industrial pharmacy* 2002;28(4):353.
56. Almeida H, Amaral MH, Lobao P, Frigerio C, Sousa Lobo JM. Nanoparticles in Ocular Drug Delivery Systems for Topical Administration: Promises and Challenges. *Curr Pharm Des* 2015;21(36):5212-24.
57. Ranta VP, Mannermaa E, Lummeppuro K, Subrizi A, Laukkanen A, Antopolsky M, Murtomäki L, Hornof M, Urtti A. Barrier analysis of periocular drug delivery to the posterior segment. *J Control Release* 2010;148(1):42-8.
58. Castellarin A, Pieramici DJ. Anterior segment complications following periocular and intraocular injections. *Ophthalmol Clin North Am* 2004;17(4):583-90, vii.
59. Yan H, Cui J, Wang Y, Yu Y. Comparison of the effects between intravitreal and periocular injections of adenoviral vectored pigment epithelium-derived factor on suppressing choroidal neovascularization in rats. *Ophthalmic Res* 2013;49(2):81-9.

60. Madaan K, Kumar S, Poonia N, Lather V, Pandita D. Dendrimers in drug delivery and targeting: Drug-dendrimer interactions and toxicity issues. *Journal of pharmacy & bioallied sciences* 2014;6(3):139.
61. Albertazzi L, Serresi M, Albanese A, Beltram F. Dendrimer internalization and intracellular trafficking in living cells. *Molecular pharmaceutics* 2010;7(3):680.
62. Menjoge AR, Kannan RM, Tomalia DA. Dendrimer-based drug and imaging conjugates: design considerations for nanomedical applications. *Drug discovery today* 2010;15(5):171.
63. Cheng Y, Xu Z, Ma M, Xu T. Dendrimers as drug carriers: applications in different routes of drug administration. *Journal of pharmaceutical sciences* 2008;97(1):123.
64. Caminade A-M, Turrin C-O, Majoral J-P. Biological properties of phosphorus dendrimers. *New Journal of Chemistry* 2010;34(8):1512.
65. Bravo-Osuna I, Vicario-de-la-Torre M, Andres-Guerrero V, Sanchez-Nieves J, Guzman-Navarro M, de la Mata FJ, Gomez R, de las Heras B, Argueso P, Ponchel G and others. Novel Water-Soluble Mucoadhesive Carbosilane Dendrimers for Ocular Administration. *Molecular Pharmaceutics* 2016;13(9):2966-2976.
66. Heredero-Bermejo I, Copa-Patino JL, Soliveri J, Fuentes-Paniagua E, de la Mata FJ, Gomez R, Perez-Serrano J. Evaluation of the activity of new cationic carbosilane dendrimers on trophozoites and cysts of *Acanthamoeba polyphaga*. *Parasitol Res* 2015;114(2):473-86.
67. Wimmer N, Marano RJ, Kearns PS, Rakoczy EP, Toth I. Syntheses of polycationic dendrimers on lipophilic peptide core for complexation and transport of oligonucleotides. *Bioorganic & medicinal chemistry letters* 2002;12(18):2635.
68. Wang W-Y, Yao C, Shao Y-F, Mu H-J, Sun K-X. Determination of puerarin in rabbit aqueous humor by liquid chromatography tandem mass spectrometry using microdialysis sampling after topical administration of puerarin PAMAM dendrimer complex. *Journal of pharmaceutical and biomedical analysis* 2011;56(4):825.
69. Sweet DM, Kolhatkar RB, Ray A, Swaan P, Ghandehari H. Transepithelial transport of PEGylated anionic poly (amidoamine) dendrimers: implications for oral drug delivery. *Journal of Controlled Release* 2009;138(1):78.

70. Kitchens KM, Kolhatkar RB, Swaan PW, Eddington ND, Ghandehari H. Transport of poly (amidoamine) dendrimers across Caco-2 cell monolayers: influence of size, charge and fluorescent labeling. *Pharmaceutical research* 2006;23(12):2818.
71. Vandamme TF, Brobeck L. Poly (amidoamine) dendrimers as ophthalmic vehicles for ocular delivery of pilocarpine nitrate and tropicamide. *Journal of Controlled Release* 2005;102(1):23.
72. Yao W-J, Sun K-X, Liu Y, Liang N, Mu H-J, Yao C, Liang R-C, Wang A-P. Effect of poly (amidoamine) dendrimers on corneal penetration of puerarin. *Biological and Pharmaceutical Bulletin* 2010;33(8):1371.
73. Bravo-Osuna I, Woodward A, Argueso P, Martínez ITM, Gómez R, de la Mata FJ, Navarro MM, Noiray M, Ponchel G, Herrero-Vanrell R. Linear Polymers Versus PAMAM Dendrimers In The Interaction With Transmembrane Ocular Mucins: Analysis By Biosensor Technology. *Investigative ophthalmology & visual science* 2012;53(14):1845.
74. Souza JG, Dias K, Silva SAM, de Rezende LCD, Rocha EM, Emery FS, Lopez RFV. Transcorneal iontophoresis of dendrimers: PAMAM corneal penetration and dexamethasone delivery. *Journal of Controlled Release* 2015;200:115.
75. Grimaudo MA, Tratta E, Pescina S, Padula C, Santi P, Nicoli S. Parameters affecting the transscleral delivery of two positively charged proteins of comparable size. *Int J Pharm* 2017;521(1-2):214-221.
76. Yao W, Sun K, Mu H, Liang N, Liu Y, Yao C, Liang R, Wang A. Preparation and characterization of puerarin–dendrimer complexes as an ocular drug delivery system. *Drug development and industrial pharmacy* 2010;36(9):1027.
77. Richichi B, Baldoneschi V, Burgalassi S, Fragai M, Vullo D, Akdemir A, Dragoni E, Louka A, Mamusa M, MOTMi D. A Divalent PAMAM-Based Matrix Metalloproteinase/Carbonic Anhydrase Inhibitor for the Treatment of Dry Eye Syndrome. *Chemistry—A European Journal* 2016;22(5):1714.
78. Mishra V, Jain NK. Acetazolamide encapsulated dendritic nano-architectures for effective glaucoma management in rabbits. *Int J Pharm* 2014;461(1-2):380-90.

79. Holden CA, Tyagi P, Thakur A, Kadam R, Jadhav G, Kompella UB, Yang H. Polyamidoamine dendrimer hydrogel for enhanced delivery of antiglaucoma drugs. *Nanomedicine: Nanotechnology, Biology and Medicine* 2012;8(5):776.
80. Iezzi R, Guru BR, Glybina IV, Mishra MK, Kennedy A, Kannan RM. Dendrimer-based targeted intravitreal therapy for sustained attenuation of neuroinflammation in retinal degeneration. *Biomaterials* 2012;33(3):979.
81. Zhao L, Chen G, Li J, Fu Y, Mavlyutov TA, Yao A, Nickells RW, Gong S, Guo LW. An intraocular drug delivery system using targeted nanocarriers attenuates retinal ganglion cell degeneration. *J Control Release* 2017;247:153-166.
82. Kambhampati SP, Mishra MK, Mastorakos P, Oh Y, Luttj GA, Kannan RM. Intracellular delivery of dendrimer triamcinolone acetonide conjugates into microglial and human retinal pigment epithelial cells. *European Journal of Pharmaceutics and Biopharmaceutics* 2015;95:239-249.
83. Kang SJ, Durairaj C, Kompella UB, O'Brien JM, Grossniklaus HE. Subconjunctival Nanoparticle Carboplatin in the Treatment of Murine Retinoblastoma. *Archives of Ophthalmology* 2017;127(8):1043-1047.
84. Yavuz B, Bozdogan Pehlivan S, Sumer Bolu B, Nomak Sanyal R, Vural I, Unlu N. Dexamethasone - PAMAM dendrimer conjugates for retinal delivery: preparation, characterization and in vivo evaluation. *J Pharm Pharmacol* 2016;68(8):1010-20.
85. Soiberman U, Kambhampati S, Wu T, Mishra M, Oh Y, Sharma R, Wang J, Al Towerki A, Yiu S, Stark W and others. Subconjunctival injectable dendrimer-dexamethasone gel for the treatment of corneal inflammation. *Biomaterials* 2017;125:38–53.
86. Kaga S, Arslan M, Sanyal R, Sanyal A. Dendrimers and Dendrons as Versatile Building Blocks for the Fabrication of Functional Hydrogels. *Molecules* 2016;21(4):497.
87. Yang H, Tyagi P, Kadam RS, Holden CA, Kompella UB. Hybrid dendrimer hydrogel/PLGA nanoparticle platform sustains drug delivery for one week and antiglaucoma effects for four days following one-time topical administration. *ACS nano* 2012;6(9):7595.

88. Wang J, He H, Cooper RC, Yang H. In Situ-Forming Polyamidoamine Dendrimer Hydrogels with Tunable Properties Prepared via Aza-Michael Addition Reaction. *ACS Appl Mater Interfaces* 2017.
89. McLaughlin MD, Hwang JC. Trends in Vitreoretinal Procedures for Medicare Beneficiaries, 2000 to 2014. *Ophthalmology* 2017.
90. Sakurai E, Ozeki H, Kunou N, Ogura Y. Effect of particle size of polymeric nanospheres on intravitreal kinetics. *Ophthalmic research* 2000;33(1):31.
91. Kim H, Robinson SB, Csaky KG. Investigating the movement of intravitreal human serum albumin nanoparticles in the vitreous and retina. *Pharmaceutical research* 2009;26(2):329.
92. Xu Q, Nicholas B, Suk JS, Wang Y-Y, Nance E, Yang J-C, McDonnell PJ, Cone RA, J. E, Duh and others. Nanoparticle diffusion in, and microrheology of, the bovine vitreous ex vivo. *Journal of Controlled Release* 2013;167(1):76–84.
93. Mehra NK, Cai D, Kuo L, Hein T, Palakurthi S. Safety and toxicity of nanomaterials for ocular drug delivery applications. *Nanotoxicology* 2016;10(7):836-60.
94. Ayalasmayajula SP, Kompella UB. Retinal delivery of celecoxib is several-fold higher following subconjunctival administration compared to systemic administration. *Pharmaceutical research* 2004;21(10):1797.
95. Kompella UB, Bandi N, Ayalasmayajula SP. Subconjunctival nano- and microparticles sustain retinal delivery of budesonide, a corticosteroid capable of inhibiting VEGF expression. *Investigative ophthalmology & visual science* 2003;44(3):1192.
96. Loftsson T, Sigurdsson HH, Hreinsdóttir D, Konradsdóttir F, Stefansson E. Dexamethasone delivery to posterior segment of the eye. *Journal of Inclusion Phenomena and Macrocyclic Chemistry* 2007;57(1-4):585.
97. Rodríguez Villanueva J, Rodríguez Villanueva L, Guzmán Navarro M. Pharmaceutical technology can turn a traditional drug, dexamethasone into a first-line ocular medicine. A global perspective and future trends. *Int J Pharm* 2017;516(1-2):342-351.

98. Yavuz B, Pehlivan SB, Vural I, Unlu N. In Vitro/In Vivo Evaluation of Dexamethasone--PAMAM Dendrimer Complexes for Retinal Drug Delivery. *J Pharm Sci* 2015;104(11):3814-23.
99. Nassiri Koopaei N, Abdollahi M. Opportunities and obstacles to the development of nanopharmaceuticals for human use. *Daru* 2016;24(1):23.
100. Dobrovolskaia MA. Pre-clinical immunotoxicity studies of nanotechnology-formulated drugs: Challenges, considerations and strategy. *J COTMrol Release* 2015;220(Pt B):571-83.
101. Korsmeyer R. Critical questions in development of targeted nanoparticle therapeutics. *Regen Biomater* 2016;3(2):143-7.
102. Kleinbeck K, Anderson E, Ogle M, Burmania J, Kao WJ. The new (challenging) role of academia in biomaterial translational research and medical device development. *Biointerphases* 2012;7(1-4):12.
103. Centers for Disease COTMrol and P. National diabetes statistics report: estimates of diabetes and its burden in the United States, 2014. Atlanta, ga: US Department of health and human services 2014.
104. Richardson T, Kerr D. Skin-related complications of insulin therapy. *American journal of clinical dermatology* 2003;4(10):661.
105. Hummel K, McFann KK, Realsen J, Messer LH, Klingensmith GJ, Chase HP. The increasing onset of type 1 diabetes in children. *The Journal of pediatrics* 2012;161(4):652.
106. Mayer-Davis EJ, Bell RA, Dabelea D, D'Agostino R, Jr., Imperatore G, Lawrence JM, Liu L, Marcovina S, Group SfDiYS. The many faces of diabetes in American youth: type 1 and type 2 diabetes in five race and ethnic populations: the SEARCH for Diabetes in Youth Study. *Diabetes care* 2009;32 Suppl 2:S99.
107. Cui F, Shi K, Zhang L, Tao A, Kawashima Y. Biodegradable nanoparticles loaded with insulin-phospholipid complex for oral delivery: preparation, in vitro characterization and in vivo evaluation. *Journal of COTMrolled Release* 2006;114(2):242.
108. Kumria R, Goomber G. Emerging trends in insulin delivery: Buccal route. *J Diabetol* 2011;2(1):1.

109. Salamat-Miller N, Chittchang M, Johnston TP. The use of mucoadhesive polymers in buccal drug delivery. *Advanced Drug Delivery Reviews* 2005;57(11):1666.
110. Sonia TA, Sharma CP. An overview of natural polymers for oral insulin delivery. *Drug discovery today* 2012;17(13):784.
111. Shojaei AH. Buccal mucosa as a route for systemic drug delivery: a review. *J Pharm Pharm Sci* 1998;1(1):15.
112. Bobade NN, Atram SC, Wankhade VP, Pande DSD, Tapar DKK. A review on buccal drug delivery system. *Int J Pharm Sci Res* 2013;3:35.
113. Sill TJ, von Recum HA. Electrospinning: applications in drug delivery and tissue engineering. *Biomaterials* 2008;29(13):1989.
114. Jintapattanakit A, Junyaprasert VB, Kissel T. The role of mucoadhesion of trimethyl chitosan and PEGylated trimethyl chitosan nanocomplexes in insulin uptake. *Journal of pharmaceutical sciences* 2009;98(12):4818.
115. Krauland AH, Guggi D, Bernkop-Schnürch A. Oral insulin delivery: the potential of thiolated chitosan-insulin tablets on non-diabetic rats. *Journal of Controlled Release* 2004;95(3):547.
116. Sarmiento B, Ribeiro A, Veiga F, Sampaio P, Neufeld R, Ferreira D. Alginate/chitosan nanoparticles are effective for oral insulin delivery. *Pharmaceutical research* 2007;24(12):2198.
117. Yin L, Ding J, He C, Cui L, Tang C, Yin C. Drug permeability and mucoadhesion properties of thiolated trimethyl chitosan nanoparticles in oral insulin delivery. *Biomaterials* 2009;30(29):5691.
118. Yuan Q, Fu Y, Kao WJ, Janigro D, Yang H. Transbuccal delivery of CNS therapeutic nanoparticles: synthesis, characterization, and in vitro permeation studies. *ACS chemical neuroscience* 2011;2(11):676.
119. Zhang Y, Wei W, Lv P, Wang L, Ma G. Preparation and evaluation of alginate–chitosan microspheres for oral delivery of insulin. *European Journal of Pharmaceutics and Biopharmaceutics* 2011;77(1):11.

120. Aduba DC, Hammer JA, Yuan Q, Yeudall WA, Bowlin GL, Yang H. Semi-interpenetrating network (sIPN) gelatin nanofiber scaffolds for oral mucosal drug delivery. *Acta biomaterialia* 2013;9(5):6576.
121. Xu L, Sheybani N, Ren S, Bowlin GL, Yeudall WA, Yang H. Semi-interpenetrating network (sIPN) co-electrospun gelatin/insulin fiber formulation for transbuccal insulin delivery. *Pharmaceutical research* 2015;32(1):275.
122. McClure MJ, Wolfe PS, Simpson DG, Sell SA, Bowlin GL. The use of air-flow impedance to cOTMrol fiber deposition patterns during electrospinning. *Biomaterials* 2012;33(3):771.
123. Marques MRC, Loebenberg R, Almukainzi M. Simulated biological fluids with possible application in dissolution testing. *Dissolution Technol* 2011;18(3):15.
124. Pakravan M, Heuzey M-C, Ajji A. A fundamental study of chitosan/PEO electrospinning. *Polymer* 2011;52(21):4813.
125. Ohkawa K, Cha D, Kim H, Nishida A, Yamamoto H. Electrospinning of chitosan. *Macromolecular Rapid Communications* 2004;25(18):1600.
126. Pillai CKS, Paul W, Sharma CP. Chitin and chitosan polymers: Chemistry, solubility and fiber formation. *Progress in polymer science* 2009;34(7):641.
127. Homayoni H, Ravandi SAH, Valizadeh M. Electrospinning of chitosan nanofibers: Processing optimization. *Carbohydrate Polymers* 2009;77(3):656.
128. Bhattarai N, Edmondson D, Veisoh O, Matsen FA, Zhang M. Electrospun chitosan-based nanofibers and their cellular compatibility. *Biomaterials* 2005;26(31):6176.
129. Ibrahim MM, Abd-Elgawad A-EH, Soliman OA, Jablonski MM. Novel topical ophthalmic formulations for management of glaucoma. *Pharmaceutical research* 2013;30(11):2818.
130. Liu S, Jones L, Gu FX. Nanomaterials for ocular drug delivery. *Macromolecular bioscience* 2012;12(5):608.
131. Patel SC, Spaeth GL. Compliance in patients prescribed eyedrops for glaucoma. *Ophthalmic Surgery, Lasers & Imaging Retina* 1995;26(3):233.
132. Coursey TG, Henriksson JT, Marciano DC, Shin CS, Isenhardt LC, Ahmed F, De Paiva CS, Pflugfelder SC, Acharya G. Dexamethasone nanowafer as an effective therapy for dry eye disease. *J COTMrol Release* 2015;213:168-74.

133. Fedorchak MV, Conner IP, Medina CA, Wingard JB, Schuman JS, Little SR. 28-day intraocular pressure reduction with a single dose of brimonidine tartrate-loaded microspheres. *Experimental eye research* 2014;125:210.
134. Peng C-C, Burke MT, Carbia BE, Plummer C, Chauhan A. Extended drug delivery by cOTMact lenses for glaucoma therapy. *Journal of COTMrolled Release* 2012;162(1):152.
135. Imayasu M, Ito I, Fukuchi H, Cavanagh HD. Effects of multipurpose care solutions for RGP cOTMact lenses on corneal epithelial tight junctions. *COTMact Lens and Anterior Eye* 2015(38):e15.
136. Yang H, Kao WJ. Dendrimers for pharmaceutical and biomedical applications. *Journal of biomaterials science, polymer edition* 2006;17(1-2):3.
137. Yang H, Leffler CT. Hybrid dendrimer hydrogel/poly(lactic-co-glycolic acid) nanoparticle platform: an advanced vehicle for topical delivery of antiglaucoma drugs and a likely solution to improving compliance and adherence in glaucoma management. *J Ocul Pharmacol Ther* 2013;29(2):166-72.
138. Aduba DC, Overlin JW, Frierson CD, Bowlin GL, Yang H. Electrospinning of PEGylated polyamidoamine dendrimer fibers. *Materials Science and Engineering: C* 2015;56:189.
139. Yang H, Morris JJ, Lopina ST. Polyethylene glycol-polyamidoamine dendritic micelle as solubility enhancer and the effect of the length of polyethylene glycol arms on the solubility of pyrene in water. *J. Colloid Interface Sci.* 2004;273(1):148-154.
140. Husain S, Abdul Y, Singh S, Ahmad A, Husain M. Regulation of nitric oxide production by delta-opioid receptors during glaucomatous injury. *PLoS One* 2014;9(10):e110397.
141. Shenoy SL, Bates WD, Frisch HL, Wnek GE. Role of chain entanglements on fiber formation during electrospinning of polymer solutions: good solvent, non-specific polymer-polymer interaction limit. *Polymer* 2005;46(10):3372-3384.
142. Yu JH, Fridrikh SV, Rutledge GC. The role of elasticity in the formation of electrospun fibers. *Polymer* 2006;47(13):4789.
143. Xiang CD, Batugo M, Gale DC, Zhang T, Ye J, Li C, Zhou S, Wu EY, Zhang EY. Characterization of human corneal epithelial cell model as a surrogate for corneal permeability

- assessment: metabolism and transport. *Drug Metabolism and Disposition* 2009;37(5):992.
144. Whitehead KA, Langer R, Anderson DG. Knocking down barriers: advances in siRNA delivery. *Nature reviews Drug discovery* 2009;8(2):129.
 145. Franciosa JA, Freis ED, Conway J. Antihypertensive and hemodynamic properties of the new beta adrenergic blocking agent timolol. *Circulation* 1973;48(1):118-24.
 146. Zimmerman TJ, Kaufman HE. Timolol. A beta-adrenergic blocking agent for the treatment of glaucoma. *Arch Ophthalmol* 1977;95(4):601-4.
 147. Coakes RL, Brubaker RF. The mechanism of timolol in lowering intraocular pressure. In the normal eye. *Arch Ophthalmol* 1978;96(11):2045-8.
 148. Bükür E, Dinç E. A New UPLC Method with Chemometric Design-Optimization Approach for the Simultaneous Quantitation of Brimonidine Tartrate and Timolol Maleate in an Eye Drop Preparation. *J Chromatogr Sci* 2017;55(2):154-161.
 149. Nieminen T, Lehtimäki T, Mäenpää J, Ropo A, Uusitalo H, Kähönen M. Ophthalmic timolol: plasma concentration and systemic cardiopulmonary effects. *Scand J Clin Lab Invest* 2007;67(2):237-45.
 150. Rana MA, Mady AF, Rehman BA, Alharthy A, Huwait B, Riaz A, Aletreby WT. From Eye Drops to ICU, a Case Report of Three Side Effects of Ophthalmic Timolol Maleate in the Same Patient. *Case Rep Crit Care* 2015;2015:714919.
 151. Ibrahim MM, Abd-Elgawad AH, Soliman OA, Jablonski MM. Natural Bioadhesive Biodegradable Nanoparticle-Based Topical Ophthalmic Formulations for Management of Glaucoma. *Transl Vis Sci Technol* 2015;4(3):12.
 152. Bravo-Osuna I, Woodward A, Argueso P, Martínez ITM, Gómez R, de la Mata FJ, Navarro MM, Noiray M, Ponchel G, Herrero-Vanrell R. Linear Polymers Versus PAMAM Dendrimers In The Interaction With Transmembrane Ocular Mucins: Analysis By Biosensor Technology. *Investigative ophthalmology & visual science* 2012;53(14):1845.
 153. Zolotarskaya OY, Xu L, Valerie K, Yang H. Click synthesis of a polyamidoamine dendrimer-based camptothecin prodrug. *RSC Adv* 2015;5(72):58600-58608.

154. Pech B, Duval O, Richomme P, Benoit J. A timolol prodrug for improved ocular delivery: Synthesis, conformational study and hydrolysis of palmitoyl timolol malonate. *International Journal of Pharmaceutics* 1996;128(1-2):179-188.
155. Sk UH, Kambhampati SP, Mishra MK, Lesniak WG, Zhang F, Kannan RM. Enhancing the efficacy of Ara-C through conjugation with PAMAM dendrimer and linear PEG: a comparative study. *Biomacromolecules* 2013;14(3):801-10.
156. Akaishi T, Odani-Kawabata N, Ishida N, Nakamura M. Ocular hypotensive effects of anti-glaucoma agents in mice. *J Ocul Pharmacol Ther* 2009;25(5):401-8.
157. Kathpalia H, Gupte A. An introduction to fast dissolving oral thin film drug delivery systems: a review. *Curr Drug Deliv* 2013;10(6):667-84.
158. Lance KD, Bernards DA, Ciaccio NA, Good SD, Mendes TS, Kudisch M, Chan E, Ishikiriya M, Bhisitkul RB, Desai TA. In vivo and in vitro sustained release of ranibizumab from a nanoporous thin-film device. *Drug Deliv Transl Res* 2016;6(6):771-780.
159. Bernards DA, Bhisitkul RB, Wynn P, Steedman MR, Lee OT, Wong F, Thoongsuwan S, Desai TA. Ocular biocompatibility and structural integrity of micro- and nanostructured poly(caprolactone) films. *J Ocul Pharmacol Ther* 2013;29(2):249-57.
160. Boateng JS, Popescu AM. Composite bi-layered erodible films for potential ocular drug delivery. *Colloids Surf B Biointerfaces* 2016;145:353-61.
161. Maki KL, Ross DS. Exchange of tears under a cOTMact lens is driven by distortions of the cOTMact lens. *Integr Comp Biol* 2014;54(6):1043-50.
162. Tieppo A, Boggs AC, Pourjavad P, Byrne ME. Analysis of release kinetics of ocular therapeutics from drug releasing cOTMact lenses: Best methods and practices to advance the field. *COTM Lens Anterior Eye* 2014;37(4):305-13.
163. Tieppo A, Pate KM, Byrne ME. In vitro cOTMrolled release of an anti-inflammatory from daily disposable therapeutic cOTMact lenses under physiological ocular tear flow. *Eur J Pharm Biopharm* 2012;81(1):170-7.
164. Yildiz HM, McKelvey CA, Marsac PJ, Carrier RL. Size selectivity of intestinal mucus to diffusing particulates is dependent on surface chemistry and exposure to lipids. *J Drug Target* 2015;23(7-8):768-74.

165. Henry CE, Wang YY, Yang Q, Hoang T, Chattopadhyay S, Hoen T, Ensign LM, Nunn KL, Schroeder H, McCallen J and others. Anti-PEG antibodies alter the mobility and biodistribution of densely PEGylated nanoparticles in mucus. *Acta Biomater* 2016;43:61-70.
166. Corey JM, Lin DY, Mycek KB, Chen Q, Samuel S, Feldman EL, Martin DC. Aligned electrospun nanofibers specify the direction of dorsal root ganglia neurite growth. *J Biomed Mater Res A* 2007;83(3):636-45.
167. Mahdizadeh Barzoki Z, Emam-Djomeh Z, Mortazavian E, Akbar Moosavi-Movahedi A, Rafiee Tehrani M. Formulation, in vitro evaluation and kinetic analysis of chitosan-gelatin bilayer muco-adhesive buccal patches of insulin nanoparticles. *J Microencapsul* 2016;33(7):613-624.
168. Benezra D, Cohen E, Maftzir G. Patterns of intraocular inflammation in children. *Bull Soc Belge Ophtalmol* 2001(279):35-8.
169. Lopez AI, Reins RY, McDermott AM, Trautner BW, Cai C. Antibacterial activity and cytotoxicity of PEGylated poly(amidoamine) dendrimers. *Mol Biosyst* 2009;5(10):1148-56.
170. Garg K, Bowlin GL. Electrospinning jets and nanofibrous structures. *Biomicrofluidics* 2011;5(1):13403.
171. Natu MV, de Sousa HC, Gil MH. Effects of drug solubility, state and loading on controlled release in bicomponent electrospun fibers. *Int J Pharm* 2010;397(1-2):50-8.

Vita

Michael George Lancina III was born January 12th, 1991, in Wyandotte, Michigan, and is an American citizen. He graduated from Airport High School, Carleton, Michigan in 2009. He received a Bachelors of Science in Biomedical Engineering from Michigan Technological University, Houghton, Michigan, in 2013.